BRITTLE FRACTURE PETROFABRIC ALONG A WEST-EAST TRAVERSE FROM THE CONNECTICUT VALLEY TO THE NARRAGANSETT BASIN

BY PAUL ORVILLE EBERLY

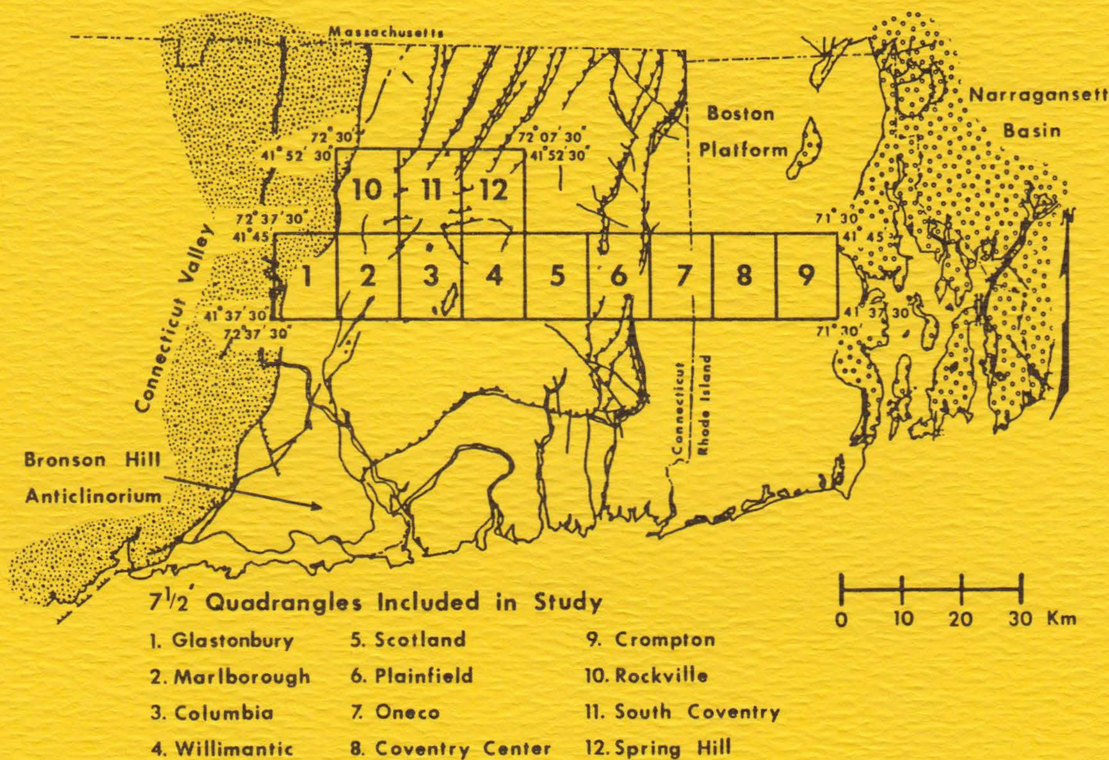

CONTRIBUTION NO. 57
DEPARTMENT OF GEOLOGY & GEOGRAPHY
UNIVERSITY OF MASSACHUSETTS
AMHERST, MASSACHUSETTS

BRITTLE FRACTURE PETROFABRIC ALONG A WEST-EAST TRAVERSE FROM THE CONNECTICUT VALLEY TO THE NARRAGANSETT BASIN

By

PAUL ORVILLE EBERLY

Contribution No. 57

Department of Geology and Geography

University of Massachusetts

Amherst, Massachusetts

September, 1985

TABLE OF CONTENTS

TABLE OF CONTENTS
(Continued)

TABLE OF CONTENTS
(Continued)

ILLUSTRATIONS

ILLUSTRATIONS
(Continued)

ILLUSTRATIONS
(Continued)

ABSTRACT

Approximately 6300 structural features, dominantly of brittle deformational origin, were examined at 105 stations along an 94 km, west-east traverse of twelve 7 1/2' quadrangles in eastern Connecticut and western Rhode Island. The data are divisible into: 1) pegmatite and aplite dikes, ductile faults, high temperature veins and high-angle brittle reverse faults of probable Alleghenian to latest Paleozoic age; 2) minor extensile and vertical dip-slip faults and lower temperature veins of probable Mesozoic age; 3.) quartz veins and faults with lateral motions that are partly contemporaneous with 1 and 2; 4.) joints and related extensile features. Joints are probable precursors of steeply dipping minor faults and may range in age from the late Paleozoic to the Quaternary. Many joints and brittle faults are mineralized. The data are dominated by two major structural trends including a NNE to NE "Merrimack" trend that is subparallel to the structural grain of the Merrimack Synclinorium and an E-W "Narragansett Pier" trend which may represent a northerly extension of a domain of E-W-trending fractures. This fracture system may have controlled emplacement of the Narragansett Pier Granite. Compressive faults in the area indicate NW-SE compression. Absence of such features in the Narragansett Pier Granite suggests late Paleozoic, counterclockwise rotation of the maximum

compressive stress from NW-SE to E-W. Mesozoic extensile faults indicate NW-SE extension that is compatible with a swarm of Mesozoic diabase dikes in this part of New England. The minor fault fabric, unlike that of areas to the west, northwest and south is dominated by dip-slip motions. The distributions of NNE-trending quartz veins, common joints and macrojoints, and minor brittle faults are influenced by major tectonic features in the area, viz., the Eastern Border Fault of the Connecticut Valley, the Willimantic Dome, the Lake Char Fault Zone (LCFZ) and the border faults of the Narragansett Basin. The correlation of minor faults with the LCFZ is particularly striking. The fabric of common joints, macrojoints and microjoints in dikes and veins is reminiscent of the rift and grain of the granite quarries of New England.

INTRODUCTION

The Problem

This study is an attempt to unravel the late, brittle deformational history of an area in eastern Connecticut and western Rhode Island. Brittle petrofabric studies were conducted at outcrops along a 94 kilometer, west-east traverse extending from the Connecticut Valley to the Narragansett Basin (Figures 1A and 1B). The traverse comprises twelve 7 1/2' quadrangles and ranges from 72° 37' 30" to 71° 30' longitude and from 41° 52' 30" to 41° 37' 30" latitude.

Several critical aspects of the late (late Paleozoic and younger) tectonic history of southern New England remain unresolved: (1) At present, the nature and extent of Alleghenian deformational events in southern New England are poorly understood. Various models have been proposed that invoke major transcurrent motions in southern New England during the late Paleozoic but little geologic evidence has been found to support them (Mosher, 1983). Further study is required to resolve the kinematic history of the late Paleozoic Narragansett Basin. (2) The relative importance of folding versus faulting in southern New England remains an item of debate. Some workers (ie: Barosh, 1981, Fig. 4) ascribe virtually the entire structural history of the area to large-scale ductile faulting. (3) Mesozoic mafic dike swarms in New England have been described by May (1971) and McHone (1978) but their tectonic significance remains unclear. (4) Crustal flexing related to the coastal plain and continental shelf (Watts, 1982) of southern New England may have occurred but no significant brittle deformational effects of this flexing have been recognized (Wise, personal communication, 1983). (5) The meaning and cause of modern seismicity in the Moodus area of Connecticut (Barosh and others, 1982) and the Narragansett Bay region of Rhode Island (McMaster and others, 1980) remain unclear.

Since low pressure/low temperature conditions prevailed during much of the late tectonic evolution of southern New England, resolution of these issues requires a fuller understanding of the area's brittle deformational history. This study closes a gap in a regional network of fracture stations and was undertaken to help clarify the later deformational events. Specifically, the objectives of the study are to provide at least partial answers to the questions listed below.

1.) What fracture patterns are of importance in eastern Connecticut and western Rhode Island? What stress fields were associated with these fracture patterns?

2.) What was the chronological sequence of the late brittle deformational events?

3.) Do fracture domain boundaries exist in the study area and, if so, what is their nature?

4.) Do fracture patterns in the area bear any special relationship to major structural features or tectonic boundaries?

5.) How do brittle fracture data for this area compare with data collected in surrounding areas by other workers?

6.) What constraints can examination of the area's brittle deformational history place on some of the tectonic models that have been proposed for the region?

Geologic Setting

The area is located within the Bronson Hill Anticlinorium and the Merrimack Synclinorium in eastern Connecticut and the Boston Platform in Connecticut and Rhode Island (Figure 2). Extensive plutonic activity, metamorphism, and widespread, penetrative, ductile deformation occurred within the area during the Taconic, Acadian and, to an uncertain extent, Alleghenian orogenic events. The Mesozoic tectonics of the region were dominated by the rifting event that produced the present Atlantic Ocean. A more complete description of the geology of the area is provided in Appendix I.

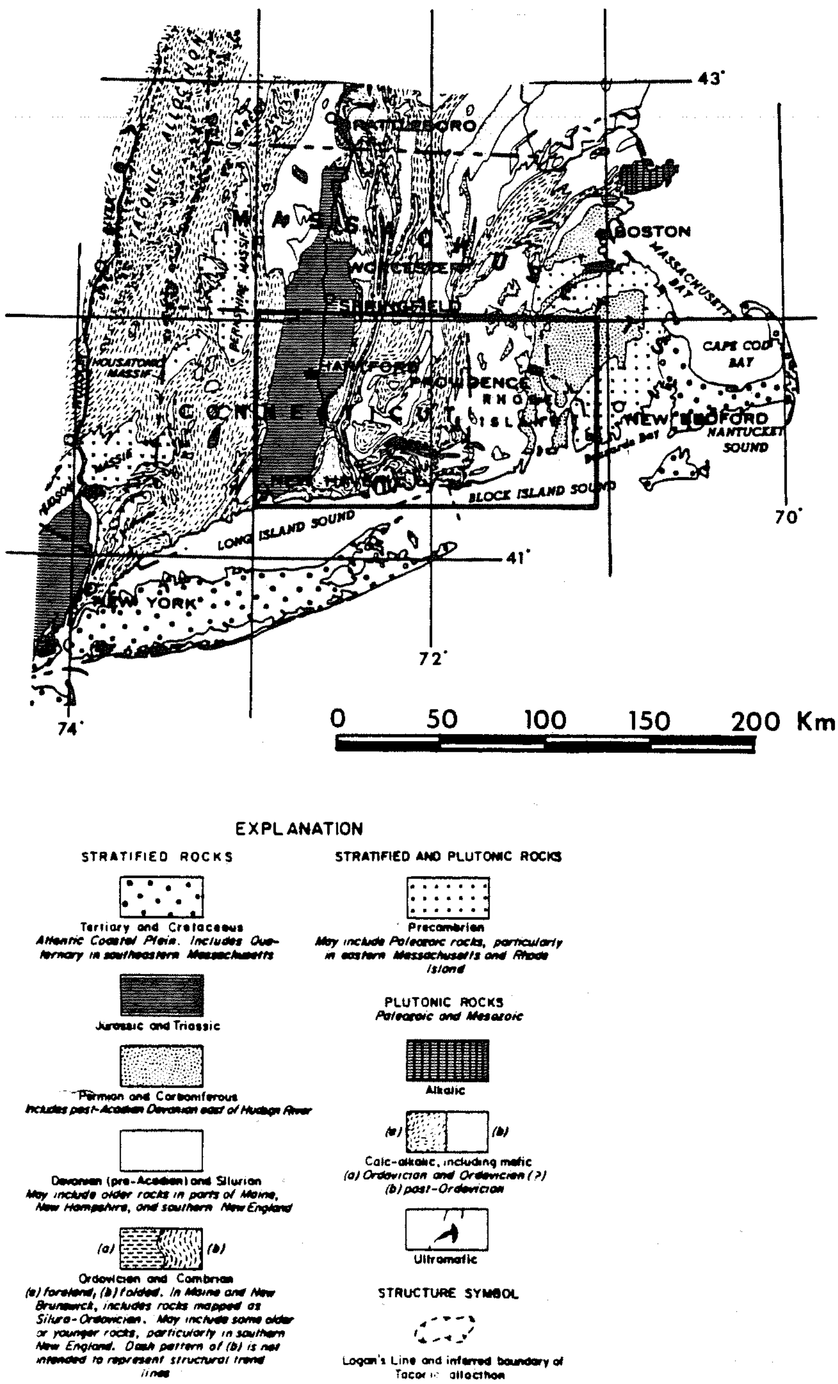

Figure 1A. Regional geologic map of southern New England (from White, 1968). The outlined area is shown in Figure 1B.

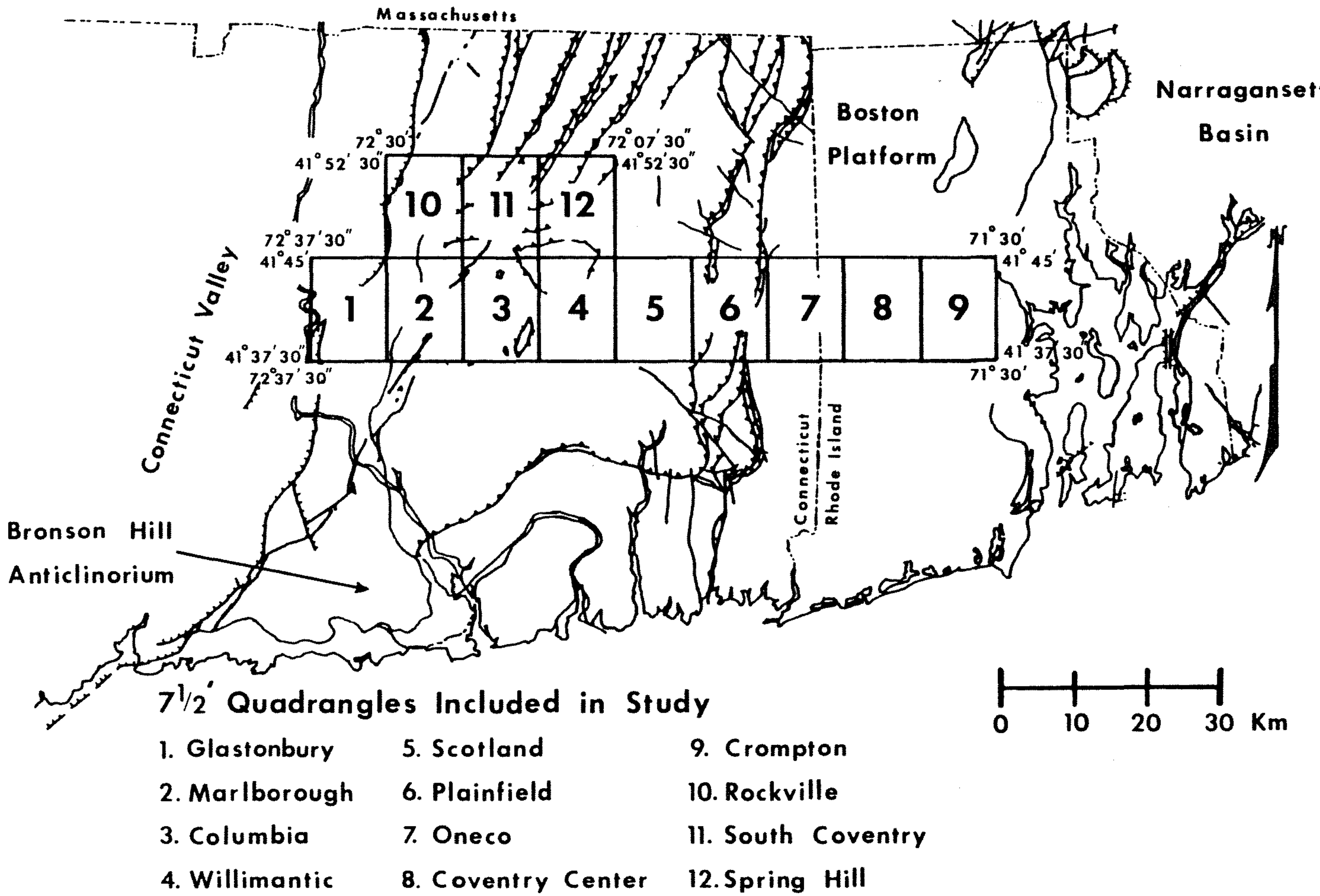

Figure 1B. Location map of the study area.

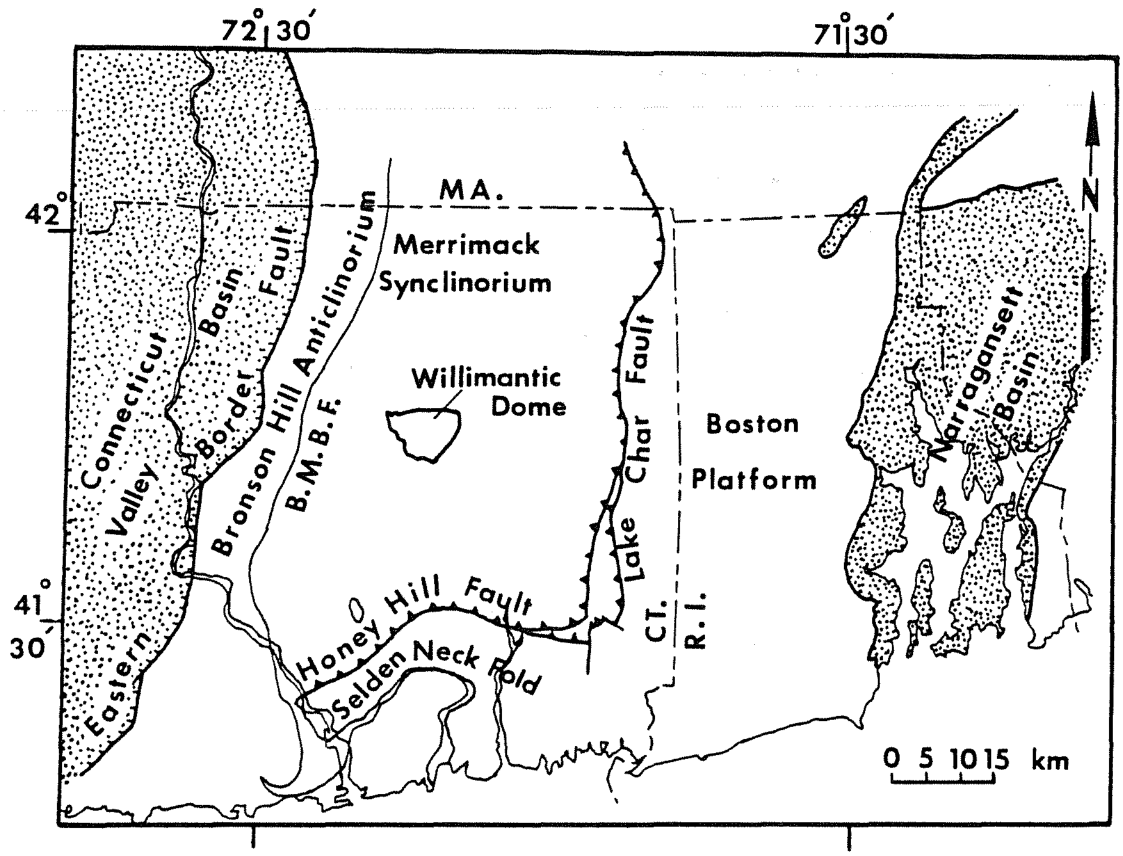

Figure 2. Simplified tectonic map of southeastern New England, B.M.B.F.=Bone Mill Brook Fault (after Dixon and Lundgren, 1968).

Previous Work

Despite considerable effort to understand the complex, early to middle Paleozoic ductile deformation of southern New England, controversy continues over the details of this portion of the area's tectonic history (ie: Quinn and Moore, 1968; Dixon and Lundgren, 1968; Tracy and Robinson, 1978; Osberg, 1980; Hall and Robinson, 1982). The late, brittle deformational history of the region, by contrast, has only recently come under vigorous investigation and its broader outlines are now beginning to emerge.

At present more than 500 fracture stations are scattered throughout the region of southern New England, making it one of the most densely sampled areas in the country for brittle deformational features. Brittle fracture studies of the Connecticut Valley and the Berkshire Anticlinorium include those of Piepul (1975); Goldstein (1975); Silverman (1976); Williams (1976); Haines and Bauer (1978); Chandler (1978); Ingari and Massaras (1978); Reks and Smith (1979); Massaras, Bauer and Wrenn (1979); Williams (1979); Maher (1979); and Peterson (1979). These studies are summarized by Wise (1981).

Field Techniques

Approximately 6300 brittle deformational features were studied during two field seasons at 105 fracture stations located throughout the twelve quadrangles of the study area.

In the 1981 field season, large outcrops throughout the area were selected for study without reference to any preestablished sampling grid, a procedure which resulted in large gaps in coverage. During the 1982 season, variants of the sampling method of Nickelsen and Hough (1967) were used. An attempt was made to study the Marlborough Quadrangle of Connecticut (Figure 1B) using the Nickelsen and Hough procedure of selecting 16 fracture stations per quadrangle but this proved to be impractical because of limited exposure. Ultimately, a procedure was chosen of making a detailed study of at least one large outcrop for each quadrant of each quadrangle, providing for a minimum of four major fracture stations per quadrangle. In addition, many small exposures were studied and recorded as mini-stations to provide more continuous coverage of the area.

The sampling procedure followed at each station was designed to minimize the sources of error listed by Wise (1964). Each station was divided into substations, the number and spacing of which were determined by the size and shape of the outcrop. Substations at roadcuts or other linear exposures were located with roughly equal spacing along the exposure. At non-linear outcrops (ie: quarries and some natural exposures), substations were scattered across the outcrop surface to ensure uniform coverage of the exposure. At individual substations, data were recorded for one member of each distinct family of brittle structural features.

For each brittle structural element considered, the type of feature (ie: joint, fault, etc.), azimuth of the plane (with dip to the right), dip, mineralogic character, surface characteristics (ie: roughness, alteration, etc.), maximum observable dimension, and any abutting, cross-cutting, or offsetting relationships were noted and recorded. Several additional features were noted for any faults observed during data collection including: the azimuth and plunge of all slickenline sets; the azimuth and plunge of the rotation axis, an imaginary line lying on the fault plane and perpendicular to the slickenlines; and the rotation sense of the fault (clockwise or counterclockwise) as viewed down the plunge of the rotation axis. The rotation axis is parallel to the intermediate compressive stress direction of the stress tensor associated with the fault (Wise, 1965). Its rotation sense was determined by offset of markers and minor drag structures (high reliability), pressure solution or frictional effects associated with surface irregularities (intermediate reliability), or by slickenline character (low reliability).

Data Analysis

Observations recorded in the study area were transferred from field records to an Interactive Data Analysis Package (IDAP) file on a Control Data Corporation Cyber 175 computer at the University of Massachusetts. IDAP, a software package by Wiedman and Hosmer (1983), allows any subset of the data to be selected for separate consideration and eliminates the need for a geologist to spend hours searching through a field notebook for data of interest. Orientations of principal stresses associated with faults were calculated according to the model of Anderson (1951) for shear failure under brittle conditions using EGYPT2, a program in Wang BASIC by D. U. Wise (1983). NETTS, a Fortran 4 program developed by G. Pferd and modified by C. Barton, was used for plotting and contouring of orientational data on lower hemispheres of equal area nets.

Areal distribution of data was studied using SYMAP, a surface-fitting software package prepared by the Harvard Spatial Analysis and Computer Graphics Laboratory. This program permits computerized production of contour maps and possesses polynomial fitting capabilities for trend surface analysis techniques (Dougenik and Sheehan, 1979). Orientational variation of steep fracture planes was analyzed using AVTD (Azimuth Versus Traverse Distance), a

Wang BASIC procedure developed by Wise (Wise and McCrory, 1982) to characterize variation of fracture azimuths along a linear traverse. Modifications by the author to AVTD made it mainframe compatible, incorporated file reading and writing capabilities, and permitted counter size adjustments to increase its suitability for large scale fracture studies.

Acknowledgement

I would like to express my heartfelt appreciation to Professor Donald U. Wise for his countless thoughtful suggestions, encouragement, and enthusiastic support of this project. Professor George E. McGill's field expertise, computing assistance, helpful observations and critical review of this manuscript are gratefully acknowledged. Professor Laurie L. Brown reviewed the manuscript and provided invaluable moral support and assistance with computing difficulties. Jamie Hall, Russell Carter, Mike Valentine, David Green, Lois Grady, Robert Snook, and Peter Morton all supplied helpful suggestions or expert field assistance. I am grateful to John Allison for the contribution of his considerable programming abilities and to Allan Swiercz for his very able assistance in the field. I am thankful also for the abundant help provided by Lee Allison. Partial financial support for field work was provided through a grant from the Department of Geology and

Geography. Finally, I would like to thank my father and mother and in particular, my wife, each of whom provided encouragement and support which made this project possible.

VEINS AND DIKES

Structural measurements and other characteristics were noted for a large number of dikes and veins in the study area. Cross-cutting relationships suggest that some of these structures are among the older features included in the data base. Mutual cross-cutting of quartz veins, aplite and pegmatite dikes and veins of more complex mineralogy indicates that emplacement of these features overlapped in time. These dikes and veins were emplaced along strength anisotropies that were repeatedly reactivated by Paleozoic and younger deformation. Dikes and veins of various types are considered below in approximate chronological order.

Pegmatite and Aplite Dikes

Cross-cutting relationships yield weak indication that the initial emplacement of aplite dikes and dikelets (n=63) in the area predated that of other mineralized fractures. Most of these features have steep dips and E-W to WNW strikes (Figure 3A). The heavy lines in this and subsequent stereonets indicate dominant trends in the data. Line lengths are proportional to strength of data concentration. If the aplite dikes are interpreted using the Anderson (1951) criterion, the orientation of the least compressive stress (sigma 3) ranges from N-S to NNE.

Pegmatite dikes (n=283) are much more common than aplites in the area. Moderately to steeply dipping pegmatite dikes and dikelets are oriented WNW and NNW (Figures 3B and 4A). Many pegmatite bodies are sill-like with gently dipping NNW orientations (compare to regional foliation, Figure 3E).

Except for a single diabase dike in Rhode Island, all dikes observed in the field (also see Miscellaneous Dikes, Appendix II) are probably of middle to late Alleghenian age or older. Most of the dikes are relatively planar and lack clear evidence for significant ductile deformation. This characteristic may indicate that most aplite, pegmatite, and other dikes do not predate the Alleghenian event. Cross-cutting relations between aplite and pegmatite dikes are ambiguous, suggesting that emplacement of these features overlapped chronologically.

Quartz Veins

Quartz veins (Figure 3C) in the study area are very consistently oriented, with most striking NNE. This strong fabric, however, is commonly only weakly developed at individual fracture stations (Figure 4B). Gently dipping, NNW-trending veins are parallel to foliation (Figure 3E) and to the pegmatite sills (Figure 3B). Cross-cutting relations show that the timing of emplacement of NNE-trending quartz veins overlapped that of a family of minor ductile faults, pegmatite and aplite dike emplacement, and at least the early stages of brittle faulting.

An approximation of the frequency of NNE-trending quartz veins at individual outcrops was obtained by calculating the percentage of such veins out of all observations collected at a station. Stations with fewer than 20 observations were eliminated or merged with nearby stations (to avoid extreme values resulting from small sample size) and digitized according to an X-Y coordinate system. The station frequencies were computer contoured (Figure 5A).

NNE-trending quartz veins are most numerous in outcrops within the Bronson Hill Anticlinorium east of the Eastern Border Fault (EBF) of the Mesozoic Connecticut Valley. The marked areal correlation of these veins with the EBF may indicate a genetic relationship between the veins and this major structure. Because movement along the EBF to the north in Massachusetts is associated with intense silicification (Chandler, 1978), some of these veins may be related to the graben tectonics of the Connecticut Valley. Veins of this type are also numerous in the Willimantic Dome area and within the Lake Char Fault Zone.

The frequency of these veins was also studied using trend surface analysis, a standard polynomial fitting technique commonly used for showing large scale trends in geological studies (Whitten, 1981; also Appendix III for

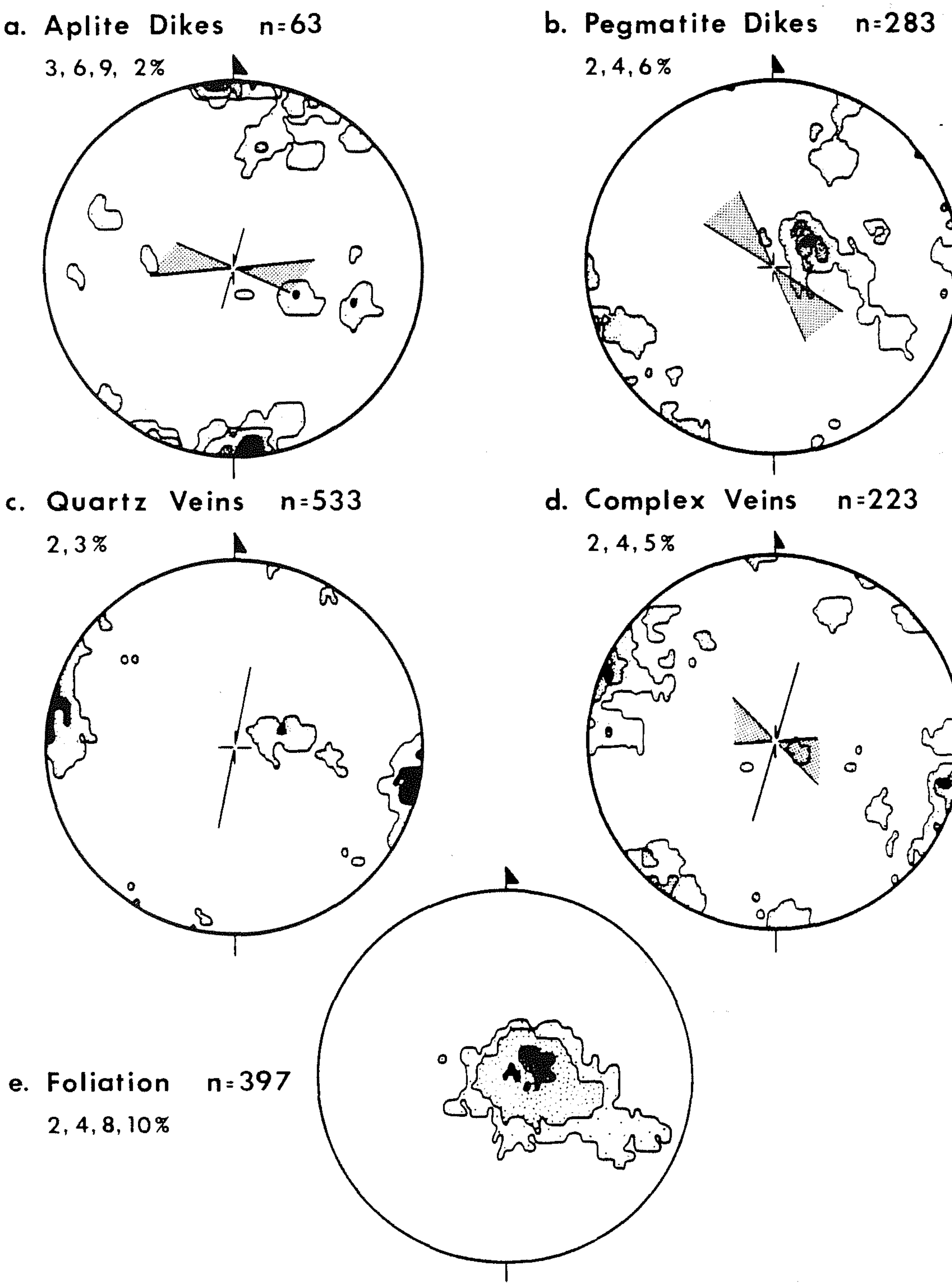

Figure 3. Equal area net plots of poles to planes for dikes, veins, and foliation within the study area. Contours are in percent per 1% area.

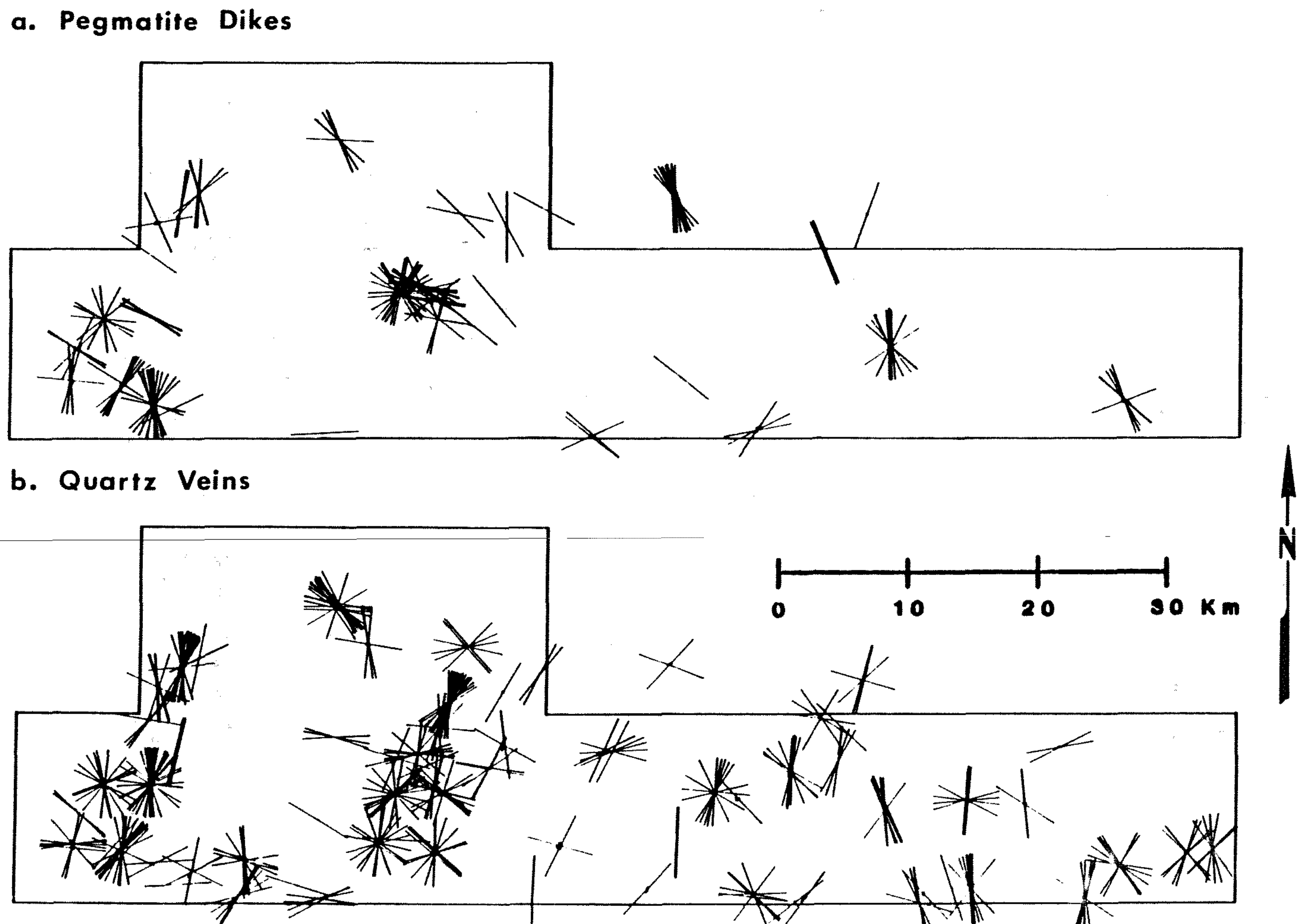

Figure 4. Azimuths of pegmatite dikes and quartz veins (Dips > 55°) at fracture stations in eastern Connecticut and western Rhode Island.

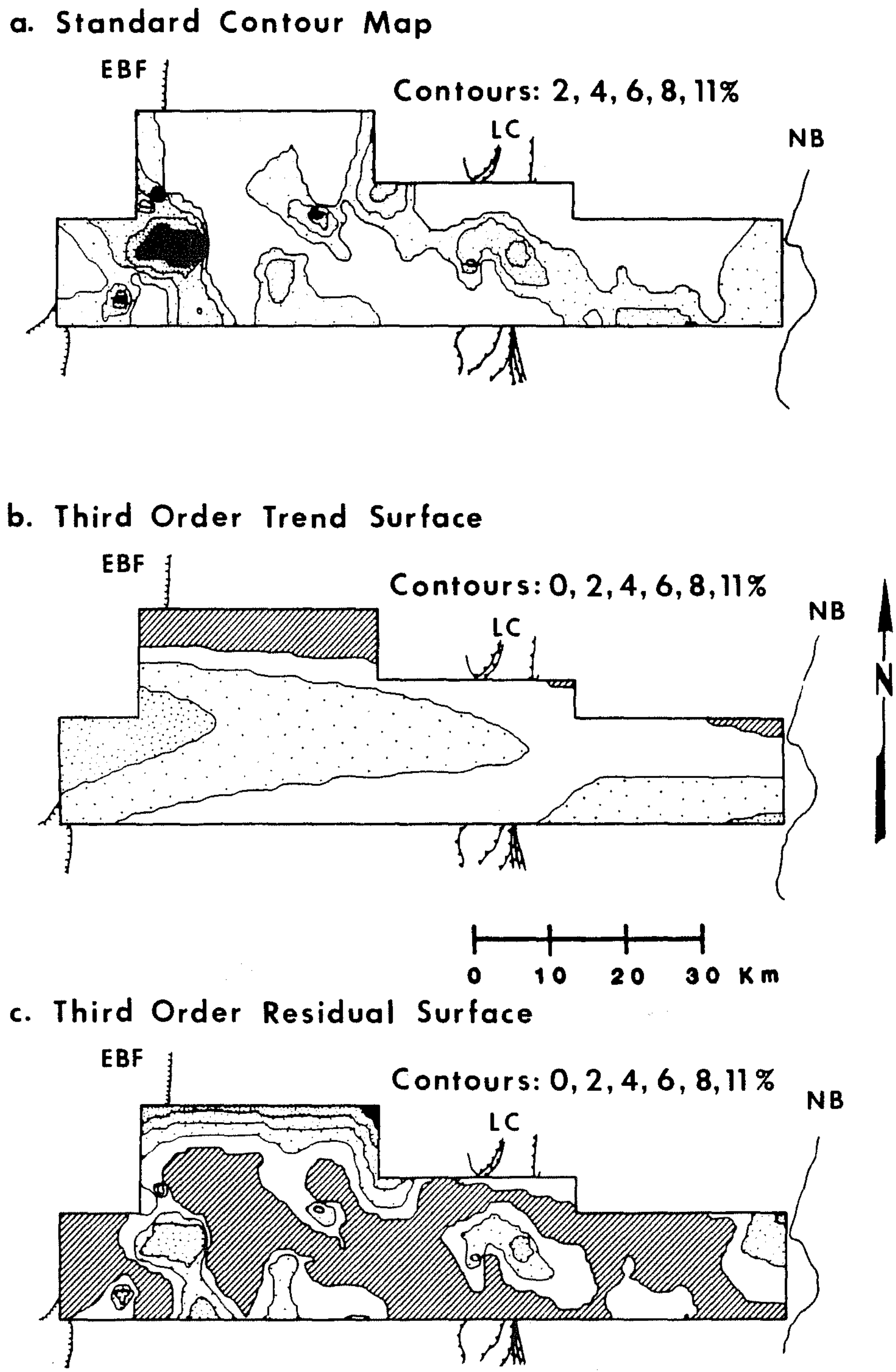

Figure 5. Distribution of NNE-trending quartz veins within the study area. See text for full discussion. EBF= Eastern Border Fault; LC=Lake Char Fault Zone; NB=Narragansett Basin.

explanation). The third order trend surface (Figure 5B) for these data shows a regional trend toward higher frequency in the western section of the study area. The zones of apparent high quartz vein frequency on the north and south boundaries of Figures 5B and 5C reflect edge effects associated with the station distribution. Residual values (Figure 5C), produced by subtraction of the regional trend surface from the standard contour map (Dougenik and Sheehan, 1979), show data concentrations related to random error and local effects of possible geological significance (Whitten, 1981). The frequency maxima near the EBF, the Willimantic Dome and the LCFZ are not part of the regional trend and may be local effects of those structures.

Complex Veins

Numerous veins (n=225) of widely varying mineralogic character (Table 1) were observed throughout the area. Structural data for these veins (Figure 3D) are similar to elements of the dike and quartz vein fabrics and suggest that a limited number of anisotropies were repeatedly reactivated during emplacement of several types of dikes and veins.

Table 1. Complex Vein Mineralogy*

Vein Mineralogy	All (%)	ENE (%)	NNE-NE (%)	NW (%)
		Vein Orientation		
Sulfide Bearing	30(13.3)	1 (9.1)	15(18.3)	3(10.0)
Silicified	2 (0.9)			
Mica Bearing	53(23.6)	1 (9.1)	18(22.0)	7(23.3)
Chlorite Bearing	24(10.7)	4(36.4)	12(14.6)	1 (3.3)
Epidote Bearing	35(15.6)	5(45.5)	14(17.1)	6(20.0)
Feldspar Bearing	37(16.4)		10(12.2)	3(10.0)
Tourmaline Bearing	36(16.0)		12(14.6)	8(26.7)
Simple Carbonate	5 (2.2)			1 (3.3)
Pseudotachylite	3 (1.3)		1 (1.2)	1 (3.3)
Total n=	225	11	82	30

*More than one mineralogic category may apply for individual veins. In each case of this type, the veins were assigned to the category having the probable greater petrogenetic significance. No veins are counted twice.

ENE, NNE to NE, and NW trends dominate the fabric of the complex veins. The strong NNE to NE trend is notably similar to the fabric displayed by quartz veins (Figure 3C). ENE-oriented elements in these data are similar to the fabric of aplite dikes (Figure 3A). A WNW- to NW-oriented fabric is found in the data for both pegmatite dikes (Figure 3B) and complex veins in the area.

Similarities in orientation and mutual cross-cutting relationships suggest that some complex veins are coeval with some of the ductile faults, aplite and pegmatite dikes, and quartz veins. The mineralogic character of the complex veins, however, indicates that their temperatures of emplacement spanned much of the cooling history of the area. Mineral assemblages of these veins range from mica bearing varieties of probable high temperature origin to chlorite bearing varieties indicative of low temperature or retrograde conditions. Cross-cutting relationships show that the time of emplacement of some of these veins overlaps that of brittle faulting. The similarity of many vein mineral assemblages to those of minor brittle faults (see Table 4) also supports this conclusion.

FAULT ANALYSIS

Ductile Faults

A small number (n=37) of minor mylonites or ductile shear zones are among the oldest structural features noted in this study. Poles to planes for these data (Figure 6) show that most minor ductile shear zones are gently dipping. Steeply dipping varieties are relatively rare and strike N-S.

Cross-cutting relationships indicate that movement on these features was coeval with the emplacement of various dikes and several families of veins. As ductile deformation of this type is a relatively high temperature and pressure phenomenon (Higgins, 1971) a late(?) Paleozoic age seems likely.

Brittle Faults

Minor faults are among the more useful structural elements to be considered in a study of a region's brittle deformational history. Given sufficient data, orientations of the principal components of the stress field in which faulting occurred can be calculated. The theoretical basis for derivation of stress tensors associated with brittle shear failure was provided by Anderson (1951) and Brace (1960). In addition, numerous laboratory studies (ie: Paterson, 1958) have supplied empirical support for the theory. Aydin and Reches (1982) questioned the validity of Anderson's model, noting that it applies strictly only under conditions of plane strain. The results of Aydin and Reches, however, differ from those of Anderson only in detail and do not seriously undermine the usefulness of Anderson's model as an analytical tool. The large sample size and area of this study would tend to obscure separate fault populations of low dihedral angle. For this study, stress orientations were calculated using the Anderson (1951) criteria. It is recognized that many of these minor faults may have reactivated older joints or other anisotropies and that a relation such as proposed by Byerlee (1968) might be more appropriate. The facts that the Anderson (1951) criteria are simpler to calculate than are the Byerlee (1968) criteria and produce a greater spread of data make this a suitable simplification.

Structural measurements were obtained for 680 minor brittle faults at 61% of the stations. Orientational data for all minor faults included in the study are summarized in Figure 7. Perhaps the most striking feature of these data is their relative simplicity. Most minor fault planes (Figure 7A) have steep dips and NE or WNW strikes. The moderately steep to vertical plunge of most slickenlines (Figure 7B) indicates that minor faults in the study area are primarily dip- to oblique-slip varieties. The stress environment calculated for most of these faults indicates NW-SE extension (Figure 7E). Most maximum compressive stress (sigma 1) axes for this population are steeply plunging (Figure 7C) whereas the average intermediate compressive stress (sigma 2) is subhorizontal and oriented NE-SW (Figure 7D). Minor populations of gently plunging sigma 1 axes and steeply plunging sigma 3 axes demonstrate that reverse motion occurred on some of the faults.

Steeply dipping to vertical faults are common in the minor fault fabric of the area (Figure 7A). The high frequency of vertical planes in the data suggests that older anisotropies were "parasitized" or reactivated during minor faulting episodes. The stress data for minor faults are well attuned to the modern vertical. This distribution of principal stress axes suggests that no appreciable tilting of the study area occurred during or after brittle faulting and, therefore, that the minor brittle faults are relatively recent (post-Acadian to Mesozoic) phenomena.

Areal Variation of Minor Fault Frequency

A primary goal of this study was to determine if the areal distribution of fracture elements bore any relationship to the major tectonic features within the area. Station frequencies of minor faults were calculated as the percentage of faults out of all data collected at each station and computer contoured on a map of the study area

(Figure 8A).

Minor faults are particularly numerous in an elongate area within and around the Lake Char Fault Zone (LCFZ). The LCFZ may have acted as a zone of weakness in the area, thereby localizing minor faulting activity. Bradley (1982), Dixon and Lundgren (1968) and other authors have suggested late Paleozoic motion on the LCFZ. If the LCFZ were a focus of late movement between North America and the Boston Platform, late Paleozoic brittle faulting activity may have been concentrated along it. Minor fault frequency values increase near the Narragansett Basin, possibly indicating that some of these brittle faults are related to the Basin's formation and so may be of late Paleozoic age. Brittle faults are also numerous in the area of the EBF. These features may be related to the movement history of that major structure.

The third order trend surface map of the data (Figure 8B) is, in some respects, similar to the contoured surface. In particular, both maps show a frequency increase in zones adjacent to the EBF and the Narragansett Basin. It is clear, however, that the third order trend surface does not describe the minor fault frequency peak associated with the LCFZ. The residual surface map (Figure 8C) suggests that the maximum in minor fault frequency within and near the LCFZ is, in fact, a local effect of that structure.

Minor Fault Subpopulations

An early attempt to analyze minor faults by orientation (Appendix II) proved to be ineffective. Classification of faults by orientation alone does not provide effective separation of families related to distinct stress fields. To address this problem, faults were categorized by dip and movement sense. Fault categories and their characteristics are summarized in Table 2. The classification scheme used in this study is identical to that employed by Wise (1981) and permits direct comparison of that data base with the data of this study.

Dip-slip varieties are dominant in the data and dip-slip normal faults are the single most common type in the study area (Table 3). Taken together, oblique- and strike-slip varieties account for roughly one third of the faults and movement on these surfaces is nearly equally divided between right- and left-lateral rotations. When compared with poles to planes for these data (Figure 7A), vertical faults seem to account for a surprisingly low proportion (15%) of the sample. This figure results from the classification scheme used (Table 3) where many steeply dipping faults are included in oblique-slip, strike-slip and unclassifiable categories. Gently dipping faults are rare in the area, comprising less than 5% of the data.

Table 2. Fault Categories Used For This Study (After Wise, 1981)

	Fault Type	Dip of Plane	Rake of Slickenlines
Dip-Slip:			
	Normal	20-80	60-90
	Reverse	20-80	60-90
Vertical:			
	Left-Lateral Oblique-Slip	>80	30-60
	Right-Lateral Oblique-Slip	>80	30-60
	Dip-Slip	>80	60-90
Strike-Slip:			
	Right-Lateral	20-90	0-30
	Left-Lateral	20-90	0-30
Oblique-Slip:			
	Reverse Left-Lateral	20-80	30-60
	Normal Left-Lateral	20-80	30-60
	Reverse Right-Lateral	20-80	30-60
	Normal Right-Lateral	20-80	30-60
Flat:	Flat	<20	0-90

Unclassified Faults: Movement sense indeterminable.

Table 3. Fault Motion Sense (Classified Faults Only)

Fault Type	n	% of data
Normal	151	28
Reverse	93	17
Left-Lateral Oblique-Slip	53	10
Right-Lateral Oblique-Slip	63	12
Left-Lateral Strike-Slip	43	8
Right-Lateral Strike-Slip	34	6
Vertical Dip Slip	83	15
Flat	22	4
Total	542	100

Dip-slip normal faults. Normal faulting in the area occurred on NE-striking planes (possibly conjugate) and a minor set of steeply dipping ENE- to WNW-trending surfaces (Figure 9A). Slickenlines (Figure 9B) are moderately to steeply plunging and clustered on the NE-trending planes. The stress field for this family is similar to that calculated for all faults (Figure 7), reflecting the large contribution (28%) of normal faults to the data. Sigma 1 axes are vertical to subvertical and the intermediate compressive stress is subhorizontal and oriented NE-SW (Figure 9C and 9D). The least compressive stress, sigma 3, plunges gently to the NW or SE (Figure 9E).

These data are shown in map form in Figure 9F and are similar to the fabric shown by Wise (1981) to the west. The NE-striking, SE-dipping normal faults are similar to a set of early normal faults in the Narragansett Pier Granite (Hozik, 1981) to the SE of my area. Similar faults are also common at the southern end of the EBF (Piepul, 1975).

Dip-slip reverse faults. Dip-slip reverse faults (Figure 10A) are remarkably similar in orientation to minor normal faults (Figure 9A) in eastern Connecticut and western Rhode Island. Most reverse motion occurred on possibly conjugate, NE-trending families of planes with slickenlines plunging to the NW or SE (Figure 10B). The maximum compressive stress for these faults plunges gently to the NW or SE (Figure 10C) and the mean sigma 2 is subhorizontal and oriented NE-SW (Figure 10D). The least compressive stress plunges steeply about the vertical (Figure 10E).

To the the west and northwest of the study area, in the Hartford and Albany 2-degree quadrangles, Wise (1981) showed fabrics trending NE and roughly E-W in the minor reverse fault data that are similar to elements of this data base (Figure 10F). NW-trending reverse faults, however, are more common to the west and northwest than they are in eastern Connecticut and western Rhode Island. Evidence for faulting of this type is lacking in the data of Hozik (1981) for the Pennsylvanian Narragansett Pier Granite in southern Rhode Island.

Dip-slip vertical faults. Evidence for dip-slip motion on vertical planes of nearly every possible orientation (Figure 11A) was observed in the study area. The data are concentrated, however, in families trending NE and E-W with slickenlines (Figure 11B) falling about the vertical. The stress field derived for vertical dip-slip faults (Figures 11C, 11D, 11E) is, in some respects, similar to that for minor normal dip-slip faults. The maximum compressive stress is subvertical; sigma 2 axes are subhorizontal and trend NE-SW and WNW-ESE. The least compressive stress plunges gently to the NNE-SSW or NW-SE. Dissimilarities between the stress fields of the normal and vertical faults may not represent real variation but may result from the inadequacy of the Anderson (1951) model when applied to preexisting, vertical planes.

A family of vertical dip-slip faults trending N-S was shown to the west and northwest by Wise (1981) but this family is only weakly developed (Figure 11F) in eastern Connecticut and western Rhode Island. The fabric observed in this study, however, does appear to extend into the areas of this earlier study. Hozik (1981) noted a late family of E-W-trending vertical faults with dip-slip motion in the Narragansett Pier Granite that may correlate with the E-W-oriented vertical dip-slip faults of this data base.

Left-lateral oblique-slip faults. Left-lateral motion, with normal or reverse components, occurred on more irregularly oriented sets of planes than the categories of faults discussed above although some orientational similarities exist. Vertical planes trending NE and WNW and NE-trending families are common in these data (Figure 12A). Most slickenlines for these faults plunge moderately within NNE- and WNW-trending planes (Figure 12B).

The maximum and intermediate compressive stress axes for these data are broadly oriented within a NE-trending plane (Figures 12C and 12D). Sigma 3 axes are comparatively stably oriented to the NW-SE and form a pole to the sigma 1-sigma 2 plane (Figure 12E). This distribution of principal stress components suggests that sigma 1 and sigma 2 were similar in magnitude and may have easily exchanged orientations.

Azimuths of planes and slickenlines for left-lateral oblique-slip faults and orientations of left-lateral faults in general (Figures 12F, 13A, and 13B) differ in some respects from the fabric to the west and northwest shown by Wise (1981). WNW and NE trends for left-lateral faults in these areas are subordinate to a strong NW-trending fabric. Left-lateral oblique-slip motion is common on minor faults oriented NE and E-W in the Narragansett Pier Granite to the SE (Hozik, 1981).

Right-lateral oblique-slip faults. Orientational maxima for right-lateral oblique-slip faults are, in general, similar to those for left-lateral varieties. Vertical WNW trends and vertical to moderately dipping NNE-NE trends are common for this family of faults (Figure 14A). Many slickenlines of right-lateral oblique-slip faults plunge to the SSE, SSW, E or W (Figure 14B). Stress orientations derived for these faults (Figures 14C, 14D, and 14E) are complex, with maximum and intermediate stress axes plunging in a variety of orientations. Sigma 3 for these faults plunges gently to the SE, SSW, NNW or SSE.

Azimuthal data for right-lateral oblique-slip faults and all faults with dextral offset in this area (Figures

14F, 15A, and 15B) are generally similar to the data shown by Wise (1981) for the Hartford sheet to the west where N-S trends also are common. NE-trending right-lateral oblique-slip faults were documented by Hozik (1981) in the western section of the Narragansett Pier Granite.

Strike-slip faults. Most minor strike-slip faults in the area trend to the NE (Figure 16A) and are subparallel to the structural grain of the Merrimack Synclinorium. Slickenlines for these faults (Figure 16B) trend NE-SW. Right- and left-lateral offset (Table 3) occurred in approximately equal proportions on these minor strike-slip faults. NE-trending, left-lateral faults are driven by horizontal, N-S-directed compression (Figure 16C). The least compressive stress for this family of structures (Figure 16E) is oriented E-W and horizontal. Right-lateral motions are associated with horizontal, E-W and NE-SW orientations of the maximum compressive stress and subhorizontal N-S- and NW-SE-trending least compressive stresses. As expected for steeply dipping strike-slip faults (Anderson, 1951), rotation axes are oriented about a vertical axis (Figure 16D).

Azimuths of planes and slickenlines for both right- and left-lateral strike-slip faults are shown in Figure 17. Strike-slip faults are more variable in azimuth to the west and northwest in the Hartford and Albany 2-degree sheets

(Wise, 1981). NNE- to NE-oriented strike-slip faults are common in the western section of the Narragansett Pier Granite to the southwest (Hozik, 1981).

Unclassified faults. A number of faults in this data base were unclassifiable by movement sense. These minor brittle faults are similarly oriented (Figure 19A) to the overall fault population (Figure 7A) and probably have similar movement histories. Steeply to moderately plunging slickenlines (Figure 19B) and horizontal to gently plunging rotation axes (Figure 19C) indicate that most of the motion was oblique- or dip-slip in nature.

Fault Plane Mineralogy

At the level of this study, the various categories of minor faults could not be distinguished reliably on the basis of their mineralogic character (Figure 18). A simplified mineralogic classification system is cross-tabulated with fault type for mineralized faults in Table 4.

Table 4A. Fault Plane Mineralogy: Raw Data**

Mineral Assemblage	Fault Type* N	R	LL	RL	SS	V	F	Total
Quartz	13	14	6	3	6	13	2	57
Sulfides	12	5	1	2	2	4	0	26
Silicified	1	0	0	1	3	1	0	6
Fe,Mn,Weathering	32	14	15	19	24	17	3	124
Mica Bearing	17	4	2	5	5	2	0	35
Chlorite Bearing	12	8	5	0	5	5	2	37
Epidote Bearing	17	16	6	9	5	13	2	68
Feldspathic	6	2	2	2	7	5	2	26
Carbonate	5	2	1	0	0	0	1	9
Pseudotachylite	0	0	1	0	1	3	0	5
Total	115	65	39	41	58	63	12	393

Table 4B. Fault Plane Mineralogy: Percentage Values

Mineral Assemblage	Fault Type* N	R	LL	RL	SS	V	F
Fe,Mn,Weathering	27.8	21.5	38.5	46.3	41.4	27.0	25.0
Quartz	11.3	21.5	15.4	7.3	10.3	20.6	16.7
Sulfides	10.4	7.7	2.6	4.9	3.4	6.3	0.0
Silicified	0.9	0.0	0.0	2.4	5.2	1.6	0.0
Mica Bearing	14.8	6.2	5.1	12.2	8.6	3.2	0.0
Chlorite Bearing	10.4	12.3	12.8	0.0	8.6	7.9	16.7
Epidote Bearing	14.8	24.6	15.4	22.0	8.6	20.6	16.7
Feldspathic	5.2	3.1	5.1	4.9	12.1	7.9	16.7
Carbonate	4.3	3.1	2.6	0.0	0.0	0.0	8.3
Pseudotachylite	0.0	0.0	2.6	0.0	1.7	4.8	0.0

*N=Dip-Slip Normal; R=Dip-Slip Reverse; LL=Left-Lateral Oblique-Slip; RL=Right-Lateral Oblique-Slip; SS=Strike-Slip; V=Vertical Dip-Slip; F=Flat.

**More than one mineralogic category may apply for individual faults. In each case of this type, the faults were assigned to the category having the probable greater petrogenetic significance. No faults are counted twice.

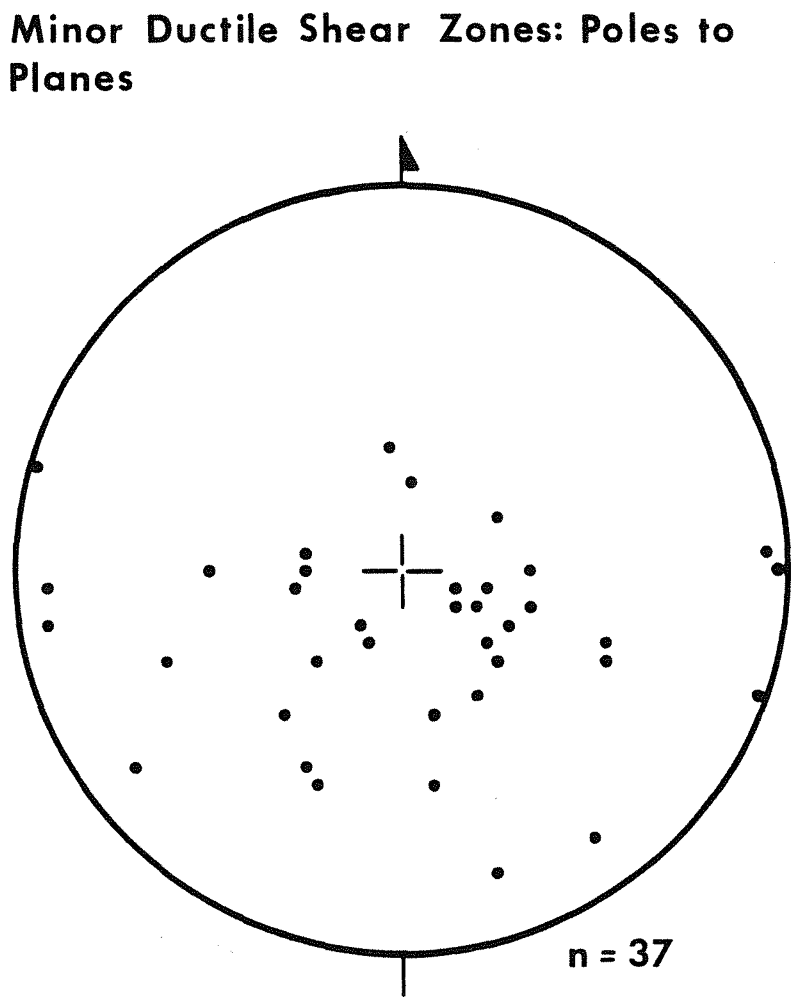

Figure 6. Equal area net plot of poles to planes for minor ductile shear zones within the study area.

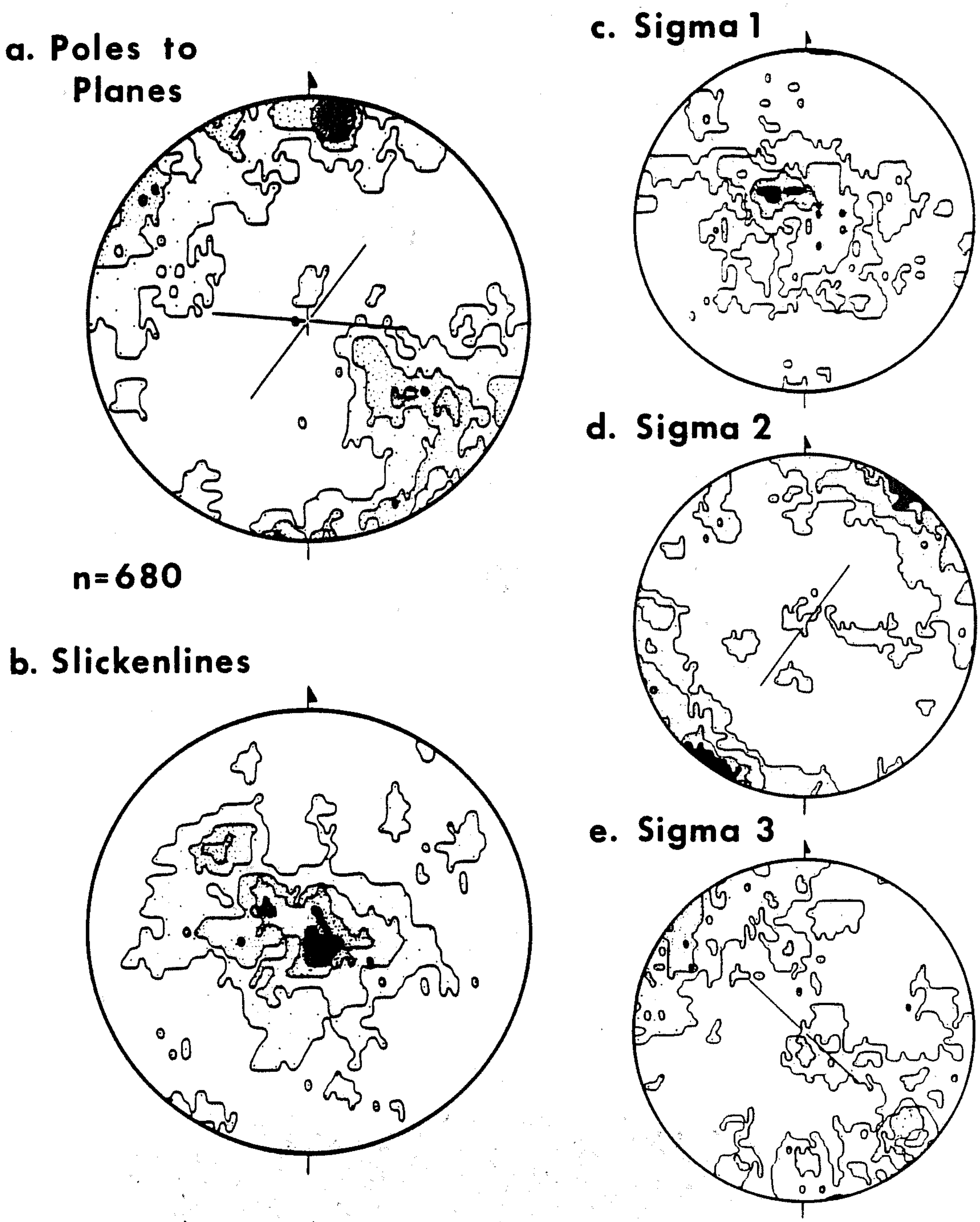

Figure 7. Equal area net plots of structural data and principal stress orientations for minor brittle faults within the study area. Contours are 1, 2, 3, 4% per 1% area.

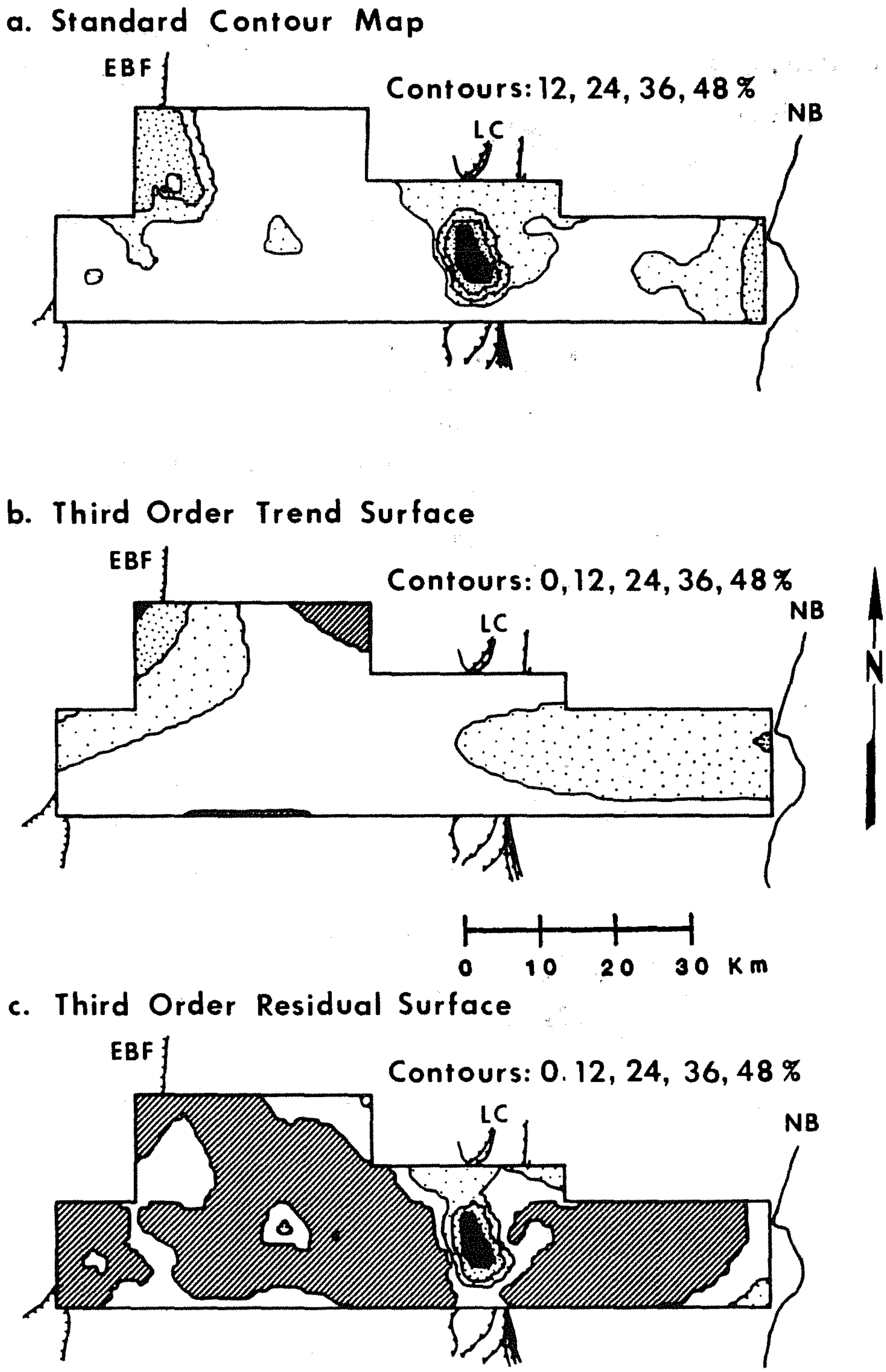

Figure 8. Distribution of minor brittle faults within the study area. See text for full discussion. EBF=Eastern Border Fault; LC=Lake Char Fault Zone; NB=Narragansett Basin.

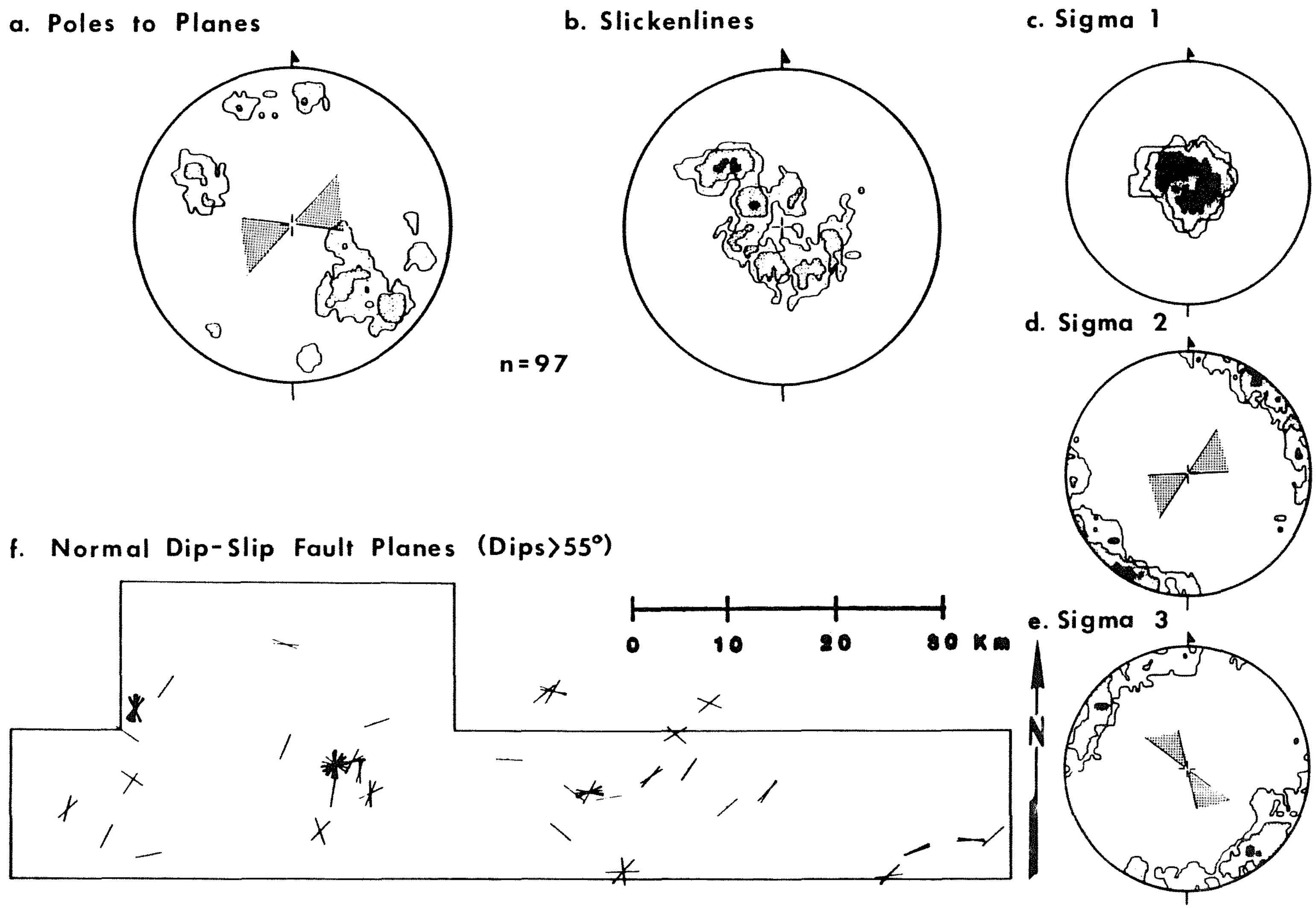

Figure 9. Structural data for normal dip-slip faults. Equal area net contours are 2, 4, 8% per 1% area.

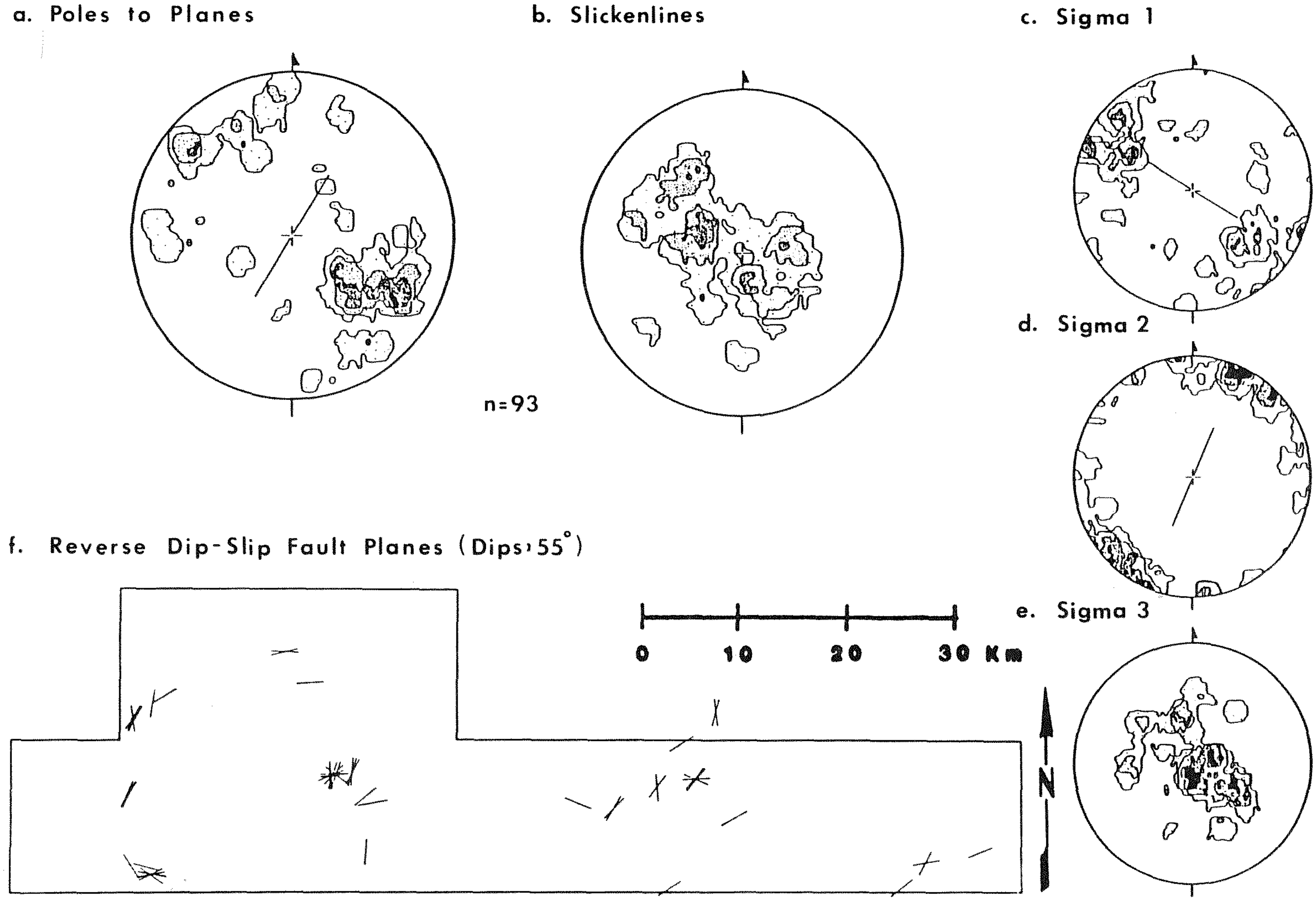

Figure 10. Structural data for reverse dip-slip faults. Equal area net contours are 2, 4, 6, 8% per 1% area.

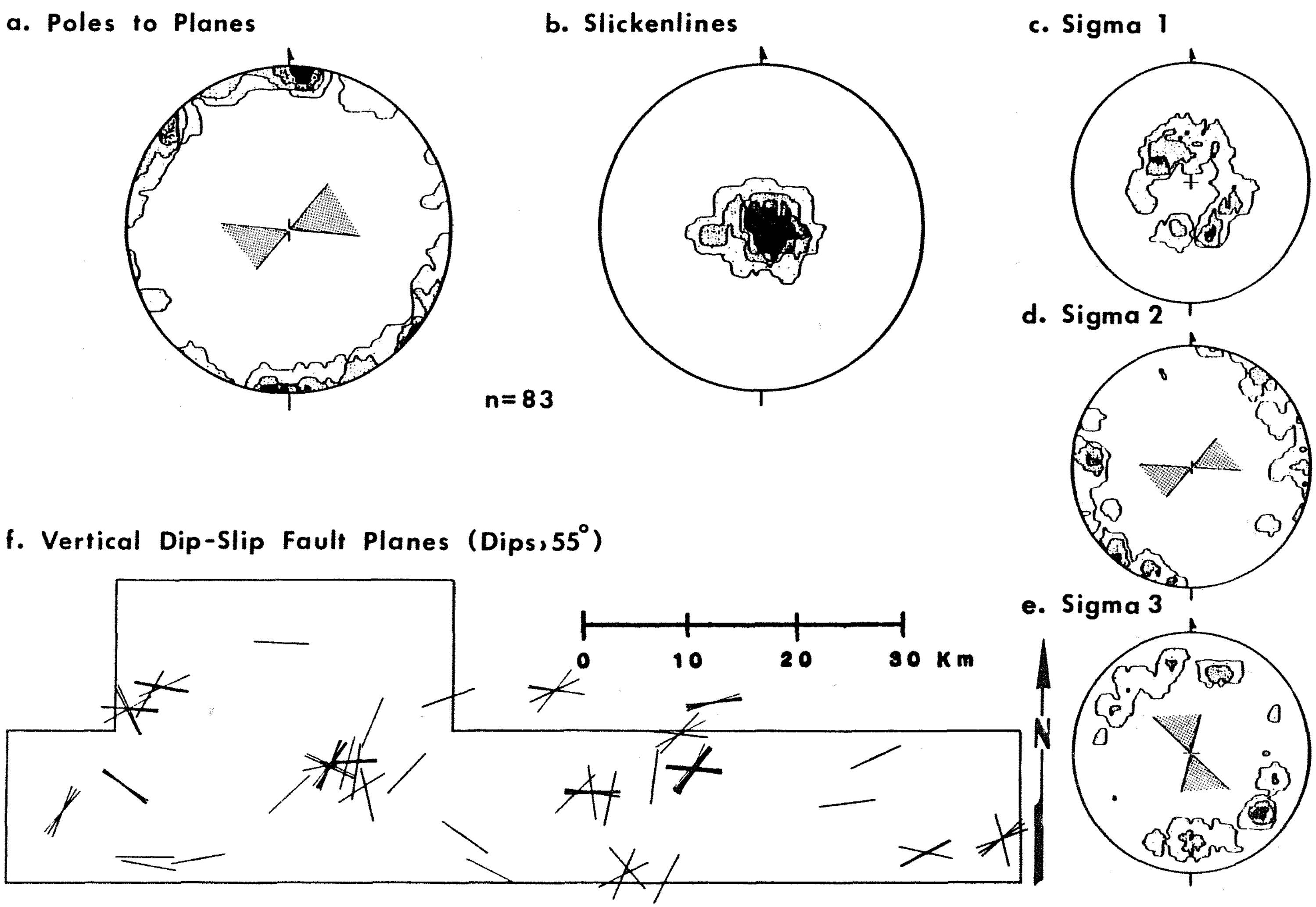

Figure 11. Structural data for vertical dip-slip faults. Equal area net contours are 2, 6, 10, 14% per 1% area.

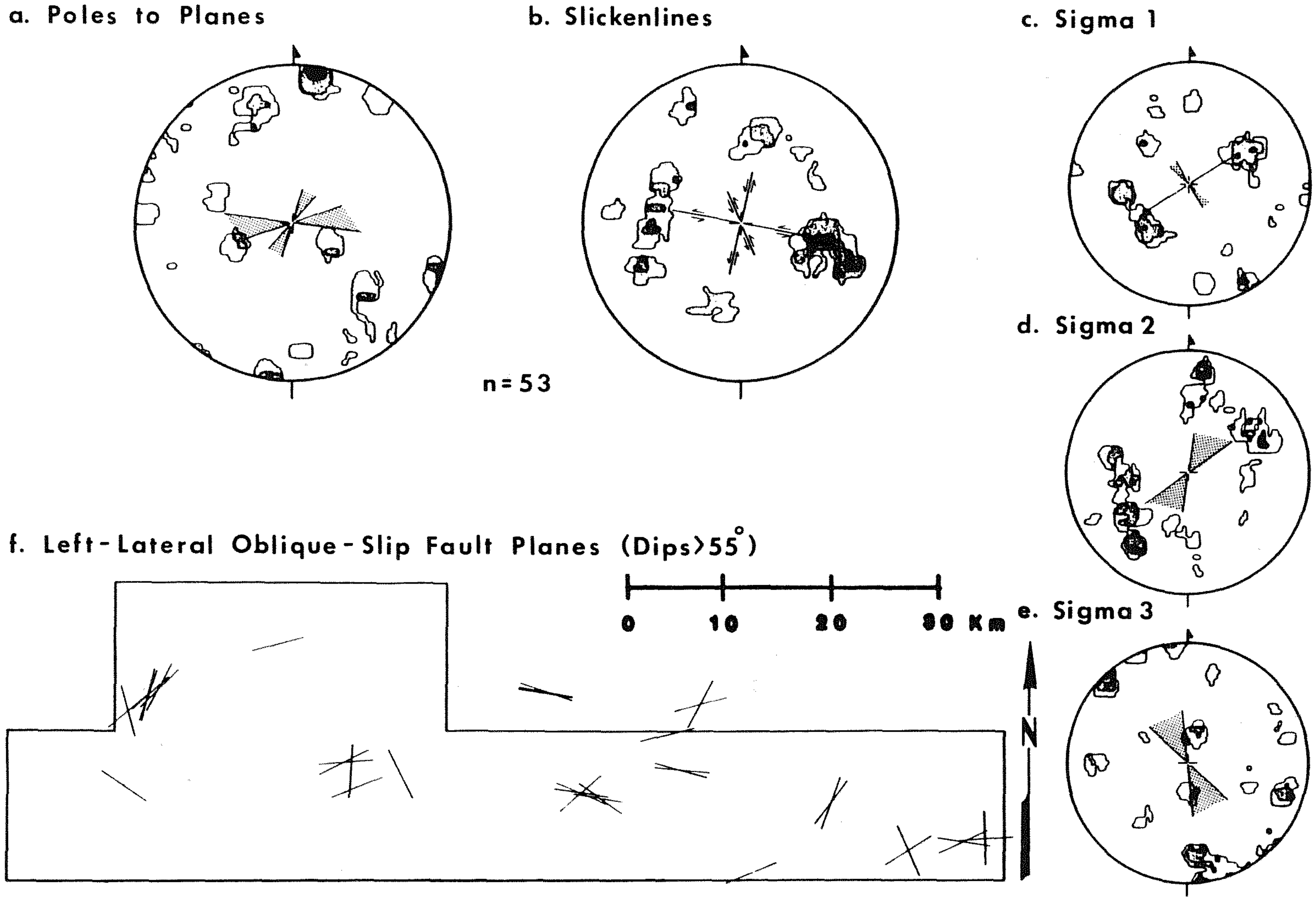

Figure 12. Structural data for left-lateral oblique-slip faults. Equal area net contours are 3, 5, 9% per 1% area.

a. Left-Lateral Strike-Slip Slickenlines

b. Left-Lateral Strike- plus Oblique-Slip Faults

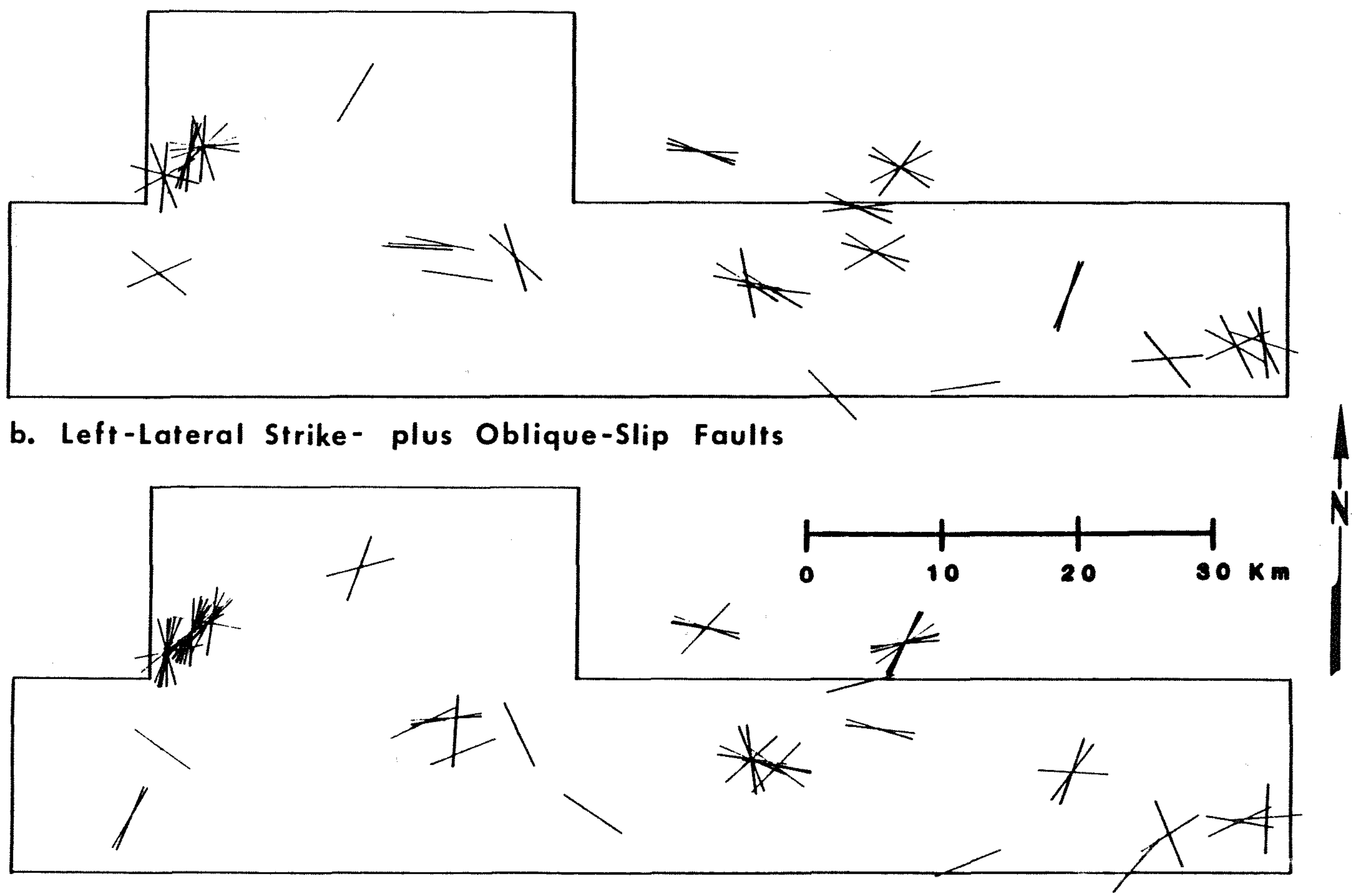

Figure 13. Slickenline azimuths for left-lateral oblique-slip faults and azimuths of planes (dips > 55°) for all faults with left-lateral components of motion.

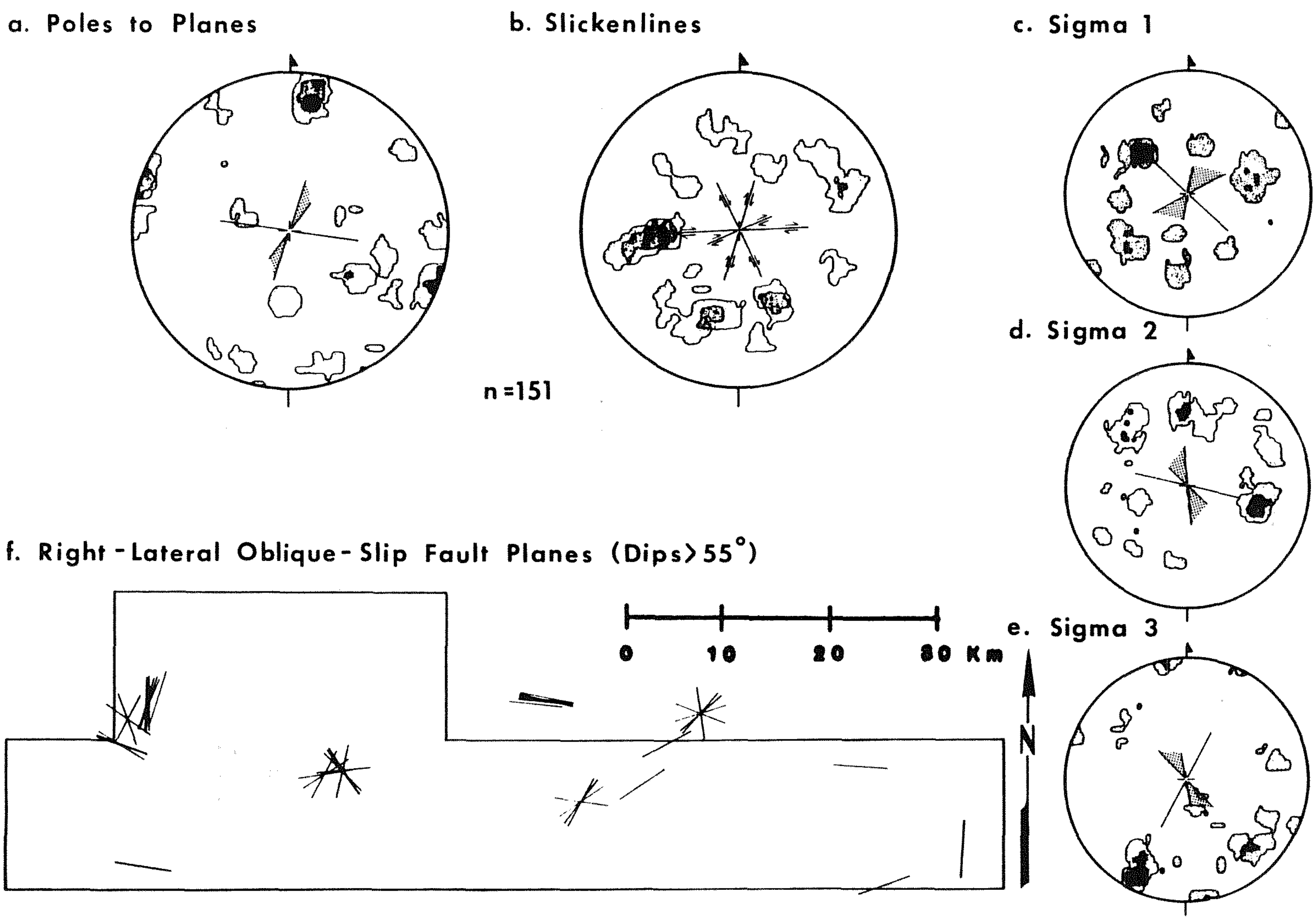

Figure 14. Structural data for right-lateral oblique-slip faults. Equal area net contours are 3, 6, 9% per 1% area.

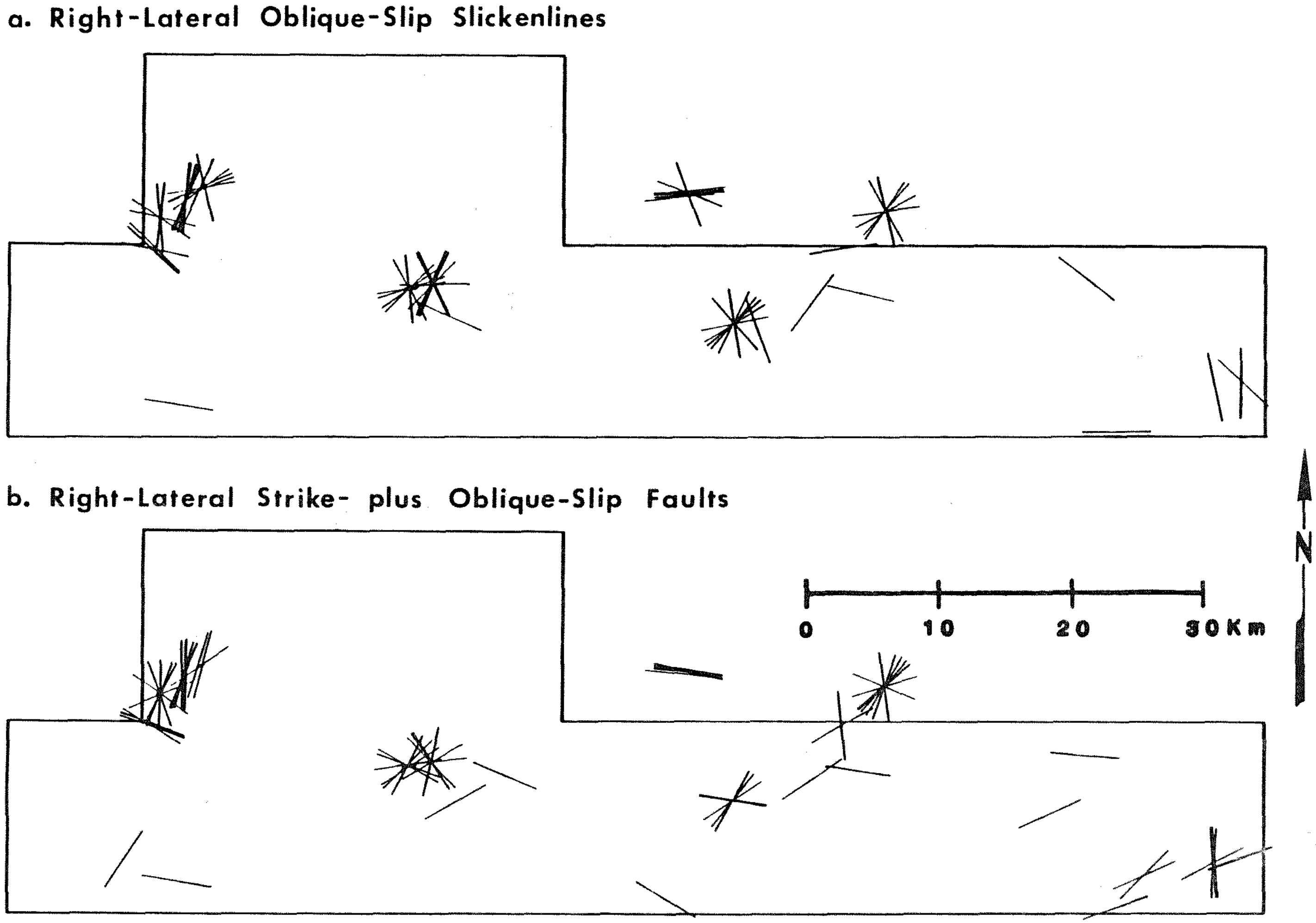

Figure 15. Slickenline azimuths for right-lateral oblique-slip faults and azimuths of planes (Dips > 55°) for all faults with right-lateral components of motion.

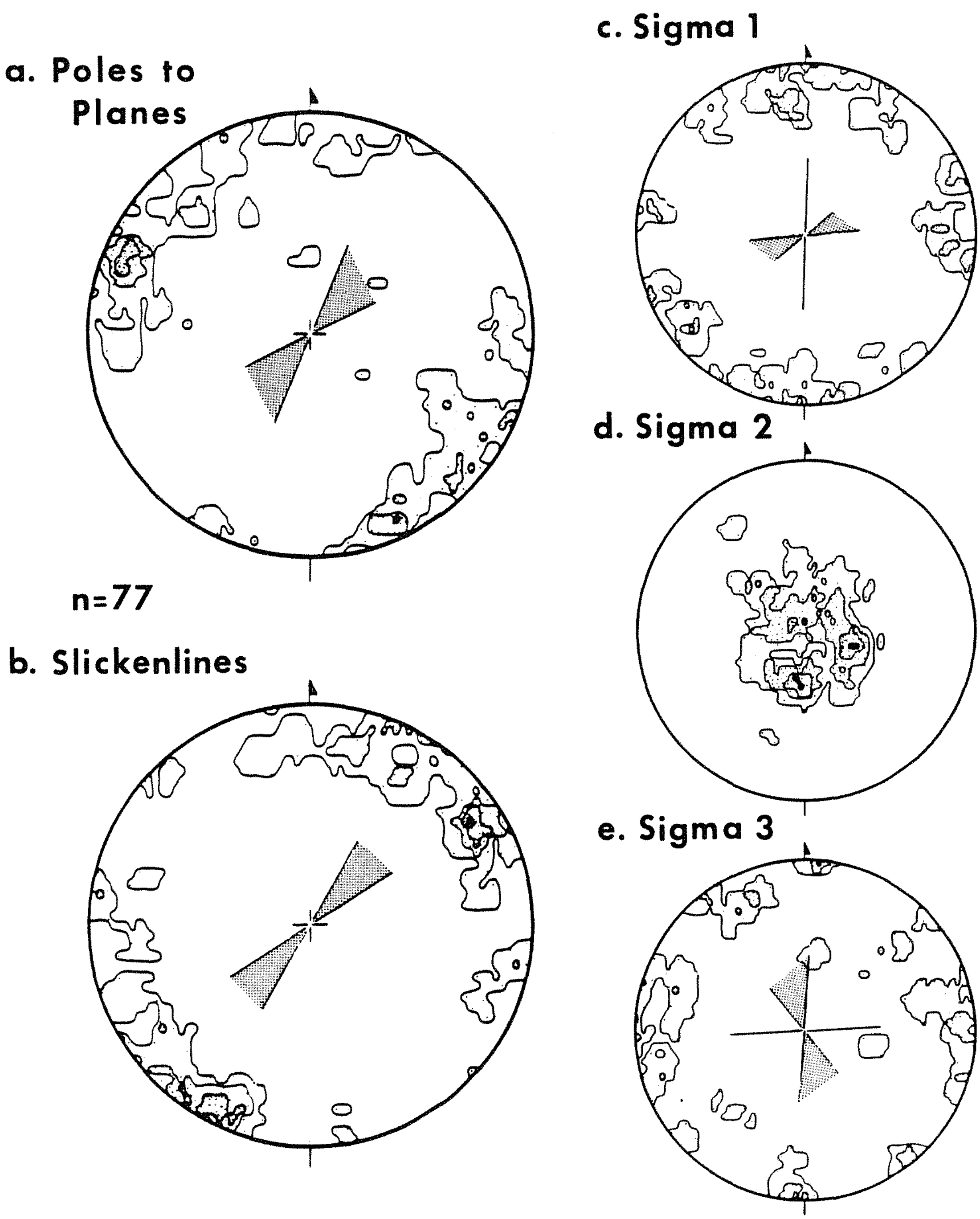

Figure 16. Structural data for strike-slip faults. Equal area net contours are 2, 5, 7, 10% per 1% area.

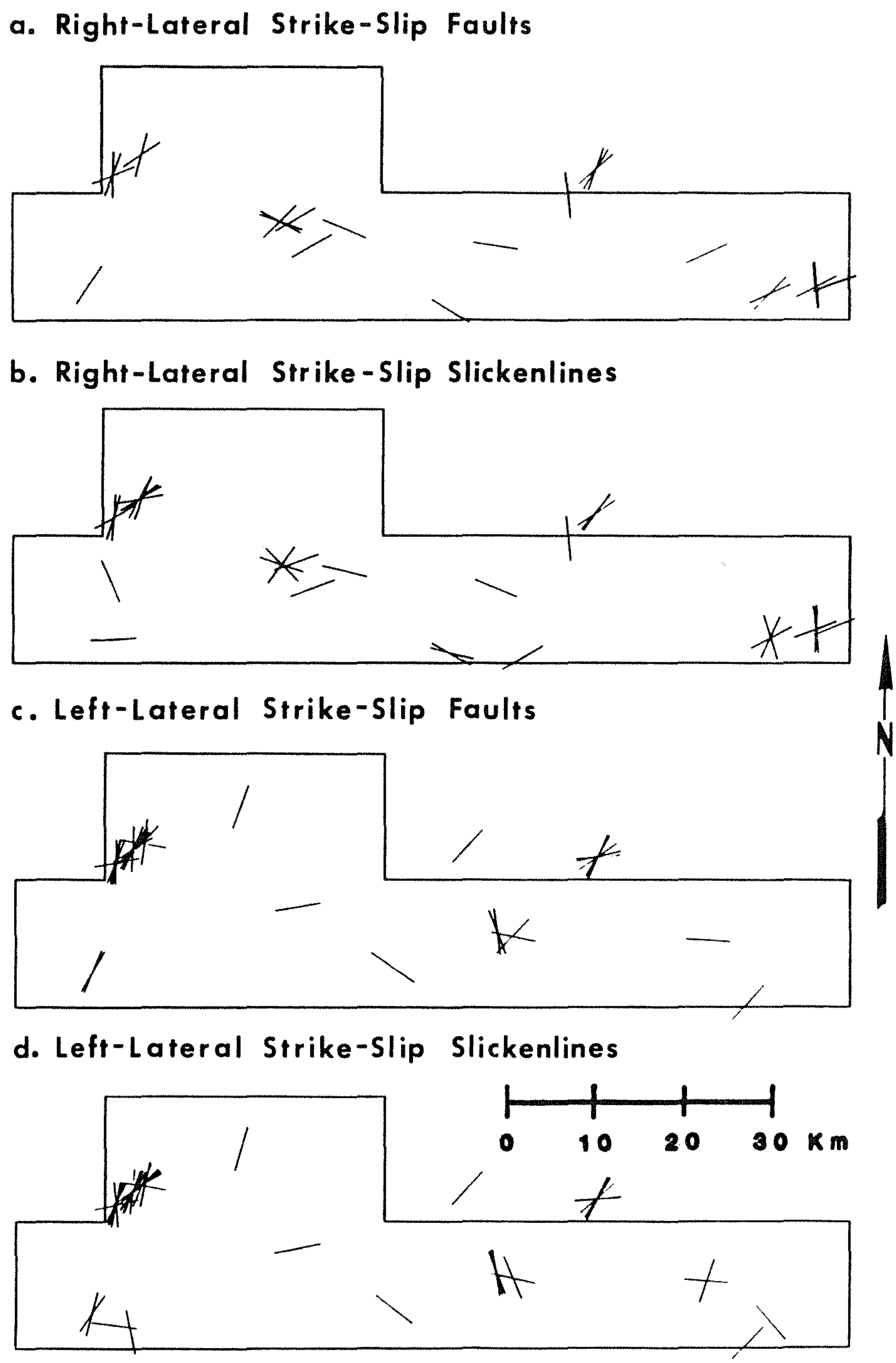

Figure 17. Azimuthal data for strike-slip faults. Fault planes have dips > 55°.

Figure 18. Fault type versus mineralogy. Vertical scales show the percentage of each category characterized by a given mineralogic assemblage. F,M,W=Fe staining, Mn staining, weathering; Q= quartz bearing; S=sulfide bearing; SI=silicified; M=mica bearing; C=chlorite bearing; E=epidote bearing; F=feldspathic; C'=simple carbonate; P=pseudotachylyte bearing.

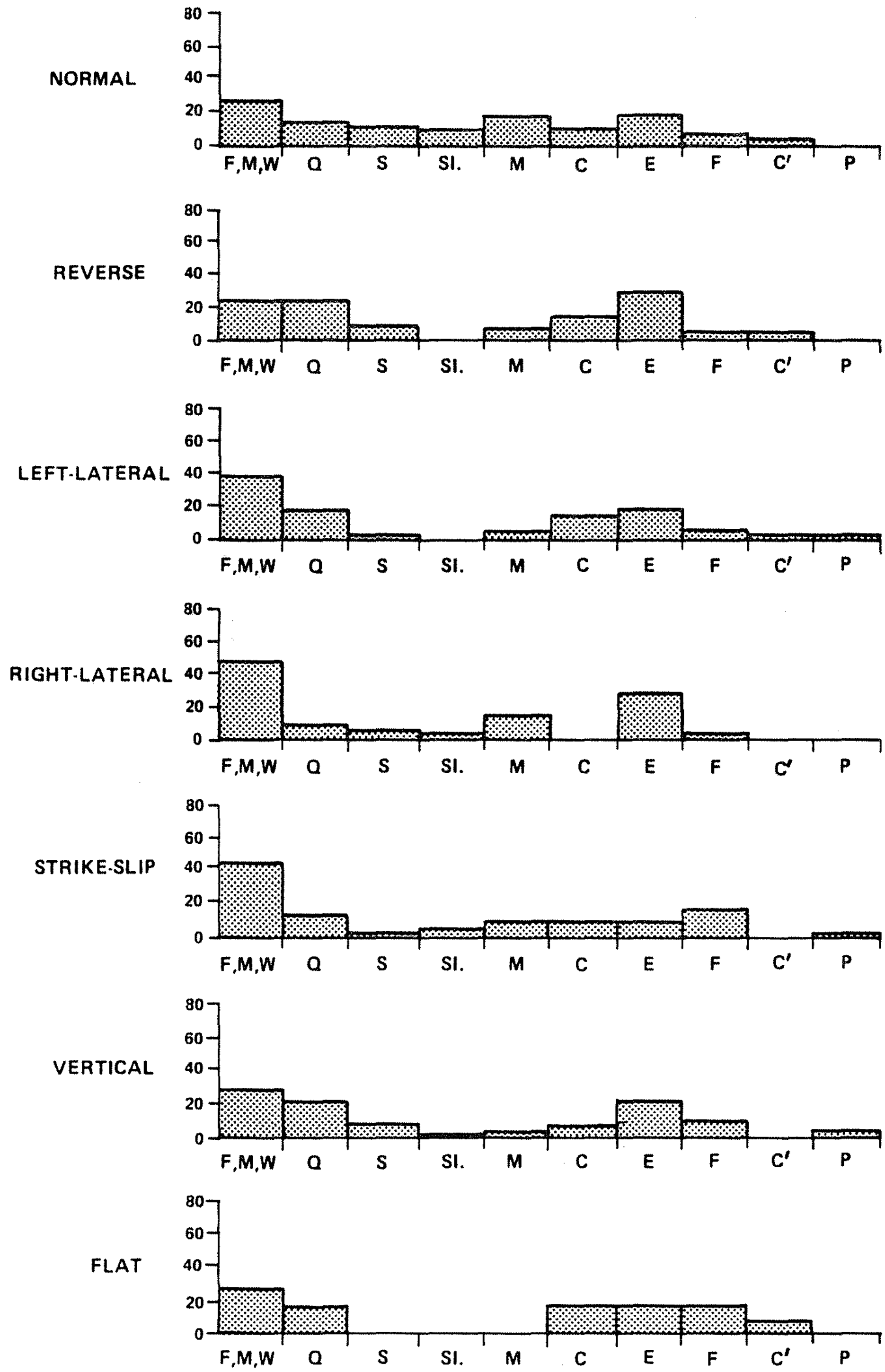
NORMAL
REVERSE
LEFT-LATERAL
RIGHT-LATERAL
STRIKE-SLIP
VERTICAL
FLAT
80
60
40
20
0
F,M,W
Q
S
Sl.
M
C
E
F
C′
P

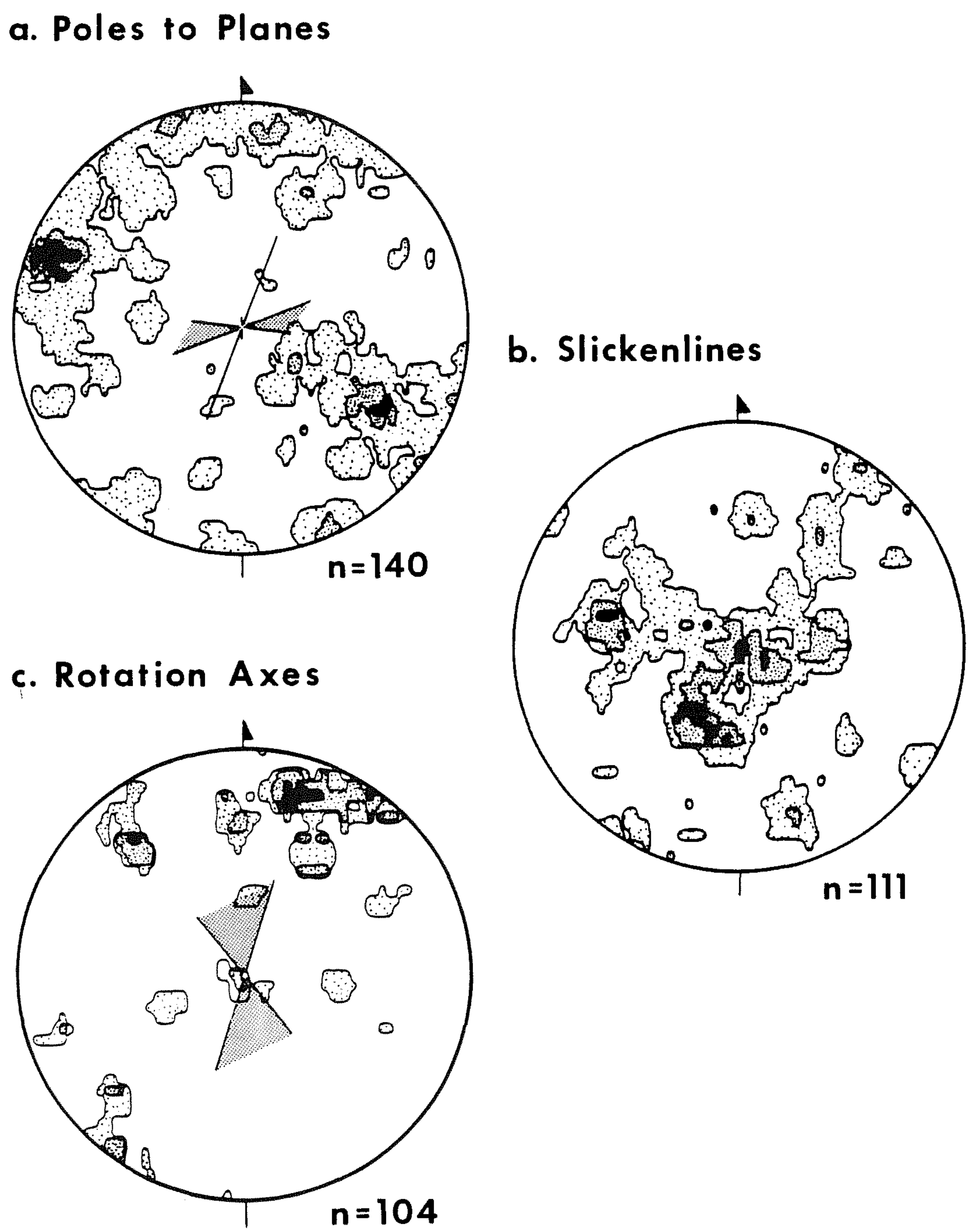

Figure 19. Structural data for unclassified faults. Equal area net contours are 1, 3, 5% per 1% area.

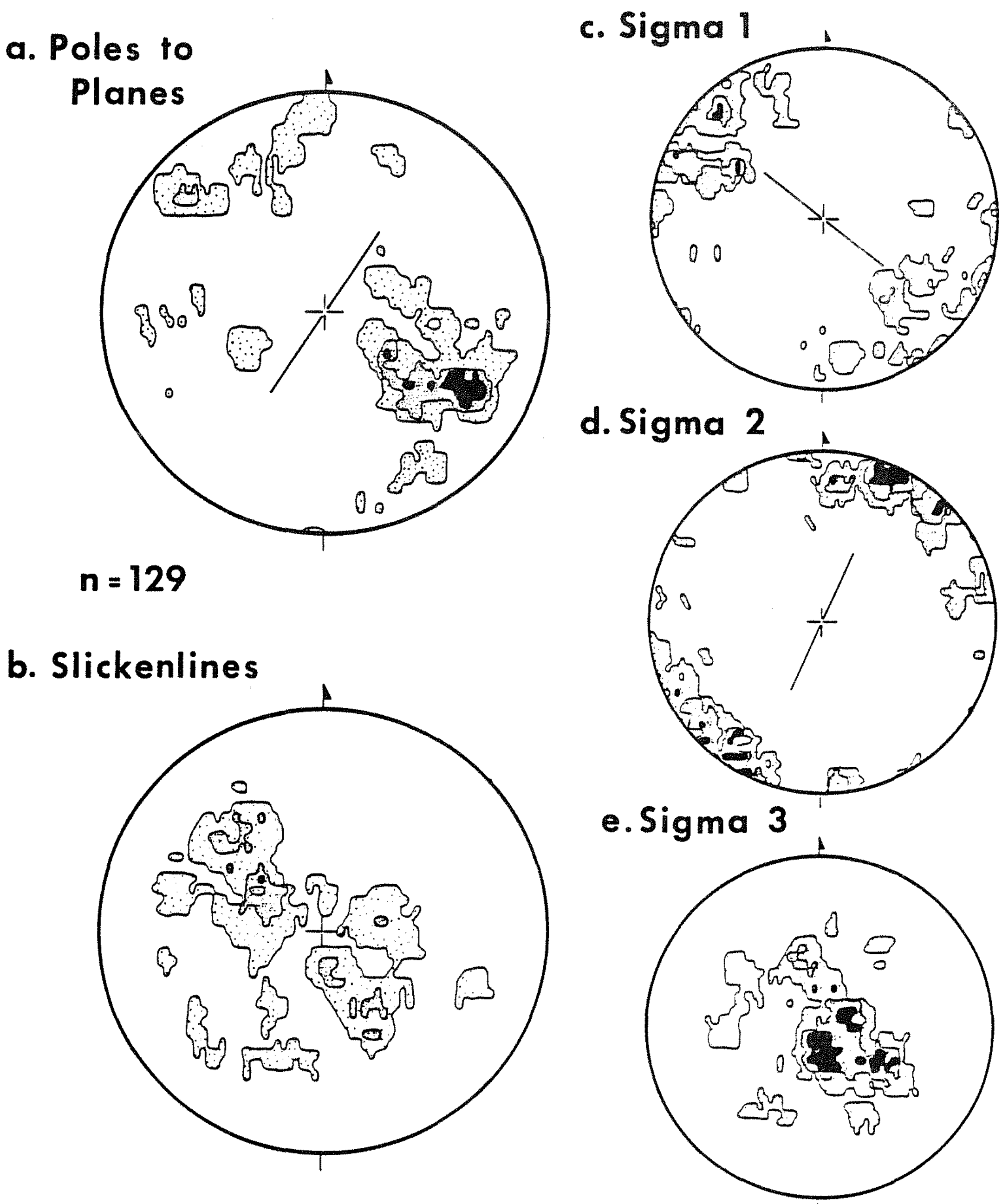

Figure 20. Structural data for faults with compressional components of motion. Equal area net contours are 2, 4, 6% per 1% area.

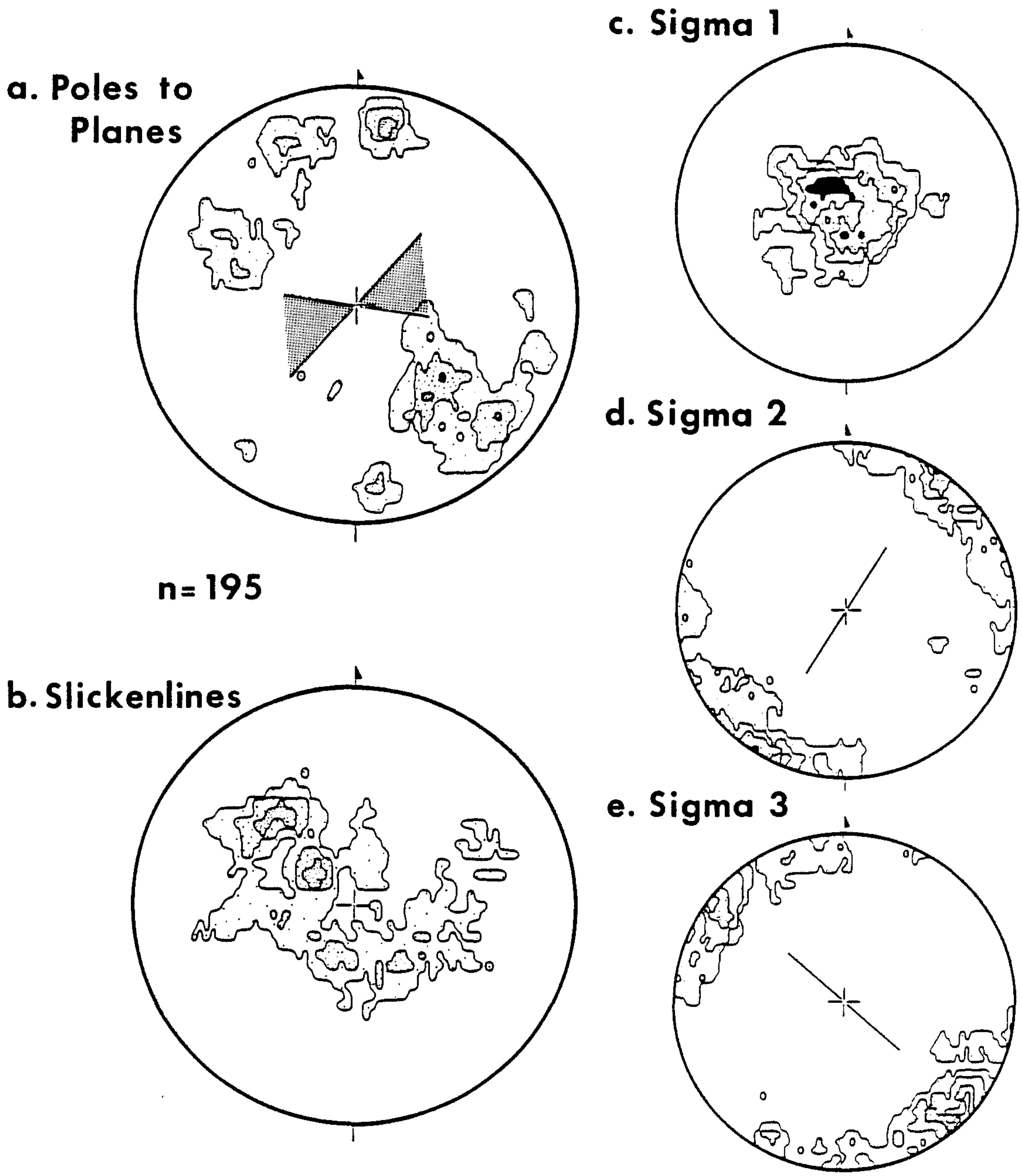

Figure 21. Structural data for faults with extensile components of motion. Equal area net contours are 2, 4, 6, 8% per 1% area.

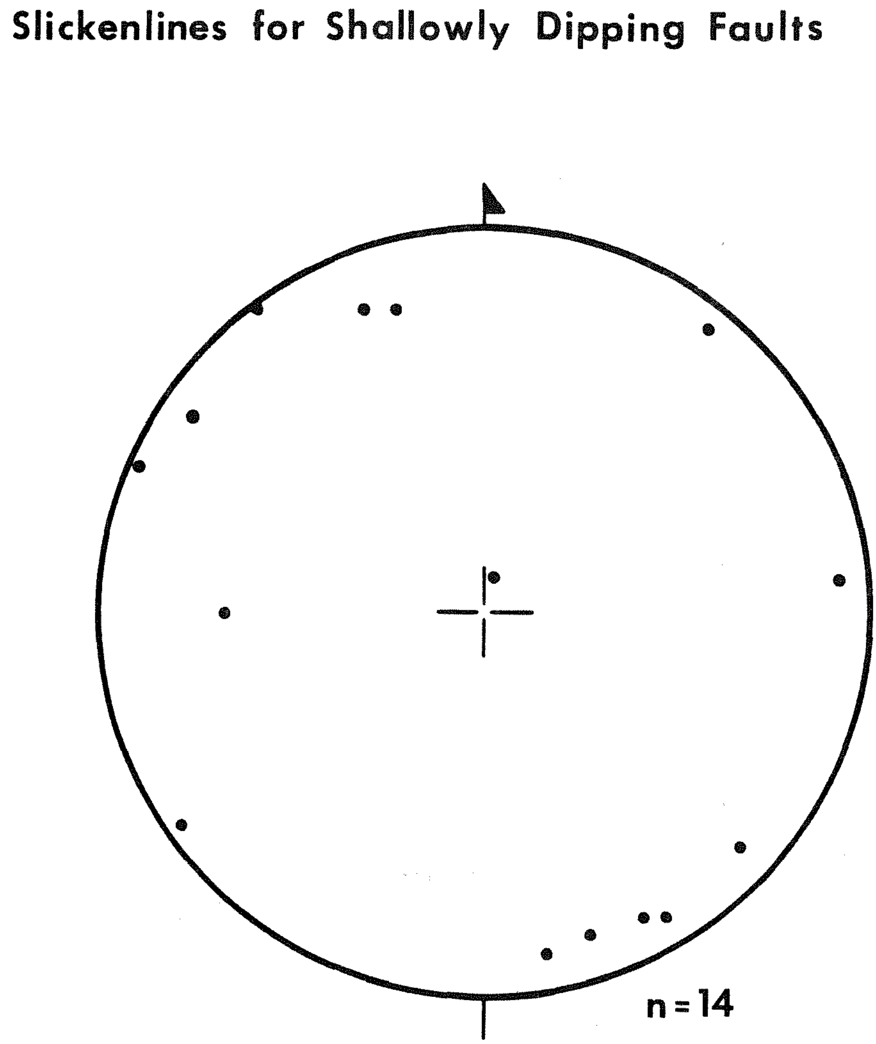

Figure 22. Equal area net plot of slickenlines for gently dipping faults.

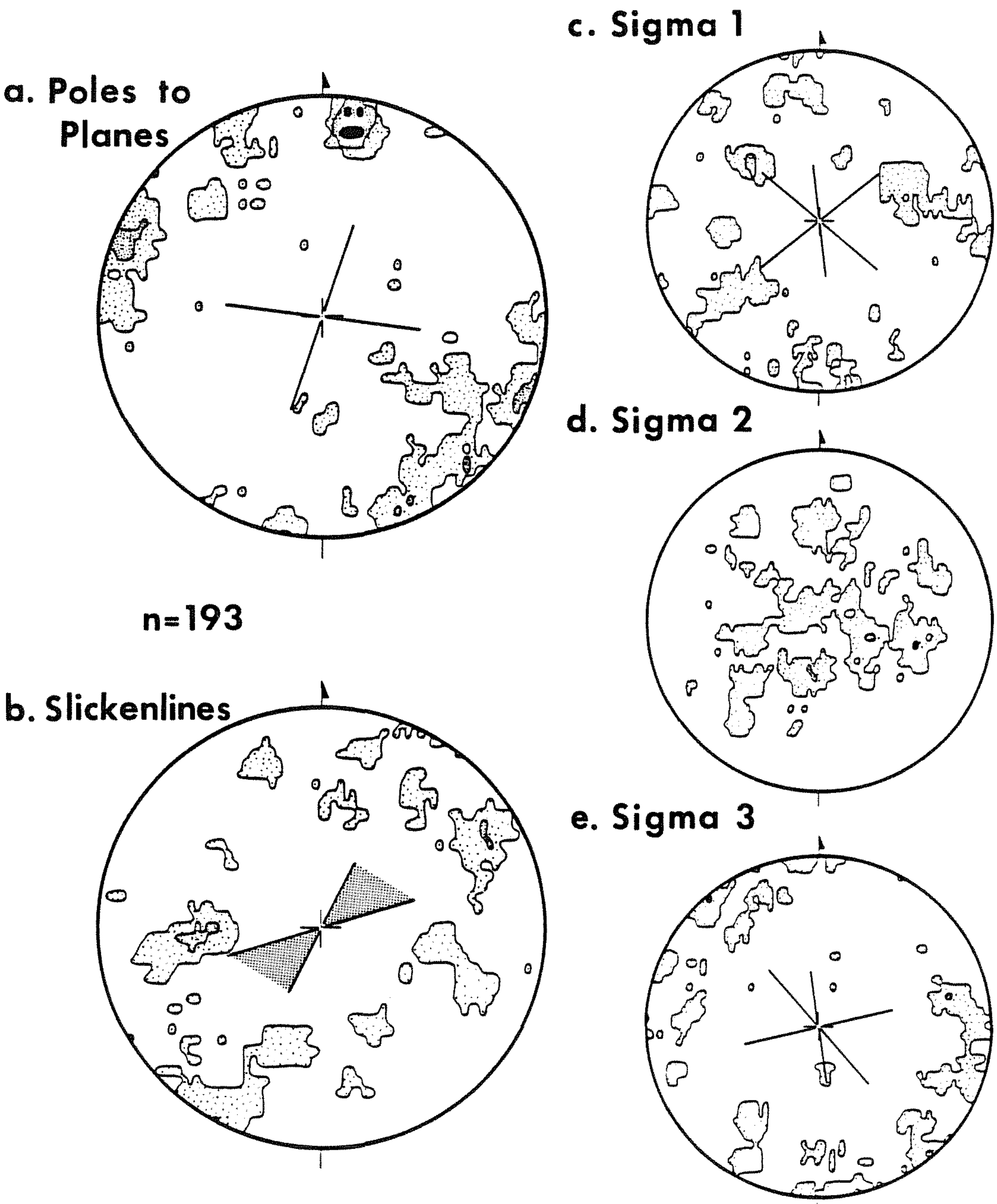

Figure 23. Structural data for faults with lateral components of motion. Equal area net contours are 2, 4, 6% per 1% area.

PATTERNS OF MINOR SLICKENSIDE MOTIONS

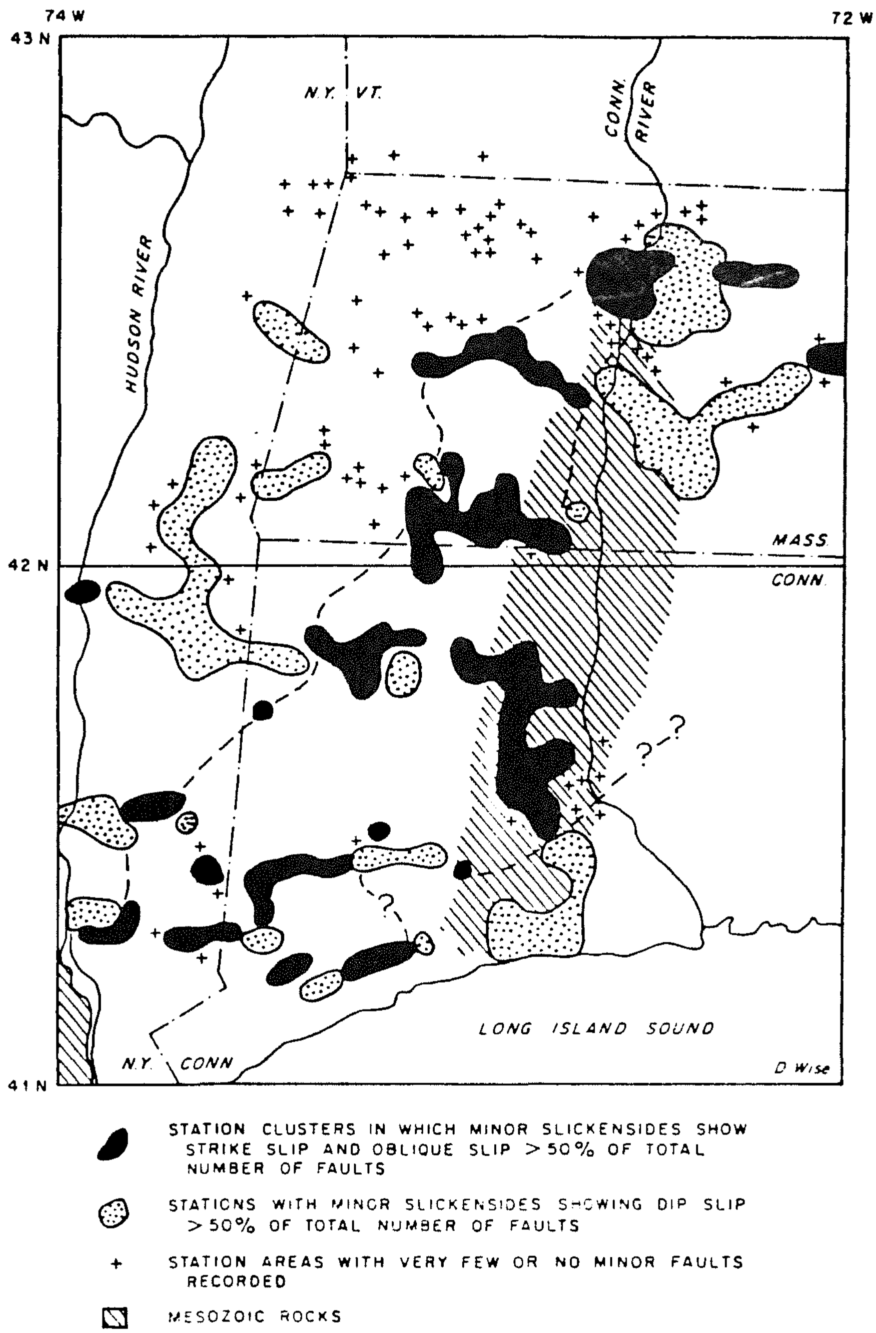

Figure 24. Zone of dominance of strike- plus oblique-slip motions on minor fault planes to the west of the study area (from Wise, 1981).

Figure 25. Distribution of families of minor faults within the study area. See text for full discussion. EBF= Eastern Border Fault; LC=Lake Char Fault Zone; NB=Narragansett Basin.

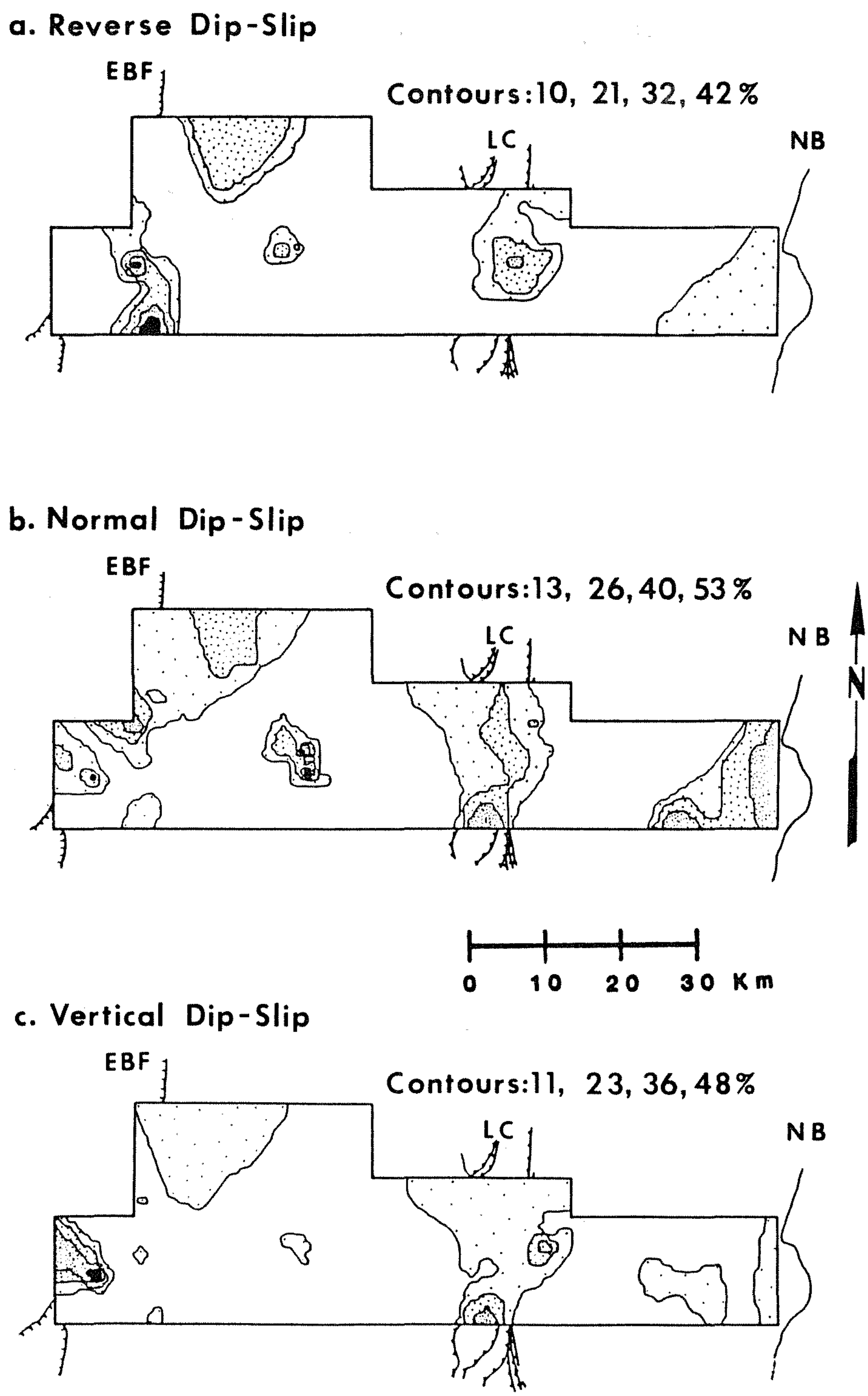
a. Reverse Dip-Slip
EBF
Contours:10, 21, 32, 42%
LC
NB
b. Normal Dip-Slip
EBF
Contours:13, 26,40, 53%
LC
NB
N
0 10 20 30 Km
c. Vertical Dip-Slip
EBF
Contours:11, 23, 36, 48%
LC
NB

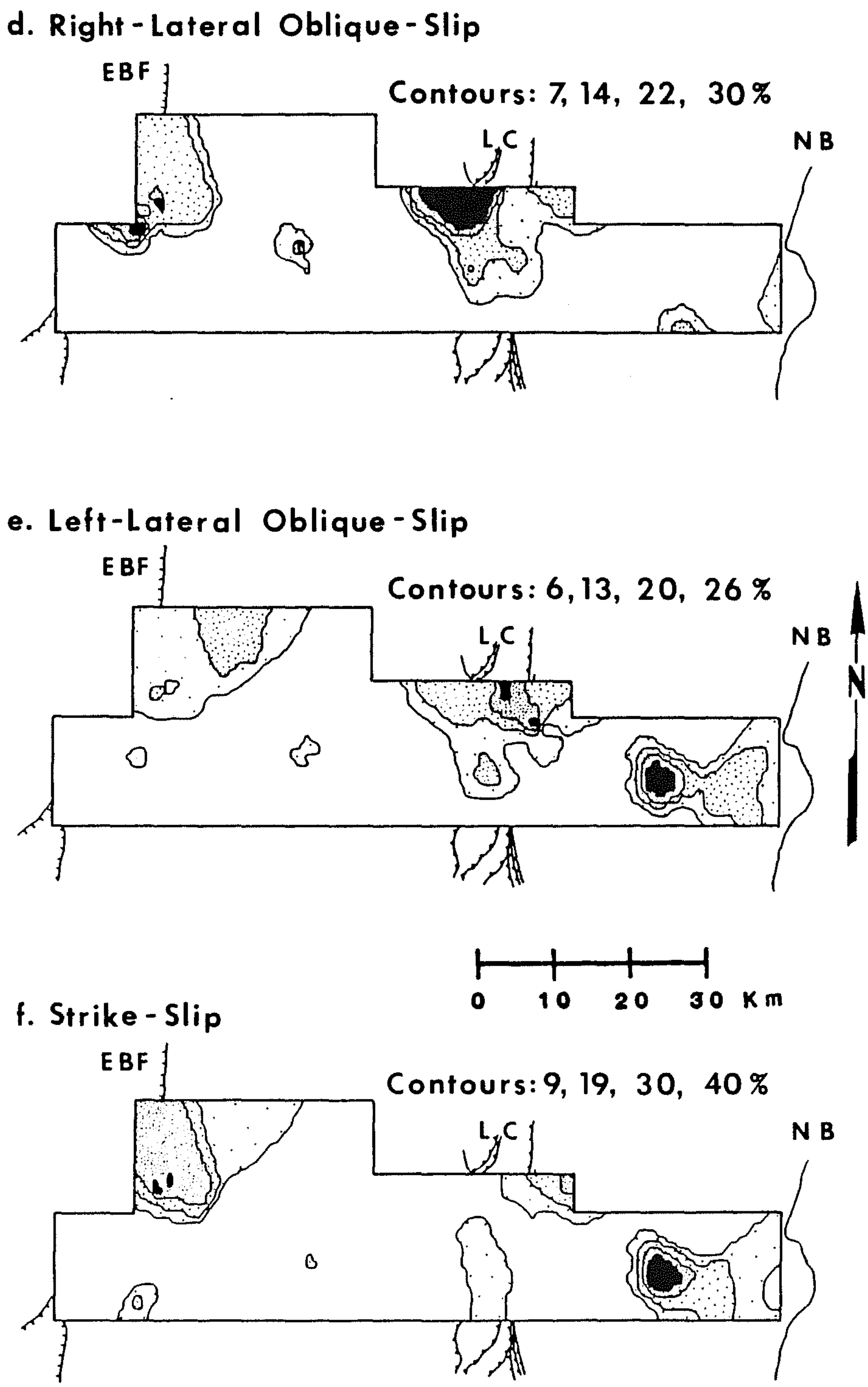
d. Right-Lateral Oblique-Slip
EBF
Contours: 7, 14, 22, 30%
LC
NB
e. Left-Lateral Oblique-Slip
EBF
Contours: 6,13, 20, 26%
LC
NB
N
0 10 20 30 Km
f. Strike-Slip
EBF
Contours: 9, 19, 30, 40%
LC
NB

g. Faults with Compressive Motions

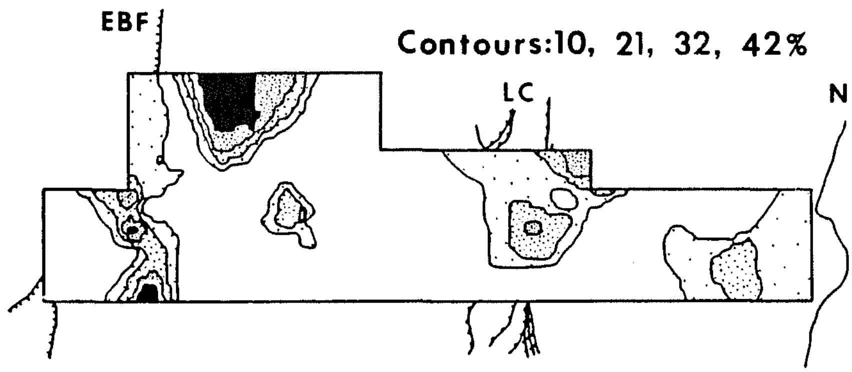

h. Faults with Extensile Motions

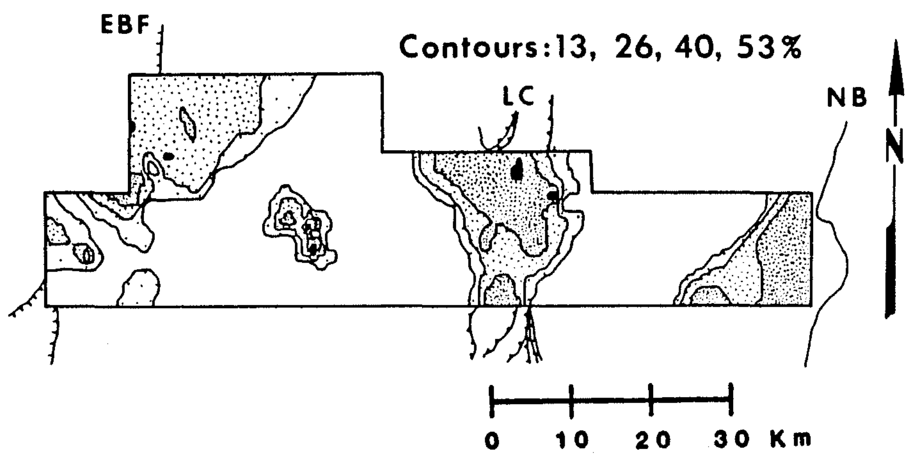

i. Faults with Lateral Motions

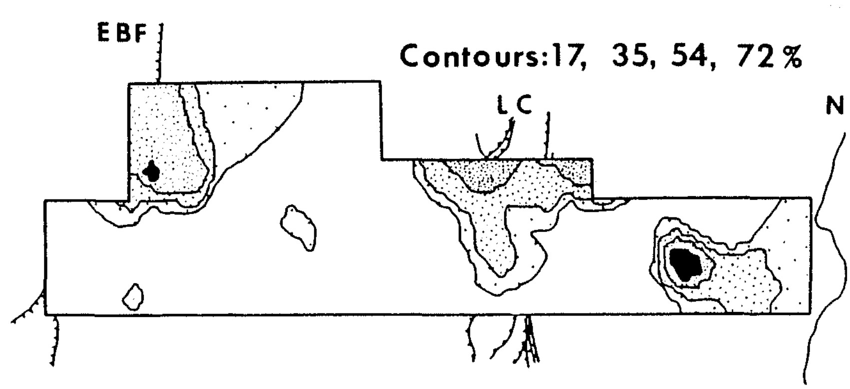

The Compressive Stress Field

In general, faults with compressional components of motion, including reverse dip- and oblique-slip varieties strike to the NE on moderately dipping, possibly conjugate planes (Figure 20A). The NW and SE trends of most slickenlines (Figure 20B) reflect the dominance of dip-slip motion on these surfaces. The maximum compressive stress for this system is subhorizontal and oriented NW-SE (Figure 20C). Sigma 2 is subhorizontal and trends NE-SW (Figure 20D) and sigma 3 is oriented about the vertical (Figure 20E).

Compressional faulting of this sort is difficult to reconcile with the extensile tectonics that have been proposed (ie: Sutter and Smith, 1979) for the Mesozoic in southern New England. Transcurrent motion during rifting between the North American and African Plates has been suggested by Wise (personal communication, 1981). Motions of this type may cause horizontal compression and minor reverse faulting activity (Wilcox, Harding, and Seely, 1977). Indeed, minor thrust faults of Mesozoic age have been documented in the Deerfield Basin of northern Massachusetts (Goldstein, 1975). Many minor extensile faults in eastern Connecticut and western Rhode Island are oriented similarly to the compressive faults (Figure 21A). It is unlikely, therefore, that these families of minor, brittle compressional and extensile faults are related to the same tectonic event. Reverse faults, moreover, are not observed in the rocks of the late Paleozoic Narragansett Pier Granite in southern Rhode Island (Hozik, 1981). This relation may suggest that minor reverse faulting in southern New England predated the emplacement of the pluton. It is possible, however, that the rocks of the Narragansett Pier Granite are within a separate fracture domain.

It seems likely, then, that this system of compressive faults represents an early phase of brittle shear failure in the region. These features may be related to the waning stages of the Alleghenian deformational event. The NW-SE compressive stress field derived for these data (Figures 20C, 20D, and 20E), then, may reflect the stress conditions that prevailed during the later stages of Alleghenian compression.

The Extensile Stress Field

Most brittle faults in the area are related to an extensile stress field of probable Mesozoic age. Extensile (dip- and oblique-slip normal) motions occurred on steep, WNW-trending planes and NE-trending, possibly conjugate families of faults (Figure 21A). Slickenline orientations (Figure 21B) indicate that dip-slip, down to the NW and SSW motions were dominant for this fault system. The stress field associated with these data indicates NW-SE-directed extension with sigma 1 subvertical (Figure 21C), sigma 2 subhorizontal and oriented NE-SW (Figure 21D), and sigma 3 subhorizontal and oriented NW-SE (Figure 21E). As noted above, these NE-trending extensile faults are markedly similar in orientation to compressive faults in the area. Many of the extensile faults, therefore, may represent a Mesozoic overprint on compressional faults of possible Alleghenian age.

The stress information derived from these data (Figures 21C, 21D, and 21E) may provide a description of the stress field for southern New England during the Mesozoic. This least compressive stress trajectory is supported by the tectonic transport direction indicated by the orientations of slickenlines on shallowly dipping faults (Figure 22) and is nearly identical to the sigma 3 orientation inferred from a family of diabase dikes of Jurassic age (May, 1971) in southern New England.

The Lateral Displacement Fault System

Faults with lateral components of motion (strike-, oblique-, and vertical oblique-slip) dip steeply and strike NNE and WNW (Figure 23A). Some of the data (reverse and normal oblique-slip faults) shown in Figure 23 were included in the discussions of the compressive and extensile stress fields above. Slickenlines for faults with lateral motions indicate NNE- or ENE-directed movement (Figure 23B).

Compressive stress orientations derived for these data are complexly distributed with sigma 1 oriented NW and in NE- and NNW-trending planes (Figure 23C); sigma 2 oriented about a partial, WNW-trending girdle (Figure 23D); and sigma 3 trending ENE-WSW, NNW-SSE, and NW-SE (Figure 23E).

The proportion (36%) of the data for minor faults with known motion vectors represented by these structures suggests that horizontal compression was relatively important in the late tectonic history of the study area. This evidence may, however, be weaker than it first appears. Many of these faults, as discussed above, represent parasitism or reactivation of older joints and/or other anisotropies. In an inhomogeneous, anisotropic medium, horizontal extension may fail to produce ideally oriented dip-slip normal faults. Rather, motion senses for many minor faults will be a partial function of the orientations of the reactivated planes. Many oblique-slip normal faults in the area, then, may result from reactivation of nonideally oriented planes in an extensile stress field.

The best criteria provided by this data base for evaluating several proposals for major transcurrent motion in southern New England may be the data for minor brittle strike-slip faults. The stress fields associated with strike-slip faults in the area provide little support for a dextral east-west megashear such as that suggested by

Arthaud and Matte (1977). In general, the paucity of true strike-slip faults in the area provides little mesoscopic structural evidence for major transcurrent motion on megashear systems. Wintsch (1984) has proposed very high temperatures and pressures for southern New England until the late Paleozoic. The transition from ductile to brittle deformation may have occurred too late in the region's history to record the effects of any major transcurrent motion(s).

Wise (1981) noted a NNE-trending zone of strike- plus oblique-slip dominance for minor faults to the west in the rocks of the Berkshire Anticlinorium and the Connecticut Valley in New York, Connecticut and Massachusetts (Figure 24). Minor faulting motions in the Narragansett Pier Granite to the south of the study area were also dominated by strike- plus oblique-slip motions (Hozik, 1981). Eastern Connecticut and western Rhode Island have a brittle deformational history which was unlike those of surrounding areas and was dominated by dip-slip motions.

Areal Distribution of Minor Fault Families

The areal distribution of the families of faults discussed above is influenced by proximity to major structural elements and tectonic features within the area. For this study, frequency values for faults of each class at individual fracture stations were defined as the percentage of such faults in the total population of faults with known motion vectors at the stations. These values were computer contoured on maps of the area (Figures 25A-25I). Data for stations with fewer than five minor faults or twenty total observations were ignored or, where appropriate, combined with data from nearby stations to suppress the misleading effects of small samples on the contouring process. N-S-trending fabrics in the fault frequency contours of Figure 25 are artifacts of the contouring process.

Several classes of minor faults, including normal and vertical dip-slip, strike- and oblique-slip, and the overall extensile and lateral fault systems (Figures 25B, 25C, 25D, 25E, 25F, 25H, and 25I) are numerous at outcrops within the Bronson Hill Anticlinorium and the Merrimack Synclinorium east of the EBF. The association of this variety of minor faults with the EBF may reflect a complex history of movement on that structure.

Faults with compressional motions (Figures 25A, and 25G) are concentrated in the Bronson Hill Anticlinorium and the Merrimack Synclinorium in the western end of the study area. These features may represent Alleghenian compression across the proposed Bone Mill Brook Fault (Pease, 1982) or Bronson Hill/Merrimack boundary.

Minor faults of all varieties are concentrated to a greater or lesser degree within the core and margin of the southwestern section of the Willimantic Dome (Figures 25A to 25I). These features may represent late strain across the Willimantic Fault or, perhaps, periods when the rate of strain was too high to be accommodated by ductile flow. Alternatively, the Dome may be a major mechanical anisotropy and may concentrate brittle shear strain in the area.

The area within and surrounding the LCFZ was a focus for minor brittle faulting activity in the study area. The affinity of minor faults with extensile components of motion (Figures 25B and 25H) for the Lake Char structure is particularly striking. This association is surprising in that the LCFZ is commonly regarded as a ductile thrust fault of regional importance (ie: Wintsch, 1984; Losh and Bradbury, 1984). The movement sense of this major structure is, however, under debate. Goldstein (1984) has suggested that the Lake Char structure is a normal fault analogous to the detachment faults of the Cordillera. Under this model, minor brittle extensile faults within and near the LCFZ may reflect late extension or high rates of strain across that structure. Bradley (1982) proposed late Paleozoic, right-lateral shear for the LCFZ. Some minor faults within and near the LCFZ may have been engendered by such transcurrent motion. The LCFZ is, however, an anisotropy of regional extent so that the high frequency of minor faults in its vicinity may be a mechanical effect.

Many faults with lateral motions (Figures 25E, 25F, and 25I) and, to a lesser degree, vertical dip-slip faults (Figure 25C) are common in outcrops in a zone within the Boston Platform east of the LCFZ. Some minor lateral motions may be related to the pull-apart tectonics that have been proposed for the Narragansett Basin (ie: Mosher, 1983). Aydin and Nur (1982) have noted that stress magnitudes are commonly low in areas surrounding large transcurrent faults. Bishop (1967), moreover, observed that most minor faults within a zone several miles wide to either side of major transcurrent faults in New Zealand are extensile varieties. These observations may explain the decrease in frequency of strike and oblique-slip motions just west of the Narragansett Basin.

All varieties of minor faults are common in an area immediately west of the Narragansett Basin (Figures 25A to 25I). This association is especially notable in the case of faults with extensile components of motion (Figures 25B and 25H). It is possible that some of these minor faults are related to the basin's kinematic history. Bradley (1982) has proposed that the basin opened as a pull-apart along NE-trending, dextral strike-slip faults. Under this model, some of the minor extensile faults may be related to the extensile component of shear stress across the basin's border faults. Mosher (1983) has suggested that the basin is a pull-apart structure related to sinistral motion on NE-trending transcurrent faults. If this interpretation is correct, minor compressional faults adjacent to the basin may be related to the compressional component of of shear stress on the basin's boundary faults.

Minor faults and major structural and tectonic features in the area are areally associated and may be related to single tectonic events. Alternatively, this association may merely indicate that large scale features in the area act as strain concentrators and thereby control the distribution of minor fault families.

Discussion

Minor faults in the study area are mainly oriented WNW and NNE to NE. Many of these faults are subparallel to the structural grain of the Merrimack Synclinorium and may be controlled by strength anisotropies associated with that grain. This pervasive NNE-NE fabric is also subparallel to one possible trend of the North American/Avalon suture zone (Gromet and O'Hara, 1984) and may be a mechanical effect of that major tectonic boundary. Many of these faults seem to have reactivated or parasitized older joints or other anisotropies.

Relative age relationships for the minor faults (as indicated by cross-cutting relations) are contradictory and faults of various types were not reliably distinguished by their mineralogic character. Minor faults with compressional components of motion, as discussed above, may reflect Alleghenian compression and, therefore, may predate other varieties of minor faults. The mineralogic similarity and relative age ambiguity of several types of extensile and lateral faults, however, make it reasonable to assume that that they are, in part, coeval. This variety of motion senses in faults of similar age may indicate that they are the response of an inhomogeneous, anisotropic medium to a uniform stress field. Hafner (1951) and Anderson (1951) observed that mechanical anisotropies may locally reorient stress trajectories, making faulting patterns difficult to interpret. Hozik (1981) proposed that brittle faults in the Narragansett Pier Granite formed under consistent NW-SE-directed extension in which maximum and intermediate compressive stresses of nearly equal magnitude rotated about sigma 3. Similar extensile stress conditions in eastern Connecticut and western Rhode Island may have contributed to the complex history of faulting motions noted in this study.

JOINTING

Introduction

Various categories of joints are, perhaps, the most ubiquitous mesoscopic deformational features observable in outcrop. While these fractures are frequently discussed in the literature, their origin and tectonic significance are unclear. The current state of disarray in the art of joint interpretation cannot be attributed to an inadequate supply of theories. In fact, the number of models for joint development may be only slightly smaller than the number of authors who have addressed this problem.

Joints are probably most commonly interpreted as extension fractures forming at 90 degrees to the axis of the least compressive stress. Extensile fractures of this sort are parallel to the sigma 1-sigma 2 plane. Blind application of this simple interpretation to all jointing phenomena may be hazardous. Only when certain surficial characteristics (ie: plumose markings, hackle) are documented on fracture surfaces can origin by extensile failure be inferred with confidence (Kulander and others, 1979). Fracture orientations may be influenced by preexisting planes of weakness or strength anisotropies that are related to earlier tectonic processes (Wise, 1964). In-situ stresses of local or regional extent may affect joint orientations. Joints are, in many cases, probably not directly caused by tectonic deformation but rather may represent stress release related to erosional unloading or deglaciation (Chapman, 1958). It seems likely that, within a given area, many factors influence the overall joint fabric.

Within the study area, joints of various types are the most commonly observed brittle deformational feature (n=4263). Joints were subdivided into several categories (Table 5) that are discussed separately below.

Common Joints

Common joints are, by far, the most numerous brittle structural feature in the study area (Table 5). Azimuthal variation of these features is extensive (Figure 26A) but pronounced N-S and E-W trends are observed in the data. Within these families, the data may be bimodally distributed among ENE- to WNW- and NNE- to NNW-oriented sets.

Orientations of prominent common joint sets at fracture stations were derived from equal area net plots of joint data (Figure 27). The bimodal distribution of the overall E-W- and N-S-trending families is readily apparent in the data for individual stations. These families are, in fact, more impressive in the aggregate than they are at individual stations where local factors may affect joint orientations. The dashed lines of Figure 27 are drawn parallel to joint azimuths in the manner of Engelder and Geiser (1980). They

Table 5. Joint Type Definitions and Number of Observations

Type	Description	n
Common Joints	Moderate to steeply dipping. Maximum Dimension $\leq$ 5 meters.	3112
Macrojoints	Moderate to steeply dipping. Maximum Dimension > 5 meters.	414
Headings (Joint Zones)	Zones of closely spaced joints with cm spacing of individual fractures.	92
Microjoints	Zones of closely spaced joints with mm spacing of individual fractures.	20
Microjoints in Dikes and Veins	Microjoints developed within quartz veins and some pegmatite dikes.	205
Sheeting	Horizontal to gently dipping.	420

represent possible sigma 1-sigma 2 planes in the area and are dominantly oriented WNW and N-S to NE.

Minerals other than hematite or pyrolusite were identified on only 15% of the joints in this data base. Mineralized fracture trends (Figure 26B) are broadly similar to the overall joint fabric but NNE trends reflect the high proportion (62%) of quartz mineralized and silicified joints (Figures 26C, 26D, and 26E) in these data (Table 6). Many features recorded as mineralized joints in this study may merely reflect reactivation of older veins and dikes.

Table 6. Mineral Coatings on Joint Surfaces+

Mineralogic Character	Joint Category					
	Common	Macro.	Micro.	Head.	MDV*	Sheeting (%)**
Weathering	1079	137	7	36	0	118
Quartz	121(28)	18(27)	1(50)	5(29)	2(67)	2(10)
Sulfides	17 (4)	1 (2)	0	0	0	0
Silic.	150(35)	24(36)	0	7(41)	0	5(25)
Mica	10 (2)	1 (2)	0	0	0	0
Chlorite	22 (5)	2 (3)	0	0	0	0
Epidote	32 (7)	1 (2)	0	3(17)	0	1 (5)
Feldspar	70(16)	14(21)	1(50)	2(11)	0	12(60)
Tourmaline	9 (2)	3 (5)	0	0	1(33)	0
Carbonate	3 (1)	1 (2)	0	0	0	0
Zeolite	0	1 (2)	0	0	0	0
Total n =	434	66	2	17	3	20

*: Microjoints in Dikes and Veins

**: Percentage not computed for stains and weathering.

+: More than one mineralogic category may apply for individual joints. In each case of this type, the joints were assigned to the category having the probable greater petrogenetic significance. No joints are counted twice.

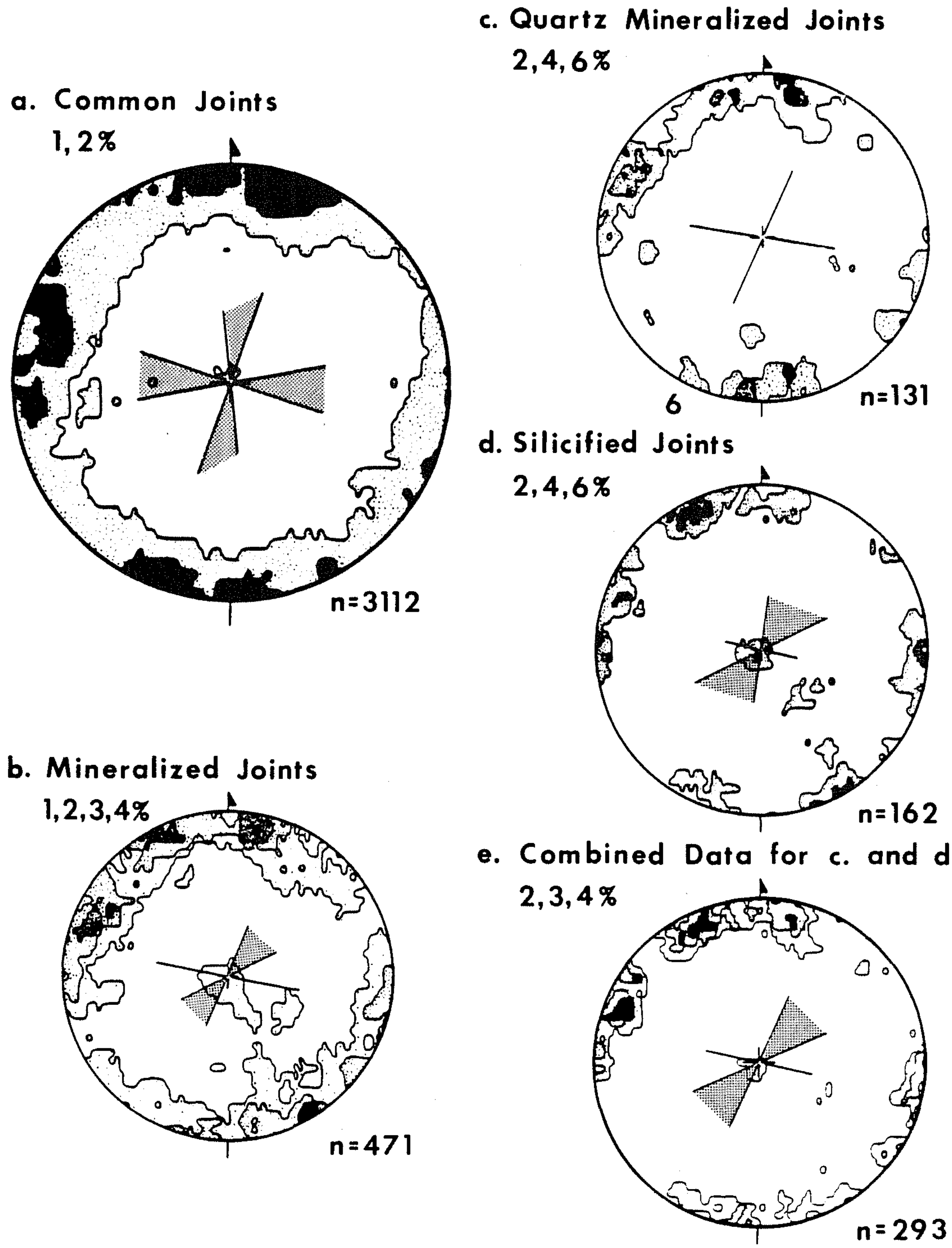

Figure 26. Structural data for common joints and several categories of mineralized joints within the study area. Contours are in percent per 1% area.

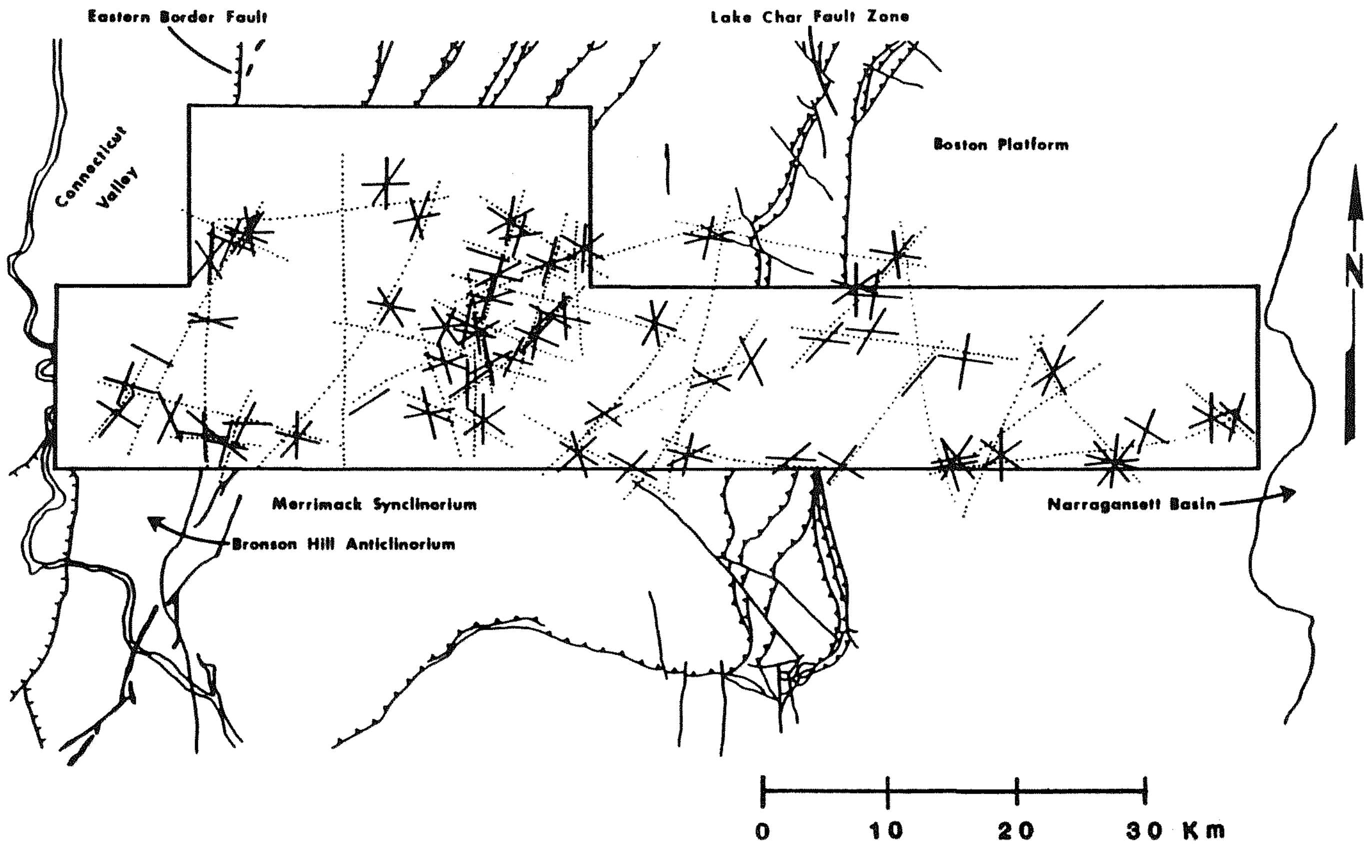

Figure 27. Trends of major joint sets at fracture stations within the study area. Dotted lines represent possible sigma 1-sigma 2 planes.

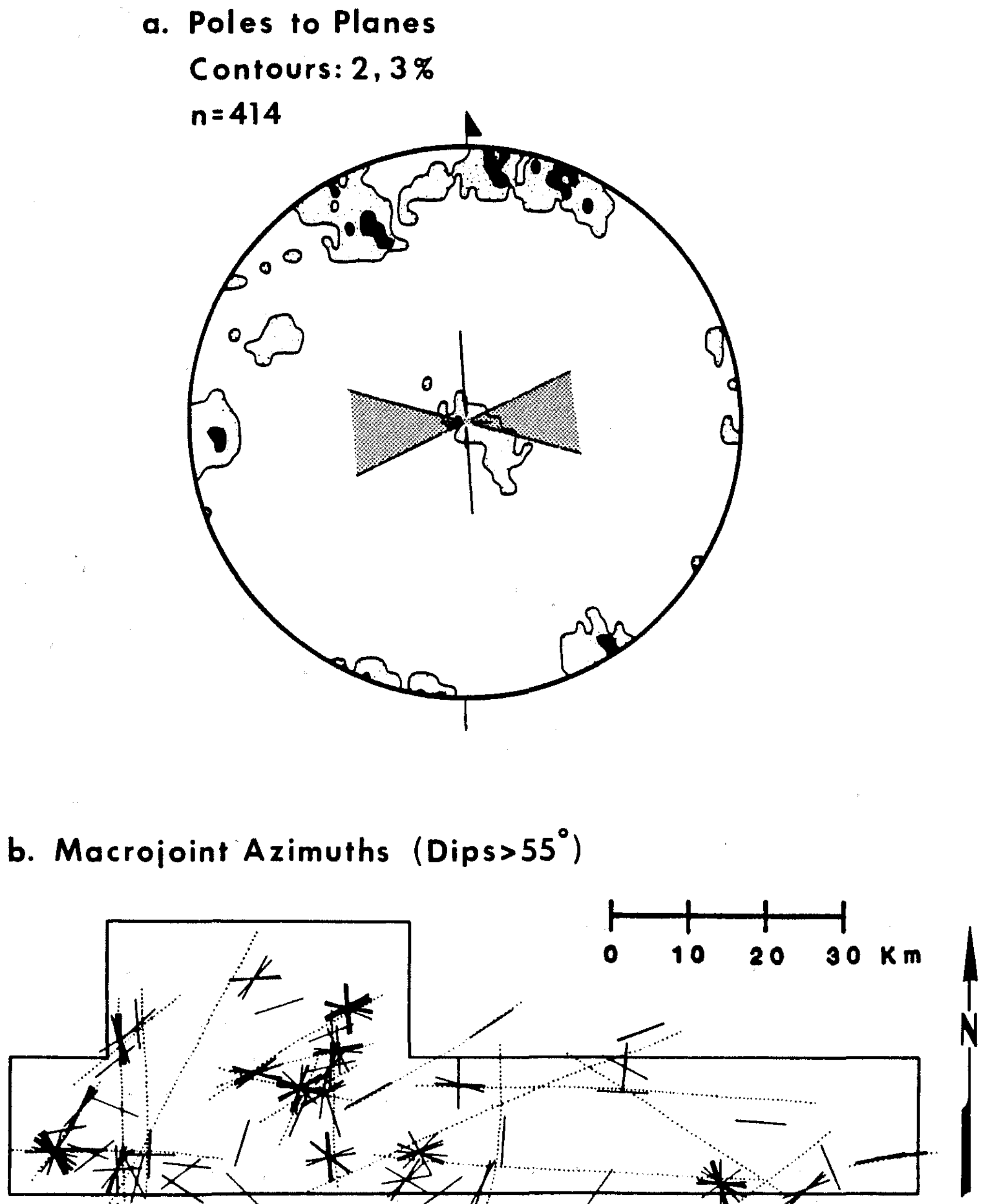

Figure 28. Structural data for macrojoints within the study area. Equal area net contours are in percent per 1% area. Dotted lines in b. represent possible sigma 1-sigma 2 planes.

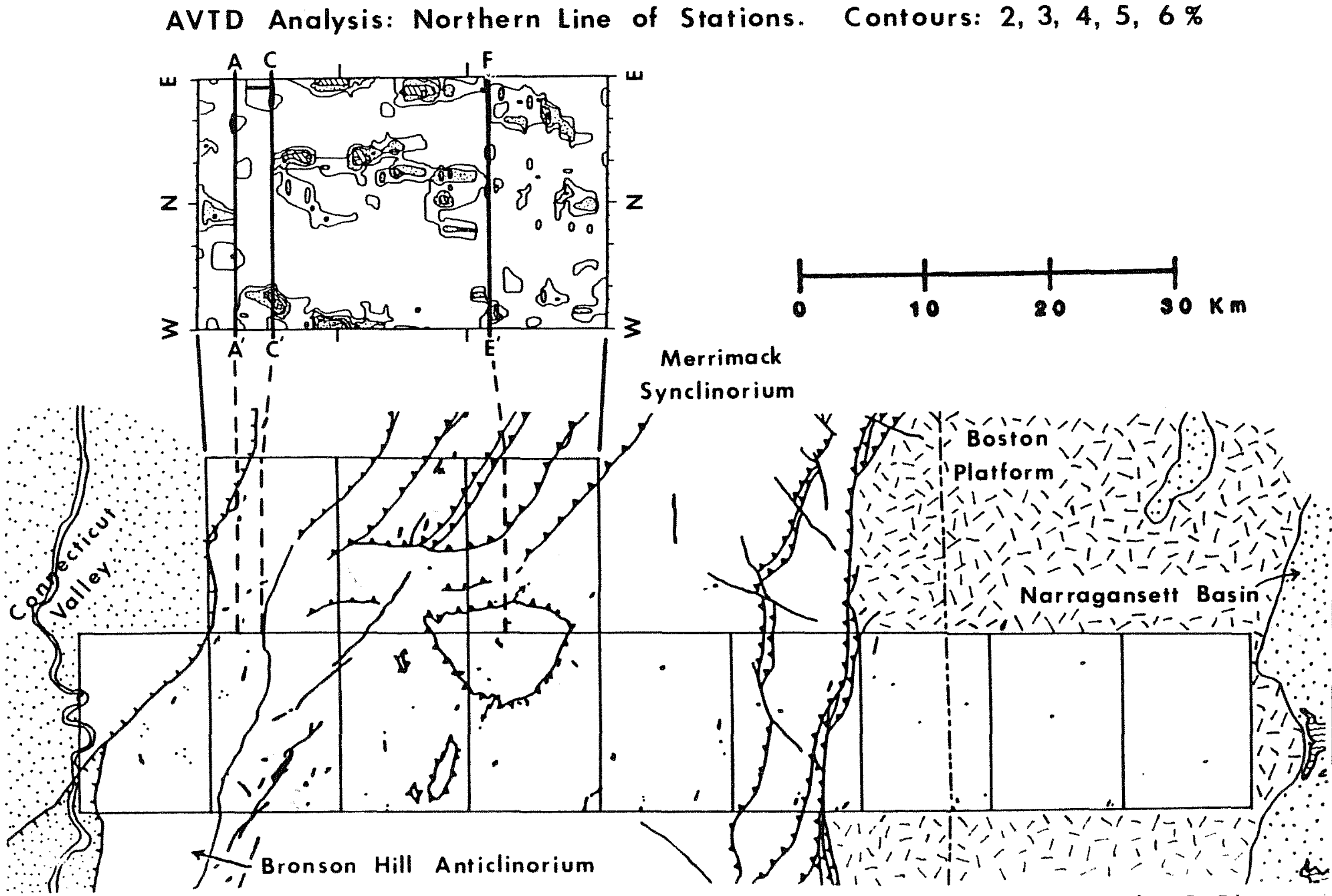

Figure 29. AVTD analysis of data for northern line of stations. A-A', C-C', and E-E' show domain boundaries and are explained in Table 7.

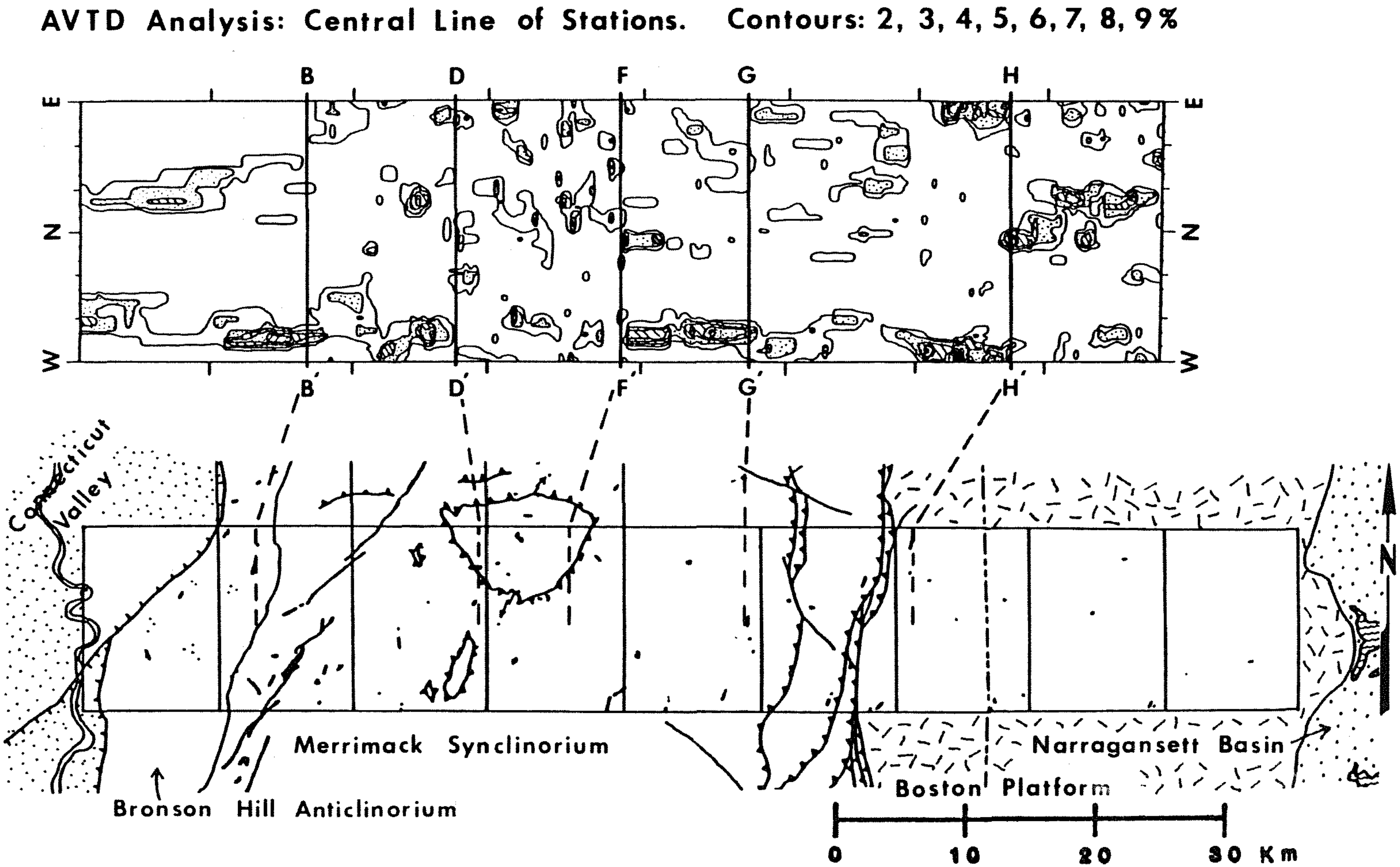

Figure 30. AVTD analysis of data for central line of stations. B-B', D-D', F-F', G-G', and H-H' show domain boundaries and are explained in Table 7.

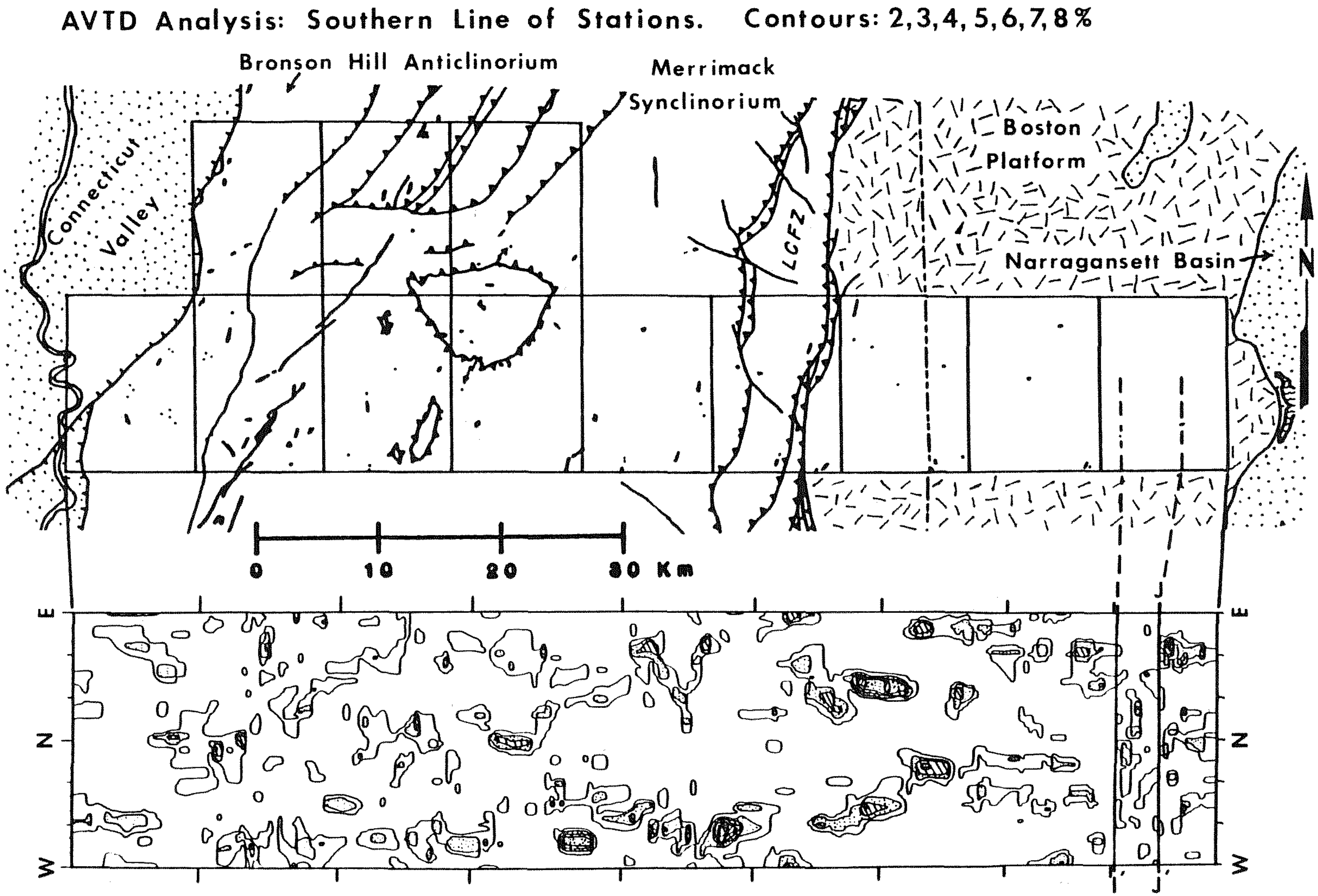

Figure 31. AVTD analysis of data for northern line of stations. I-I' and J-J' show domain boundaries and are explained in Table 7.

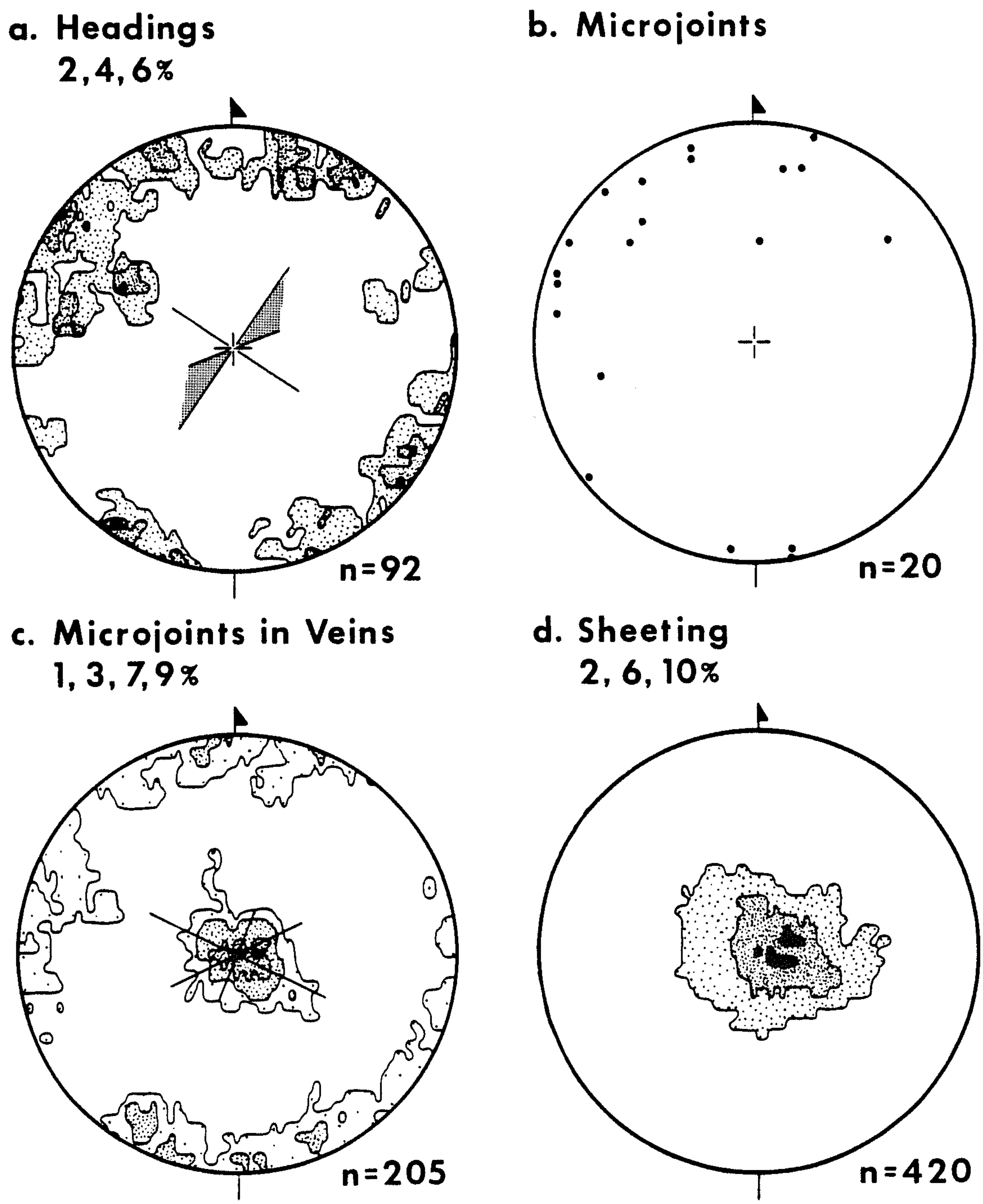

Figure 32. Structural data for several categories of joints in the study area. Equal area net contours are in percent per 1% area.

Figure 33. Fracture data from previous studies: a. prominent joint sets of the Hartford and Albany 2-degree sheets (from Wise, 1981); b. joint data from the Hartford and Albany 2-degree sheets (from Wise, 1981); c. joint data for the Moodus Quadrangle (Weston Geophysical, unpublished data); d. rift and grain of granite quarries of New England (from Wise, 1964).

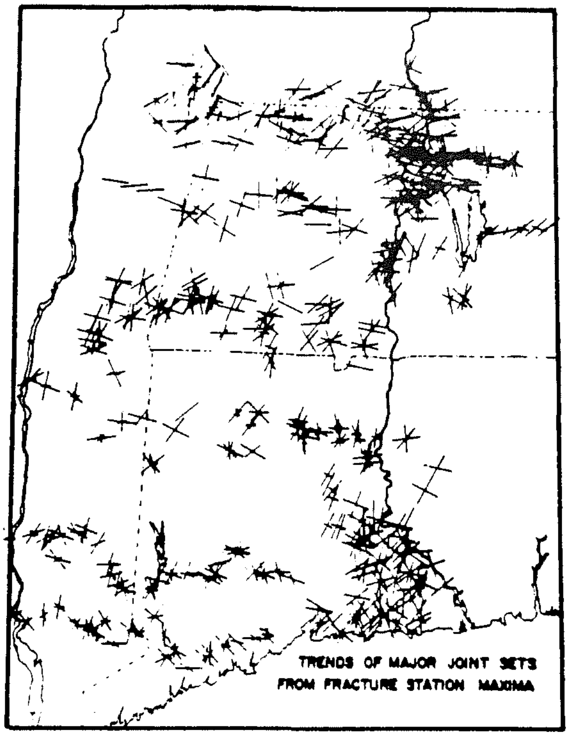

a.

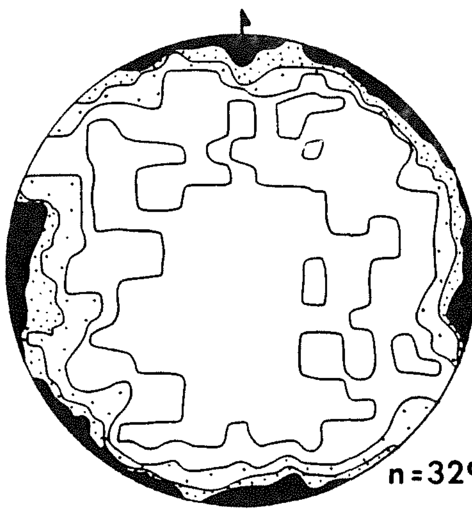

n=329

Contours: 1, 2,4,6%

c.

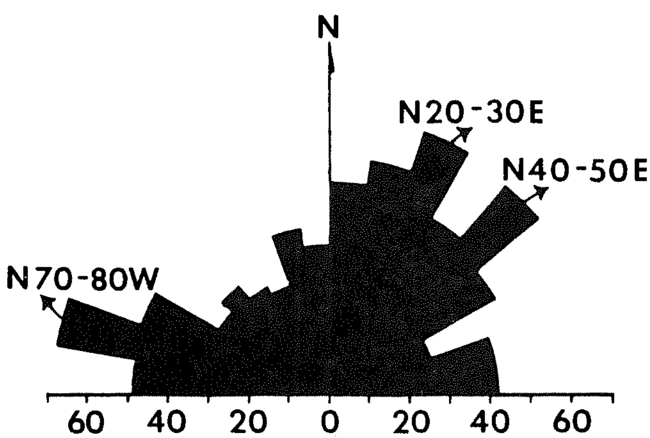

b.

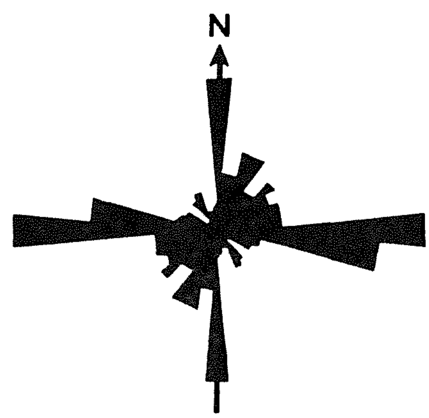

d.

Macrojoints

Macrojoints are similar in orientation to common joints and are characterized by NNW and broadly E-W-trending families. Azimuths of macrojoints with dips greater than 55 are shown in Figure 28B. Possible sigma 1-sigma 2 planes (the dotted lines of Figure 28B) are oriented N-S, NE, and E-W. Mineral coatings on macrojoint surfaces are similar to those observed for common joints (Table 6). Like the smaller fractures, these mineralized features probably include many reactivated veins and dikes.

Azimuth Versus Traverse Distance Analysis

Areal variation of combined orientational data for common joints and macrojoints was examined using Azimuth Versus Traverse Distance (AVTD) analysis. AVTD analysis is a sensitive tool for detecting domain boundaries and orientational variation of structural elements. For the purposes of this study, a modified version of the AVTD program was developed to permit variation of counter size during program execution. This feature permits AVTD plots to be adjusted to correspond with map distance and removes the dependence of plot length on data density.

Three AVTD traverses were produced for the study area. Stations within the northern three quadrangles (Figure 29) and the northern (Figure 30) and southern (Figure 31) halves of the main line of quadrangles were considered as separate traverses to provide control over latitudinal as well as longitudinal variation in joint orientations. The information presented on the AVTD plots of joint data for the area is summarized in Table 7. The analysis suggests that major structural elements within the area influence the orientations of joints in their vicinity and shows that orientations of common joints and macrojoints are more variable along the southern line of stations.

Table 7. AVTD Summary   *******: Domain Boundary

Northern Traverse

NNW trends E of EBF.

A *********** A'

NNW trends die out. Bimodal E-W trends appear.

C *********** C'

Bimodal N-S trends appear W of BMBF.

E *********** E'

E-W elements curve NE N of Willimantic Dome. N-S trends sporadically developed.

Central Traverse

NNE and WNW trends dominate.

B *********** B'

NNE trends die out. WNW trends dominate.

D *********** D'

Chaotic jointing in Willimantic Dome area.

F *********** F'

WNW trends dominate. N-S trends sporadically developed.

G *********** G'

ENE trends appear W of LCFZ.

H *********** H'

E-W trends diminish E of LCFZ. N-S-NNE trends dominate.

Southern Traverse

Zone of complex jointing with elements of ENE-WNW and NNE-NNW families.

I *********** I'

Zone of extremely complex jointing on Boston Platform.

J *********** J'

NW, N-S, and NE trends appear W of Narragansett Basin.

Headings and Microjoints

A WNW-oriented family of joint zones or headings (Figure 32A) is similar in orientation to elements of the fabrics of common and macrojoints in the area. The data for the headings is dominated, however, by NNE trends which are more similar to elements of the fabrics of the quartz veins and silicified and quartz mineralized joints (Figures 3C, 26C, 26D, and 26E).

In the Rocky Mountains, microjoints are commonly older, less chaotically oriented, and more reliable than common joints for providing useful stress information (Wise, 1964). Microjoints noted in this study strike mainly to the NE (Figure 32B) but the data are too sparse to indicate a clear trend.

A broadly E-W-trending, bimodally distributed fabric is observed in the data for closely spaced fractures or microjoints in veins and dikes (Figure 32C). Horizontal to gently dipping fractures of this type may be related to deglaciation or regional erosional unloading.

Sheeting

Sheeting joints (Figure 32D) are horizontal to gently dipping fractures that may or may not be parallel to bedding or metamorphic foliation. They probably result from stress release related to erosional and/or glacial unloading.

Timing

Abutting relationships between the various families of joints are ambiguous. In fact, contradictions in the relative age of distinct joint sets are sometimes observed within the same outcrop! If, as discussed in Chapter 4, vertical and steeply dipping faults formed by reactivating older joints, some joints must predate many of the minor brittle faults in the study area. These joints may be of early Mesozoic or late Paleozoic age. In outcrop steeply dipping joints of all types are truncated by very young features, related to unloading phenomena. Some steep joints, therefore, opened during the latest deglaciation in the Quaternary.

The dominant WNW-ENE and NNE-NNW trends in the joint data seem to have persisted from a time prior to minor brittle faulting until the very recent deglaciation and erosional denudation of the area. This consistency suggests that these trends are fundamental anisotropies which were repeatedly reactivated in the area's later history. This coherent fabric may also be related to in-situ stresses that were active over a large area and exerted control over fracture orientations.

Comparison with Data from Other Workers

While there is significant variation in common joint fabrics in southern New England, some elements of the common joint data of this study seem to extend into surrounding areas. Azimuths of joint sets at individual fracture stations in the Hartford and Albany sheets to the west and northwest of this study are shown in Figure 33A. Elements of the study area's dominant broad N-S and E-W joint trends are observed to the west as indicated by WNW and NNE maxima (Figure 33B) in the data of Wise (1981). WNW and NNE trends are also prominent in the common joint data for the Narragansett Pier Granite where a westerly-striking joint set appears to predate northerly-striking joints (Hozik, 1981). South of the study area in the Moodus Quadrangle of Connecticut, many common joints (Figure 33C) are broadly oriented N-S and E-W (Weston Geophysical, unpublished data, 1982). McMaster and others (1980) investigated fracture patterns in the sediments of the Narragansett Basin of Rhode Island but did not show separate plots of data for joints and faults.

Summary and Speculation

Clear trends in the data for joints and related features are persistent across the area. Broadly E-W- and N-S-oriented fabrics in the data for common joints, macrojoints and microjoints in dikes and veins are similar to fabrics observed in nearby areas. This fabric is similar to the rift and grain of the granite quarries of New England (Dale, 1923) and may be part of the same regional system of anisotropies (Figure 33D). Microjoints, quartz mineralized joints and headings strike NE and may represent the anisotropies on which some of the NE-trending vertical faults formed. Joint development in the area seems to have extended from the late Paleozoic or early Mesozoic to the Quaternary.

AVTD analysis of data for common joints and macrojoints suggests that structural domain boundaries for these features are controlled, in part, by proximity to major tectonic features. In particular, joint orientations seem to vary with proximity to the EBF of the Connecticut Valley, the Willimantic Dome, the LCFZ and the western margin of the Narragansett Basin in Rhode Island.

CONCLUSIONS

Summary

A somewhat speculative sequence of brittle deformation, based upon mineralization and cross-cutting relationships, is presented in Figure 34. Minor ductile shear zones are among the oldest features noted in this study. Timing of the ductile faults appears to overlap that of aplite and pegmatite dikes, some quartz veins and higher temperature complex veins. Dikes and veins follow strength anisotropies which were reactivated repeatedly during the area's cooling history. A family of high-angle compressional faults is of probable late Paleozoic age and may reflect a late stage of Alleghenian compression. A brittle faulting episode indicating NW-SE-directed extension occurred, along with emplacement of lower temperature veins, during the Mesozoic. Minor vertical dip-slip faults were probably coeval with this family of extensile faults. Faults with lateral components of motion are of indeterminate age but probably span much of the area's brittle faulting history. Joints of various categories are probable forerunners of minor vertical faults and must, in some cases, have preceded them. Steep joints of all categories, however, are truncated by gently dipping joints related to regional erosional unloading and/or deglaciation. Joint development in this area, then, may have occurred from the late Paleozoic or early Mesozoic to the Quaternary.

The late Paleozoic and younger tectonic history of southern New England comprises a complex series of brittle deformational events. The fracture fabric of eastern Connecticut and western Rhode Island, however, is characterized by elements that are found in data of various classes (Table 8). These fundamental anisotropies seem to have persisted through much of the area's later tectonic history and include a broadly E-W-oriented "Narragansett Pier" trend and a NNE-NE-oriented "Merrimack" trend (Figure 35).

Hozik (1984) and Murray (personal communication, 1984) have suggested that emplacement of the Narragansett Pier Granite Batholith and the dikes of the Westerly Granite was controlled by an E-W-trending fracture system. The Narragansett Pier trend of this study may represent a northward continuation of that domain. The NNE-NE-oriented Merrimack trend is parallel to the structural grain of the Merrimack Synclinorium and may reflect control of fracture orientations by that anisotropy.

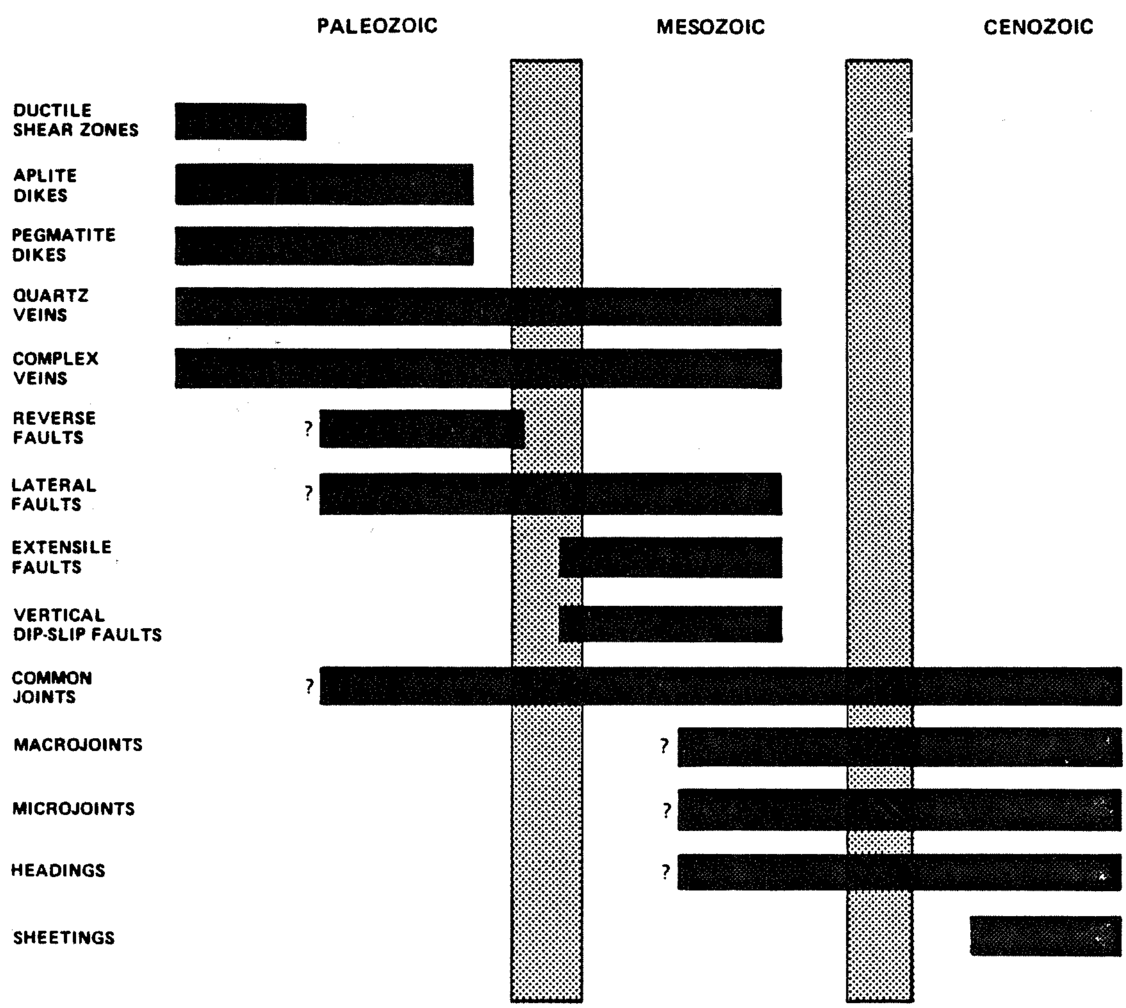

Figure 34. Relative age relations for brittle deformational features in eastern Connecticut and western Rhode Island.

Figure 35. Data showing the "Merrimack" and "Narragansett Pier" structural trends: a. aplite dikes; b. pegmatite dikes; c. quartz veins; d. complex veins; e. all brittle faults; f. reverse dip-slip faults; g. normal dip-slip faults; h. vertical dip-slip faults; i. left-lateral oblique-slip faults; j. right-lateral oblique-slip faults; k. strike-slip faults; l. unclassified faults; m. compressional faults; n. extensile faults; o. lateral displacement faults; p. common joints; q. mineralized joints; r. quartz mineralized joints; s. silicified joints; t. silicified and quartz mineralized joints; u. macrojoints; v. headings; w. microjoints; x. microjoints in veins and dikes.

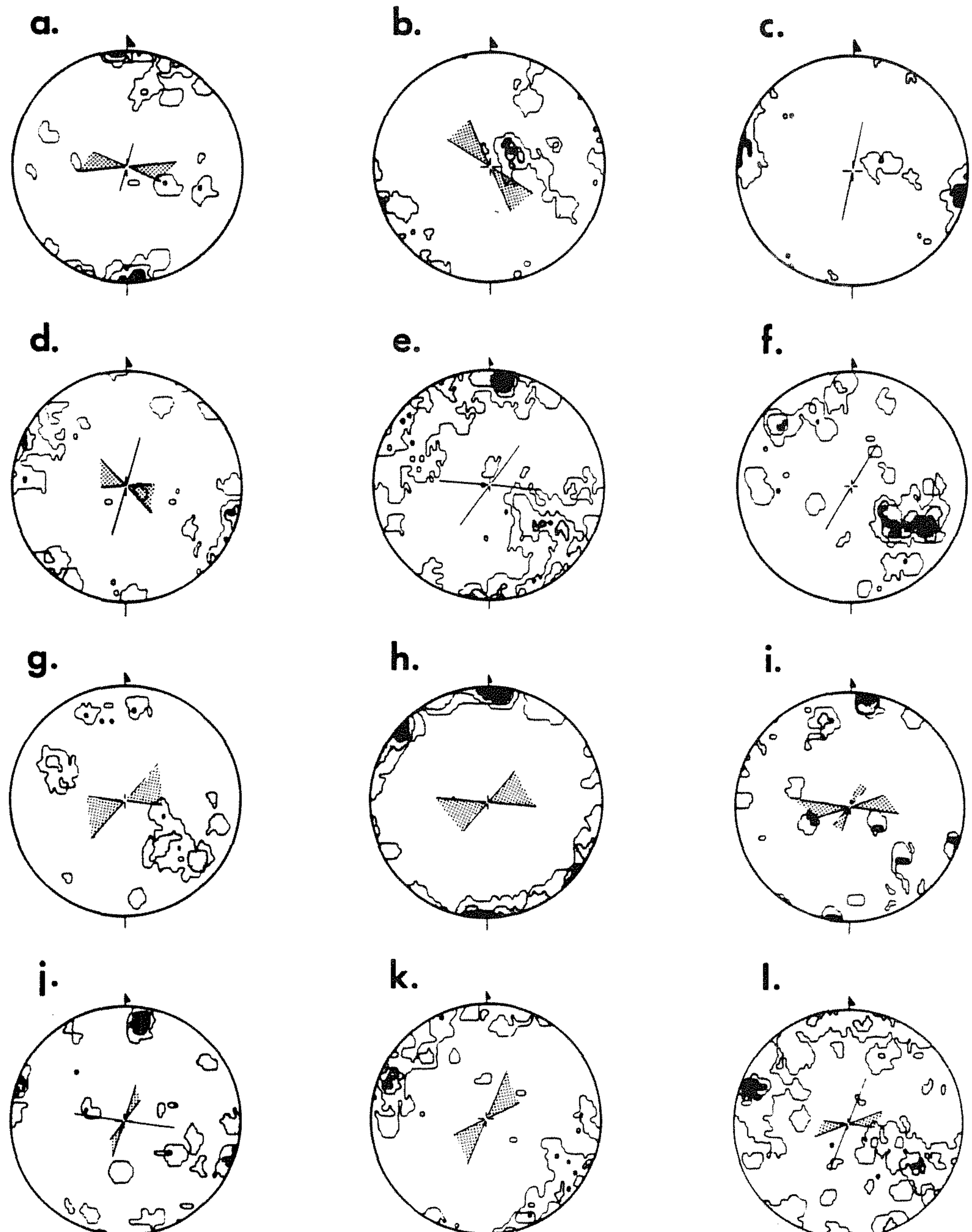
a.
b.
c.
d.
e.
f.
g.
h.
i.
j.
k.
l.

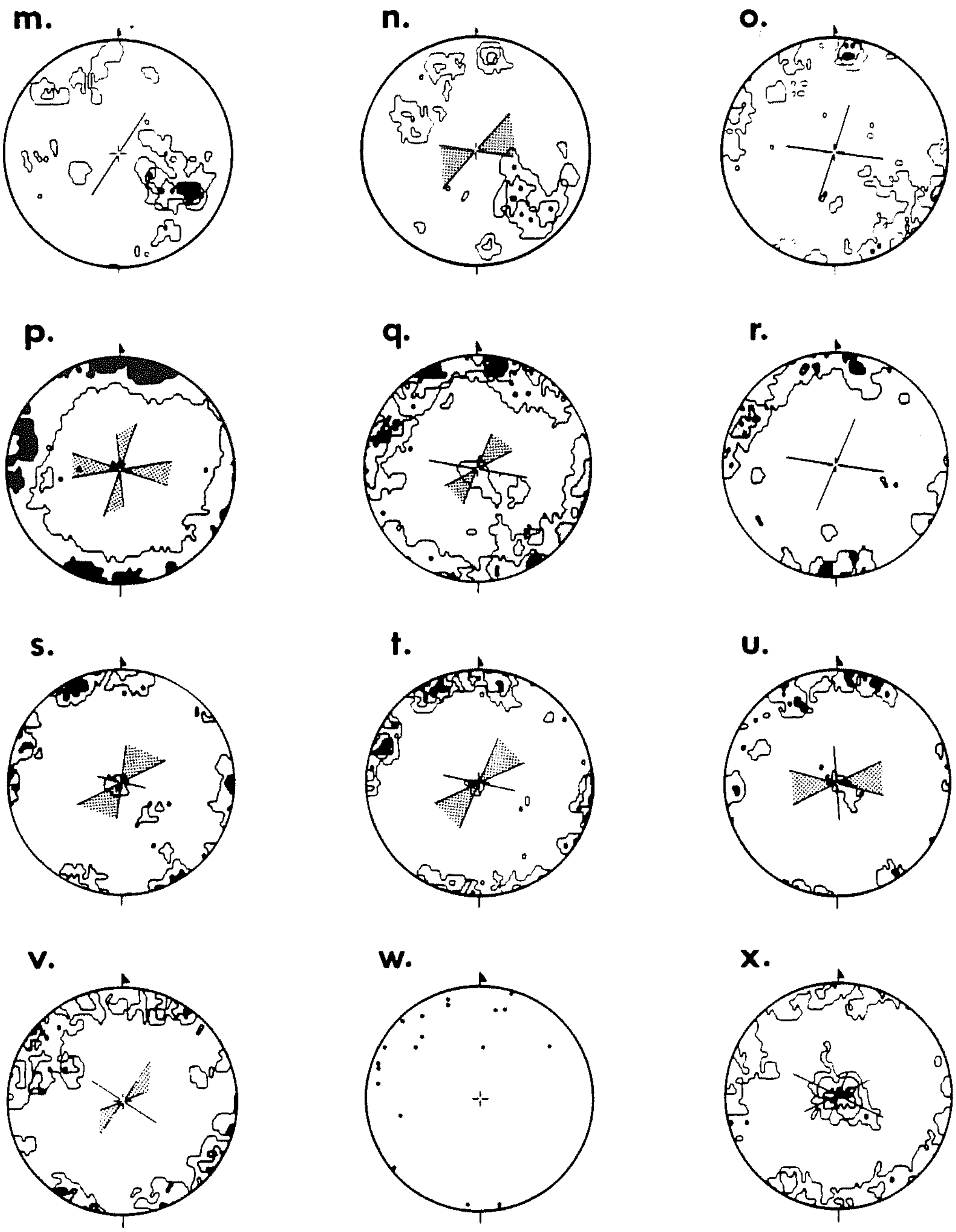
m.
n.
o.
p.
q.
r.
s.
t.
u.
v.
w.
x.

Table 8: Elements of Major Structural Trends

Narragansett Pier (E-W)	Merrimack (NNE-NE)
Extensile Structural Trends	
Sigma 3 approximately N-S	Sigma 3 (WNW-NW)
Aplite Dikes	Quartz Veins
Pegmatite Dikes	NNE Complex Veins
ENE Complex Veins	NE Extensile Faults
WNW Extensile Faults	NNE-NE Vertical Dip-Slip Faults
WNW Vertical Dip-Slip Faults	Quartz Min. Joints
Microjoints in Veins and Dikes	Silicified Joints
WNW Headings	NNE Headings
ENE-WNW Macrojoints	Microjoints
ENE-WNW Common Joints	NNE Common Joints
Compressional Structural Trends	
WNW Lateral Faults (Left-Lateral: Sigma 1 NE or SW) (Right-Lateral: Sigma 1 NW)	Compressional Faults (Sigma 1 NW)
	NNE Lateral Faults (Left-Lateral: Sigma 1 NNW-SSE or NW) (Right-Lateral: Sigma 1 NE or SW)
	Strike-Slip Faults (Left-Lateral: Sigma 1 N-S) (Right-Lateral: Sigma 1 E-W or NE)

Most minor brittle fault data for the area can be subdivided into four categories: 1) A compressive system of probable late Paleozoic age. This system indicates NW-SE compression and may reflect the latest stages of Alleghenian deformation. 2) An extensile system of probable Mesozoic age. The NW-SE direction of extension indicated by these data is consistent with that inferred from NE-trending mafic dikes of Mesozoic age in southern New England (May, 1971) and is probably related to the continental rifting that produced the present Atlantic Ocean. 3) A system of faults with lateral components of motion. This category includes data from systems 1 and 2 and is not associated with any unique stress field. These structures probably formed over a large portion of the area's later tectonic history. They may reflect warping of stress trajectories near crustal anisotropies, variation in the regional stress field, or simple reactivation of nonideally oriented, preexisting planes. Faults with lateral motions comprise 35% and true strike-slip varieties represent only 14% of the data for faults with known motion vectors. This proportion seems surprisingly low in light of recently proposed models for major transcurrent motions in this area (ie: Arthaud and Matte, 1977; Bradley, 1982; Mosher, 1983). The later history of the area seems to have differed fundamentally from that of areas in Connecticut and Massachusetts to the west and northwest (Wise, 1981) and the Narragansett Pier Granite to the south (Hozik, 1981) where dominance of strike- plus oblique-slip motions was noted. 4) A system of vertical dip-slip faults of probable Mesozoic age. Most of these structures indicate NW-SE and NNE-SSW extension. WNW-oriented members of this system may correlate with similar faults noted by Hozik (1981) in the Narragansett Pier Granite to the south. These may be the youngest brittle faults in the batholith and may reflect a change in the direction of continental drift at approximately 80 MABP (Hozik, 1981).

The areal distribution of minor brittle faults is at least partially controlled by major structural and tectonic features in the study area. The affinity of minor faulting motions for the area surrounding the LCFZ is particularly striking. This geographic coincidence may indicate that minor structures were produced by the same tectonic events as were major structures in the area. These large-scale features, however, may act as major crustal anisotropies and thereby serve to localize later brittle strain in this part of New England.

Joint development probably occurred from the late Paleozoic or early Mesozoic to the Quaternary. Domain boundaries for common and macrojoints seem to be influenced by major tectonic features. Elements of the overall, broad

E-W and N-S-trending fabrics observed in the data for common joints and macrojoints extend into surrounding areas and are reminiscent of the rift and grain of granite quarries in New England (Dale, 1923).

Speculation

The Merrimack trend of this study includes features of probable Paleozoic age (older quartz veins, high temperature complex veins, minor reverse faults). Late Acadian extension related to normal motions on the LCFZ (Goldstein, 1981, 1984) may have produced this pervasive anisotropy. The trend may also have been engendered by the extensile component of right-lateral shear across a northerly trending ductile shear zone of late Paleozoic age (Gromet and O'Hara, 1984) within the Boston Platform. Alternatively, relaxation of Alleghenian NW-SE-directed compression is a possible cause of the Merrimack fracture trend.

Hozik (1981) has proposed that the Narragansett Pier Granite was emplaced under E-W-directed compression. Supporting structural evidence for early Permian, E-W-oriented compression is found in the sediments of the Narragansett Basin (Mosher, 1983). The anisotropies of the Narragansett Pier trend could be related to compression of this type. NE-trending compressional faults are not found in the rocks of the Narragansett Pier Granite. This absence may indicate that the NW-SE-directed compression in eastern

Connecticut and western Rhode Island represents a slightly older stress field. If the compressional faults of this study predate the Narragansett Pier Granite, a counterclockwise rotation of the maximum compressive stress occurred in the late Paleozoic. This rotation is in the opposite sense of that proposed by Wintsch (1984) and Wintsch and Fout (1982) on the basis of mineral lineation orientations in the Honey Hill, Willimantic, and Lake Char Fault Zones.

REFERENCES CITED

Aydin, A., and Nur, A., 1982, Evolution of pull-apart basins and their scale independence: Tectonics, v. 1, p. 91-105.

Aydin, A., and Reches, Z., 1982, Number and orientation of fault sets in the field and in experiments: Geology, v. 10, p. 107-112.

Anderson, E. M., 1951, The dynamics of faulting: London, Oliver and Boyd, 206 p.

Arthaud, F., and Matte, P., 1977, Late Paleozoic strike-slip faulting in southern Europe and northern Africa: result of a right-lateral shear zone between the Appalachians and the Urals: Geological Society of America Bulletin, v. 88, p. 1305-1320.

Barosh, P. J., 1982, Structural patterns at the junction of the Merrimack Province, Nashoba thrust belt, and the southeast New England platform in the Webster-Oxford area, Massachusetts, Connecticut, and Rhode Island, in Joeston, R., and Quarrier, S.S., eds. Guidebook for Field Trips in Connecticut and South Central Massachusetts, 74th Annual Meeting New England Intercollegiate Geological Conference: State Geological and Natural History Survey of Connecticut, Guidebook No. 5, p. 395-418.

Barosh, P. J., London, D., and de Boer, J., 1982, The structural geology of the Moodus seismic area, south-central Connecticut, in Joeston R., and Quarrier, S. S., eds., Guidebook for Fieldtrips in Connecticut and South Central Massachusetts, 74th Annual Meeting New England Intercollegiate Geological Conference: State Geological and Natural History Survey of Connecticut, Guidebook No. 5, p. 419-451.

Bishop, D. G., 1967, The geometric relationships of structural features associated with major strike-slip faults in New Zealand: New Zealand Journal of Geology and Geophysics, v. 11, p. 405-417.

Boucot, A. J., and Gray, J., 1983, A Paleozoic Pangea: Science, v. 222, p. 571-581.

Brace, W. F., 1960, An extension of the Griffith theory of fracture to rocks: Journal of Geophysical Research, v. 65, p. 3477-3480.

Bradley, D. C., 1982, Subsidence in late Paleozoic basins in the northern Appalachians: Tectonics, v. 1, p. 107-123.

Byerlee, J. D., 1968, Brittle-ductile transition in rocks: Journal of Geophysical Research, v. 73, p. 4741-4750.

Chandler, W. E., Jr., 1978, Graben mechanics at the junction of the Hartford and Deerfield Basins of the Connecticut Valley, Massachusetts (M.Sc. Thesis): Amherst, Massachusetts, Contribution No. 33, Department of Geology and Geography, University of Massachusetts, 151 p.

Chapman, C. A., 1958, Control of jointing by topography (Maine): Journal of Geology, v. 66, p. 552-558.

Dale, T. N., 1923, The commercial granites of New England: U. S. Geological Survey Bulletin, 738, 488 p.

Dixon, H. R. and Lundgren, L. W., Jr., 1968, Structure of eastern Connecticut, in Zen, E-an, White, W. S., Hadley, J. B., and Thompson, J. B., Jr., eds., Studies of Appalachian Geology: Northern and Maritime: New York, Interscience Publishers, p. 219-229.

Dougenik, J. A., and Sheehan, D. E., SYMAP users reference manual: Cambridge, Lab for Computer Graphics and Spatial Analysis, 197 p.

Engelder, T., and Geiser, P., 1980, On the use of regional joint sets as trajectories of paleostress fields during the development of the Appalachian Plateau, New York: Journal of Geophysical Research B., v. 85, p. 6319-6341.

Goldstein, A. G., 1975, Brittle fracture history of the Montague Basin, north-central Massachusetts (M.Sc. Thesis): Amherst, Massachusetts, Contribution No. 25, Department of Geology and Geography, University of Massachusetts, 151 p.

Goldstein, A. G., 1981, Tectonics of ductile faulting in a portion of the Lake Char Mylonite Zone, Massachusetts and Connecticut, (Ph.D. dissertation), University of Massachusetts, Amherst, Massachusetts, 189 p.

Goldstein, A. G., 1984, Kinematic Indicators in Lake Char Fault Mylonites: Geological Society of America Abstracts with Programs, v. 16, no. 1, p. 18.

Grew, E. S., 1973, Stratigraphy of the Pennsylvanian and pre-Pennsylvanian rocks of the Worcester area, Massachusetts, American Journal of Science, v. 273, p. 113-129.

Gromet, L. P., and O'Hara, K. D., 1984, Two distinct late Precambrian terranes within the "Avalon Zone", southeastern New England, and their late Paleozoic juxtaposition: Geological Society of America Abstracts with Programs, v. 16, p. 20.

Hafner, W., 1951, Stress distributions and faulting: Geological Society of America Bulletin, v. 62, p. 373-398.

Haines, D., and Bauer, P., 1978, An east-west brittle fracture report across the Berkshires through Pittsfield, Massachusetts (Undergraduate Student Report): Department of Geology and Geography, University of Massachusetts, 41 p.

Hall, L. M., and Robinson, Peter, 1982, Stratigraphic-tectonic subdivisions of southern New England, in St. Julien, P., and Beland, J., eds, Major Structural Zones and Faults of the Northern Appalachians: Geological Society of Canada Special Paper 24, p. 15-41.

Higgins, M. W., 1971, Cataclastic rocks: U.S.G.S. Professional Paper 687, 97 p.

Hozik, M. J., 1981, Brittle fracture history of the Narragansett Pier Granite, Rhode Island, (Ph.D. dissertation), University of Massachusetts, Amherst, Massachusetts, 309 p.

Hozik, M. J., 1984, Brittle fracture history of the Narragansett Pier Granite, Rhode Island: Geological Society of America Abstracts with Programs, v. 16, no. 1, p. 25.

Ingari, J., and Massaras, D., 1978, Brittle fracture patterns across southwestern Massachusetts and adjacent New York (Undergraduate Student Report): Department of Geology and Geography, University of Massachusetts, 53 p.

Kent, D. V., and Opdyke, N. D., 1979, The early Carboniferous paleomagnetic field of North America and its bearing on tectonics of the northern Appalachians: Earth and Planetary Science Letters, v. 44, p. 365-372.

Kent, D. V., and Opdyke, N. D., 1984, A revised paleopole for the Mauch Chunk Formation and its tectonic implications: EOS, v. 65, p. 200.

Kocis, D. E., Hermes, O. D., and Cain, J. A., 1978, Petrologic comparison of the pink and white facies of the Narragansett Pier Granite, Rhode Island: Geological Society of America Abstracts with Programs, v. 10, no. 2, p. 71.

Kulander, B. R., Barton, C. C., and Dean, S. L., 1979, The application of fractography to core and outcrop fracture investigation: U. S. Department of Energy, METC/SP-79/3, 174 p.

Losh, S., and Bradbury, H. J., 1984, Late Paleozoic deformation within the Honey Hill-Lake Char Fault Zone, southern New England: Geological Society of America Abstracts with Programs, v. 16, no. 1, p. 48.

Maher, T. H., 1979, The eastern Border Fault and Deerfield Basin of north-central Massachusetts: a compilation of previous work with additional data and interpretation (Senior Research Problem), Department of Geology and Geography, University of Massachusetts, 62 p.

Massaras, D., Bauer, P., and Wrenn, S., 1979, Brittle fracture patterns on two traverses across southwestern Connecticut and adjacent New York (Post-B.S. Student Report): Department of Geology and Geography, University of Massachusetts, 54 p.

May, P. R., 1971, Pattern of Triassic-Jurassic diabase dikes around the North Atlantic in the context of the pre-drift positions of the continents: Geological Society of America Bulletin, v. 82, p. 1285-1292.

McHone, J. G., 1978, Distribution, orientations, and ages of mafic dikes in central New England: Geological Society of America Bulletin, v. 89, p. 1645-1655.

McMaster, R. L. de Boer, J., and Collins, B. P., 1980, Tectonic development of southern Narragansett Bay and offshore Rhode Island: Geology, v. 8, p. 496-500.

Mosher, S., 1983, Kinematic History of the Narragansett Basin, Massachusetts and Rhode Island, constraints on late Paleozoic plate reconstructions: Tectonics, v. 2, p. 327-344.

Nickelsen, R. P., and Hough, V. N. D., 1967, Jointing in the Appalachian Plateau of Pennsylvania: Geological Society of America Bulletin, v. 78, p. 609-630.

Osberg, P. H., 1980, Stratigraphic and structural relations in the turbidite sequence of south-central Maine: New England Intercollegiate Geological Conference, 72nd Annual Meeting, Guidebook, p. 278-296.

Page, L. R., 1968, Devonian plutonic rocks in New England, in Zen, E-an, White, W. S., Hadley, J. B., and Thompson, J. B., Jr., eds., Studies of Appalachian Geology: Northern and Maritime: New York, Interscience Publishers, p. 371-383.

Paterson, M. S., 1958, Experimental deformation and faulting in the Wombeyan Marble: Geological Society of America Bulletin, v. 69, p. 465-476.

Pease, M. H., Jr., 1982, The Bonemill Brook Fault Zone, Eastern Connecticut, in Joeston, R., and Quarrier, S. S., eds., Guidebook for Fieldtrips in Connecticut and South Central Massachusetts, 74th Annual Meeting New England Intercollegiate Geological Conference: State Geological and Natural History Survey of Connecticut, Guidebook No. 5, p. 465-482.

Peterson, C., 1979, Brittle deformation in and along the line of the Quabbin Aqueduct Tunnel, central Massachusetts (Senior Honors Thesis): Amherst, Massachusetts, Department of Geology and Geography, University of Massachusetts.

Piepul, R., 1975, An analysis of jointing and faulting at the southern end of the eastern border fault, Connecticut (M.Sc. Thesis): Amherst, Massachusetts, Contribution No.23, Department of Geology and Geography, University of Massachusetts, 109 p.

Quinn, A. W., and Moore, G. E., Jr, 1968, Sedimentation, tectonism, and plutonism of the Narragansett Basin Region, in Zen, E-an, White, W. S., Hadley, J. B. and Thompson, J. B., Jr., eds., Studies of Appalachian Geology: Northern and Maritime: New York, Interscience Publishers, p. 269-280.

Reks, I., and Smith, G., 1979, Brittle fracture analyses northwest Connecticut traverse (Undergraduate Student Report): Department of Geology and Geography, University of Massachusetts, 21 p.

Robinson, P., and Hall, L. M., 1980, Tectonic synthesis of New England, in Wones, D. R., ed., The Caledonides in the USA: I.G.C.P. Project 27: Caledonide Orogen, 1979 Meeting, Blacksburg, Virginia: Virginia Polytechnic Institute and State University Memoir, no. 2, p. 73-82.

Rogers, J., 1982, Yet another preliminary geologic map of Connecticut, in Joeston, R., and Quarrier, S. S., eds., Guidebook for fieldtrips in Connecticut and south central Massachusetts: 74th Annual Meeting New England Intercollegiate Geological Conference: State Geological and Natural History Survey of Connecticut, Guidebook No. 5, p. 1-4.

Russell, W. L., 1922, The structural and stratigraphic relations of the great Triassic fault of southern Connecticut: American Journal of Science, v. 4, p. 483-497.

Silverman, J. N., 1976, An analysis of brittle deformation along an east-west line in north-central Massachusetts (Senior Honors Thesis): Department of Geology and Geography, University of Massachusetts, 50 p.

Skehan, J. W., S. J., and Murray, D. P., eds., 1978, The coal-bearing Narragansett Basin of Massachusetts and Rhode Island: Geology, Volume I: Weston, Massachusetts, Weston Observatory, Department of Geology and Geophysics, Boston College, 99 p.

Sutter, J. F., and Smith, T. E., 1979, $^{40}Ar/^{39}Ar$ ages of diabase intrusions from Newark trend basins in Connecticut and Maryland: initiation of central Atlantic rifting: American Journal of Science, v. 279, p. 808-831.

Tracy, R. J., and Robinson, Peter, 1978, Metamorphic isograd mapping in central Massachusetts and the study of changing mineral compositions in metamorphism. Geological Society of America, Abstracts with Programs v. 10, p. 89.

Watts, A. B., 1982, Tectonic subsidence, flexure and global changes of sea level: Nature, v. 279, p. 469-474.

Wheeler, G., 1937, The west wall of the New England Triassic lowland: Connecticut State Geological and Natural History Survey Bulletin 58, p. 73.

Wheeler, G., 1939, Triassic fault line deflections and associated warpings: Journal of Geology, v. 47, p. 337-370.

White, W. S., 1968, Generalized geologic map of the Northern Appalachian Region, in Zen, E-an, White, W. S., Hadley, J. B., and Thompson, J. B., Jr., eds., Studies of Appalachian Geology: Northern and Maritime: New York, Interscience Publishers, p. 269-280.

Whitten, E. H. T., 1975, The practical use of trend-surface analyses in the geological sciences, in Davis, J. C., and McCullagh, M. J., eds., Display and Analysis of Spatial Data: London, John Wiley and Sons, p. 282-297.

Whitten, E. H. T., 1981, Trends in computer applications in structural geology, in Merriam, D. F., ed., Computer Applications in the Earth Sciences, An Update of the 70's: New York, Plenum Press, p. 323-368.

Wiedman, C., and Hosmer, T., 1983, IDAP: Interactive Data Analysis Package: Amherst, Massachusetts, University Computing Center, University of Massachusetts, 88 p.

Williams, G., 1976, An analysis of brittle deformation in the area of the northern portion of the Pelham Dome, north-central Massachusetts (Senior Thesis): Department of Geology and Geography, University of Massachusetts, 47 p.

Williams, G., 1979, Transition from ductile to brittle deformation at the head of the Deerfield Basin, Bernardston-Leydon area, Massachusetts (M.Sc. Thesis): Amherst, Massachusetts, Contribution No. 35, Department of Geology and Geography, University of Massachusetts, 151 p.

Wilcox, R. E., Harding, T. P., and Seely, D. R., 1973, Basic wrench tectonics: American Association of Petroleum Geologists Bulletin, v. 57, p. 74-96.

Wintsch, R. P., 1979, The Willimantic fault: a ductile fault in eastern Connecticut: American Journal of Science, v. 279, p. 367-393.

Wintsch, R. P., and Fout, J. S., 1982, Structure and petrology of the Willimantic Dome and the Willimantic fault, eastern Connecticut, in Joeston, R., and Quarrier, S. S., eds., Guidebook for Fieldtrips in Connecticut and South Central Massachusetts, 74th Annual Meeting New England Intercollegiate Geological Conference: State Geological and Natural History Survey of Connecticut, Guidebook No. 5, p. 465-482.

Wintsch, R. P., 1984, A tectonic model for the late Paleozoic of southeastern New England: Geological Society of America Abstracts with Programs, v. 16, no. 1, p. 71.

Wise, D. U., 1964, Microjointing in basement, middle Rockie Mountains of Montana and Wyoming: Geological Society of America Bulletin, v. 75, p. 287-306.

Wise, D. U., 1965, Rotation axis method for detecting conjugate planes in calcite petrofabric: American Journal of Science, v. 263, p. 289-301.

Wise, D. U., 1981, Fault, fracture and lineament data for western Massachusetts and western Connecticut: United States Nuclear Regulatory Commission, NUREG/CR-2292, 253 p.

Wise. D. U., and McCrory, T. A., 1982, A new method of fracture analysis; Azimuth Versus Traverse Distance plots: Geological Society of America Bulletin, v. 93, p. 889-897.

Zartman, R. E., Hurley, P. M., Krueger, H. W., and Giletti, B. J., 1970, A Permian disturbance of K-Ar radiometric ages in New England: its occurrence and cause: Geological Society of America Bulletin, v. 82, p. 937-958.

APPENDIX I

GEOLOGIC SETTING AND HISTORY

Major Geologic Elements and Boundaries

Geologic provinces and major tectonic elements within and adjacent to the study area are shown in Figure 2, a generalized tectonic map of eastern Connecticut and western Rhode Island.

The geologic provinces of interest to this study are listed (from west to east) and briefly described below:

1) Connecticut Valley: One of a series of grabens and half-grabens that trend sub-parallel to the eastern continental margin of North America. It is filled with clastic terrigenous sediments (Russell, 1922) and basaltic volcanic rocks that may be related to a NNE-trending basaltic dike swarm of Jurassic age in New England (May, 1971).

2) Bronson Hill Anticlinorium: A line of Devonian mantled gneiss domes penetrating and incorporating a series of Devonian nappes. The rocks within this geologic province are late Precambrian through Devonian metasedimentary varieties (Dixon and Lundgren, 1968; Robinson and Hall, 1980; Rogers, 1982).

3) Merrimack Synclinorium: In the study area, an isoclinal, synclinal nappe. It is deformed by the Seldon Neck Fold in southern Connecticut. The synclinorium

includes late Precambrian through Devonian metasediments (Dixon and Lundgren, 1968; Robinson and Hall, 1980).

4) Willimantic Dome: A low amplitude structure that deforms the rocks of the Merrimack Synclinorium (Dixon and Lundgren, 1968). The dome is cored by gneissic units that may have an affinity with the Avalonian rocks of the Boston Platform (Wintsch and Fout, 1982). Erosion of the dome may have produced a window exposing the lower plate of the Lake Char-Honey Hill Fault Zone. A disturbed horizon in the dome's stratigraphy, characterized by rotated tectonic blocks, may represent the Lake Char-Honey Hill surface of decollement (Wintsch, 1979). Alternatively, this horizon may be a Cordilleran type detachment fault (Goldstein, 1984).

5) Boston Platform: Late Precambrian sedimentary rocks and plutonic rocks, which range in composition from quartz diorite to granite (Dixon and Lundgren, 1968; Quinn and Moore, 1968). The Boston Platform is intruded by Devonian and younger granitic plutons (Page, 1968) and includes a late Alleghenian ductile shear zone separating distinct Precambrian terranes (Gromet and O'Hara, 1984).

6) Narragansett Basin: A fault-bounded, later Paleozoic trough filled with Pennsylvanian terrigenous clastic sediments and coal bearing horizons (Quinn and Moore, 1968). Intense, multiphase, Alleghenian, ductile

through brittle deformation is observed in Pennsylvanian sediments within the basin (Mosher, 1983). The Narragansett Basin is intruded at its southwestern end by the late Paleozoic Narragansett Pier Granite (Hozik, 1981).

A series of major faults bounds these geologic provinces (see Figure 2). These major boundaries are listed (from west to east) and discussed briefly below.

a) Eastern Border Fault: The master fault of the Connecticut Valley Graben. This feature is a NNE-trending, west dipping, Triassic to Jurassic normal fault that extends at least from the Vermont-Massachusetts border to the Long Island Sound (Wheeler, 1937, 1939; Chandler, 1978).

b) Bone Mill Brook Fault: A proposed west over east Alleghenian thrust fault separating the rocks of the Bronson Hill Anticlinorium from those of the Merrimack Synclinorium (Pease, 1982).

c) Lake Chargoggagoggmanchauggagoggchaubunagungamaugg (Lake Char)-Honey Hill Fault Zones: Continuous zones of intense cataclasis separating the rocks of the Merrimack Synclinorium from the Boston Platform. These zones are commonly considered to be west over east (Lake Char) and north over south (Honey Hill) thrust faults (ie: Dixon and Lundgren, 1968). The movement sense of these features is under debate as Goldstein (1984) has shown that small scale structures near the Lake Char Fault indicate normal displacement.

d) Border Faults of the Narragansett Basin: The nature of these faults is controversial. Mosher (1983) has suggested that the Narragansett Basin opened as a pull-apart along NE-trending, left-lateral post-Acadian strike-slip faults. Bradley (1982) and McMaster and others (1980), however, have proposed that the basin is a pull-apart structure associated with right-lateral motion along NE-trending structures.

General Geologic History

The tectonics of southern New England during the early to middle Paleozoic were dominated by compressional deformation associated with the Taconic and Acadian events. The late Precambrian crystalline rocks of the Avalon Platform may have "docked" with the North American Plate in the Devonian producing penetrative ductile deformation across the region (Robinson and Hall, 1980). The boundary between the North American Plate and the Avalon Platform may be located east of the Lake Char Fault Zone in Massachusetts, Connecticut, and Rhode Island (Gromet and O'Hara, 1984).

Large scale, early Devonian, recumbent isoclinal folds and middle Devonian backfolds in southern New England were further deformed by the Seldon Neck Fold and mantled gneiss domes in the middle Devonian (Robinson and Hall, 1980).

Movement on the Lake Char-Honey Hill Fault Zone and, possibly, the Bone Mill Brook Fault may have been coeval with middle Devonian backfolding and may have continued, with interruptions, into the Permian (Dixon and Lundgren, 1968; Robinson and Hall, 1980).

The late Paleozoic tectonic history of southern New England is now under intense scrutiny. Numerous observations provide evidence for an Alleghenian disturbance in the region. Penetrative, multiphase, ductile deformation occurred in Pennsylvanian and Permian formations in the Narragansett Basin (Skehan and Murray, 1978; Mosher, 1983). Pennsylvanian meta-anthracite coals in the Worcester (Grew, 1973) and Narragansett (Skehan and Murray, 1978) Basins, late Paleozoic radiometric dates (Zartman and others, 1970) and the Permian Narragansett Pier Granite (Kocis and others, 1978) indicate a late Paleozoic thermal event.

Several models of large scale transcurrent motion have been proposed for this part of New England. On the basis of paleomagnetic evidence, Kent and Opdyke (1979) suggested that coastal New England and the Canadian Maritime Region (Acadia) have moved approximately 1500 kilometers northward to their present position along a sinistral transcurrent shear zone. While this proposal of transcurrent emplacement of Acadia has engendered one of the more puzzling problems of Appalachian tectonics in recent years, it is based on an inaccurate post-Acadian pole position for North America (Kent and Opdyke, 1984). Boucot and Gray (1983) have underscored such hazards by noting that Paleozoic and older plate reconstructions based purely on paleomagnetic evidence run into serious difficulties when paleogeographic, paleontologic, paleoclimatic, and lithostratigraphic data are taken into account.

Arthaud and Matte (1977) have proposed a late Paleozoic east-west trending dextral megashear system separating a northern master plate comprising the Canadian Shield and the European and Asian plates, and a southern master plate composed of Africa and an unknown eastern plate. The area of this study is located in the zone of transition between the transcurrent motion of this megashear system and the Alleghenian compressional tectonics of the southern Appalachians. Mosher (1983) has invoked this model to explain late stage deformation of the Narragansett Basin and its sediments.

Most field evidence for post-Acadian transcurrent motion in the Northern Appalachians indicates dextral displacement (Bradley, 1982). The predominance of dextral motion on recognized strike-slip faults in the Northern Appalachians has led Bradley (1982) to propose a late Paleozoic dextral shear zone between continental plates. Under this model, as much as 200 kilometers of displacement was concentrated along the Acadian suture and within the Avalonian basement. Within the study area, the Ponkapoag Fault of Rhode Island and the Lake Char-Clinton Newbury Fault Zones of Connecticut and Massachusetts may be components of this proposed shear system (Bradley, 1982).

The Triassic marked the close of a Paleozoic Wilson Cycle in the Appalachian system and the beginning of a new cycle with the initiation of continental rifting to form the present day Atlantic Ocean. The Connecticut Valley half-graben and swarms of mafic (diabase) dikes in southern New England are related to this Mesozoic crustal extension (Sutter and Smith, 1979; May, 1971). Radiometric dating of these dikes shows that actual opening of the Atlantic Ocean did not begin until approximately 175 MABP (Sutter and Smith, 1979). Multiple swarms of Mesozoic mafic dikes in northern New England indicate a complex history of stress reorientation in that area. The plutons of the White Mountain Magma Series of Canada and northern New England were emplaced during the Mesozoic in several pulses of magmatic activity (McHone, 1978). These and other features attest to robust tectonic activity in southern New England during the Mesozoic.

APPENDIX II

MISCELLANEOUS STRUCTURAL DATA

Structural data for granite, syenite, diabase and felsic dikes are shown in Figure 37. In general, these features are similar in orientation to the aplite and pegmatite dikes (Figures 3A and 3B). An early effort to analyze the minor brittle fault population involved separation of data clusters by orientation. The results of this analysis are shown in Figures 37 to 40. NE-striking, NW-dipping faults and NE-striking vertical faults (Figures 37 and 39) are part of the Merrimack fracture trend of eastern Connecticut and western Rhode Island. E-W-striking vertical faults (Figure 38) are part of the Narragansett Pier structural trend. Many minor faults did not fit a classification system based solely on orientation. Data for these features is shown in Figure 40.

Figure 41 shows locations where strike- plus oblique-slip faults comprise over 50% of the minor faults observed at fracture stations. Locations where these families are subordinate to dip-slip faults or where minor faults are rare are also shown.

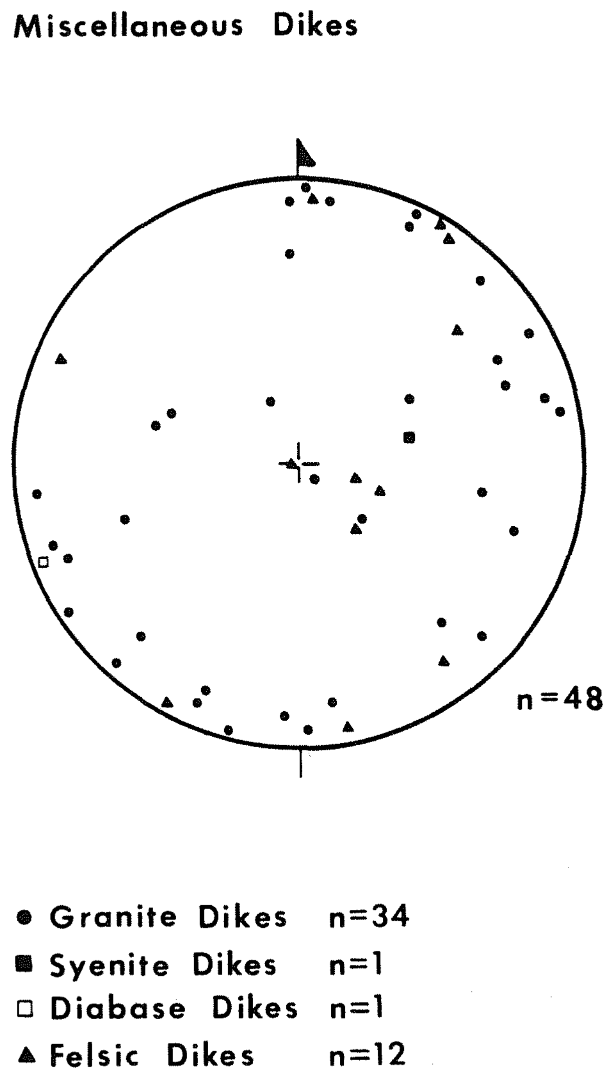

Figure 36. Equal area net plot of poles to planes for miscellaneous dikes.

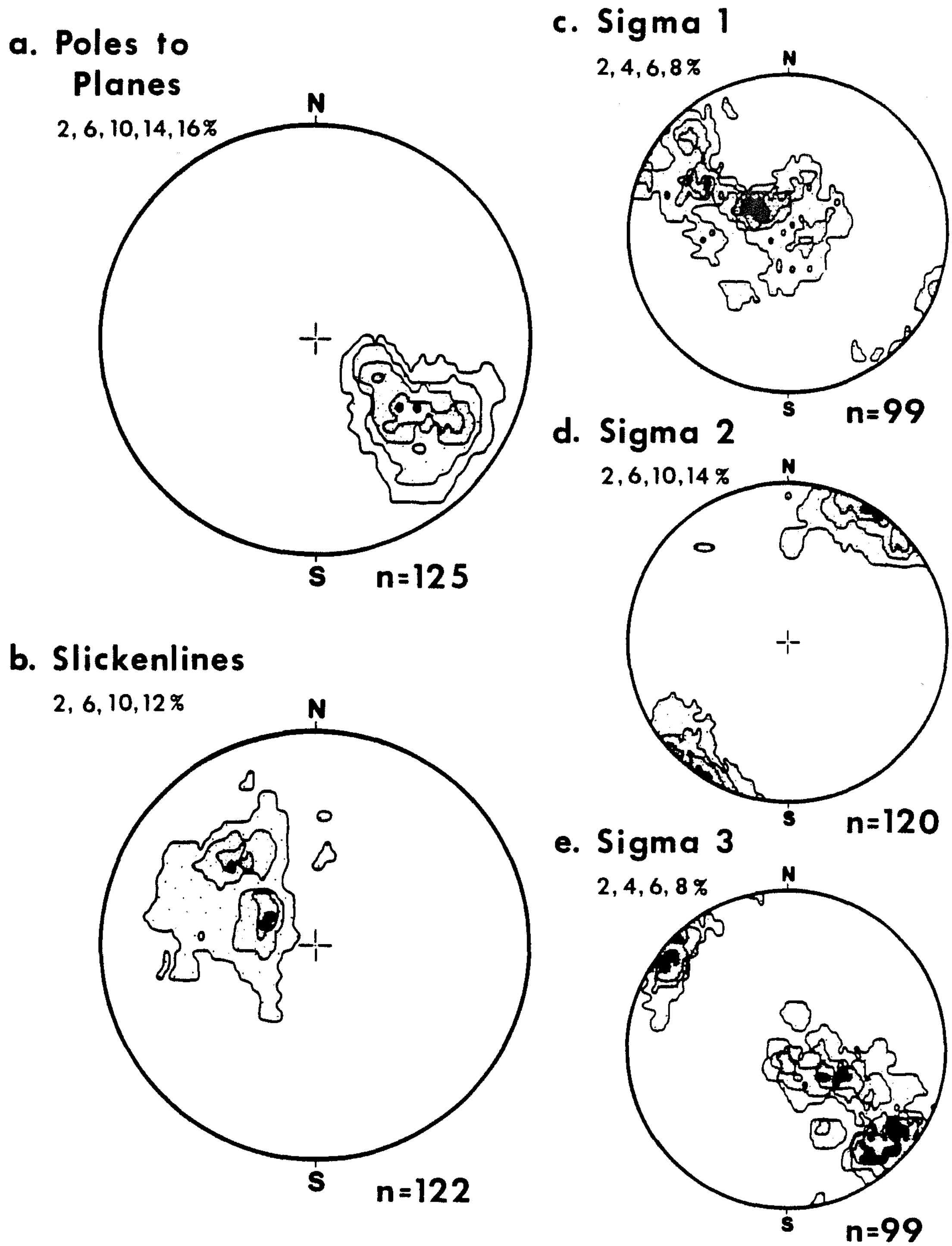

Figure 37. Classification of minor faults by orientation. NE-striking (Merrimack Trend), NW-dipping faults (mostly normal dip-slip). Contours on equal area nets are in percent per 1% area.

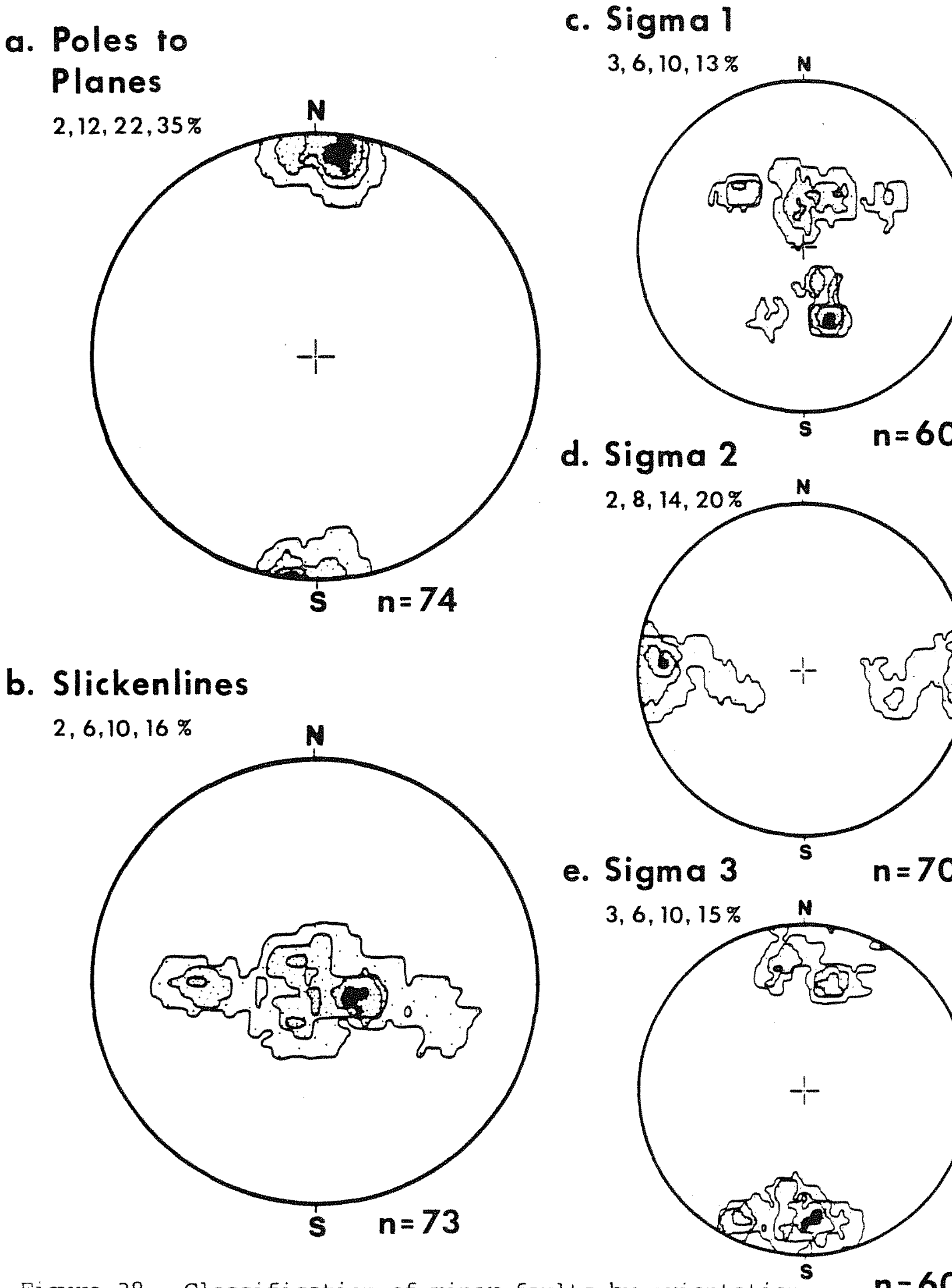

Figure 38. Classification of minor faults by orientation. E-W striking (Narragansett Pier Trend), vertical faults (dip- and oblique-slip). Contours on equal area nets are in percent per 1% area.

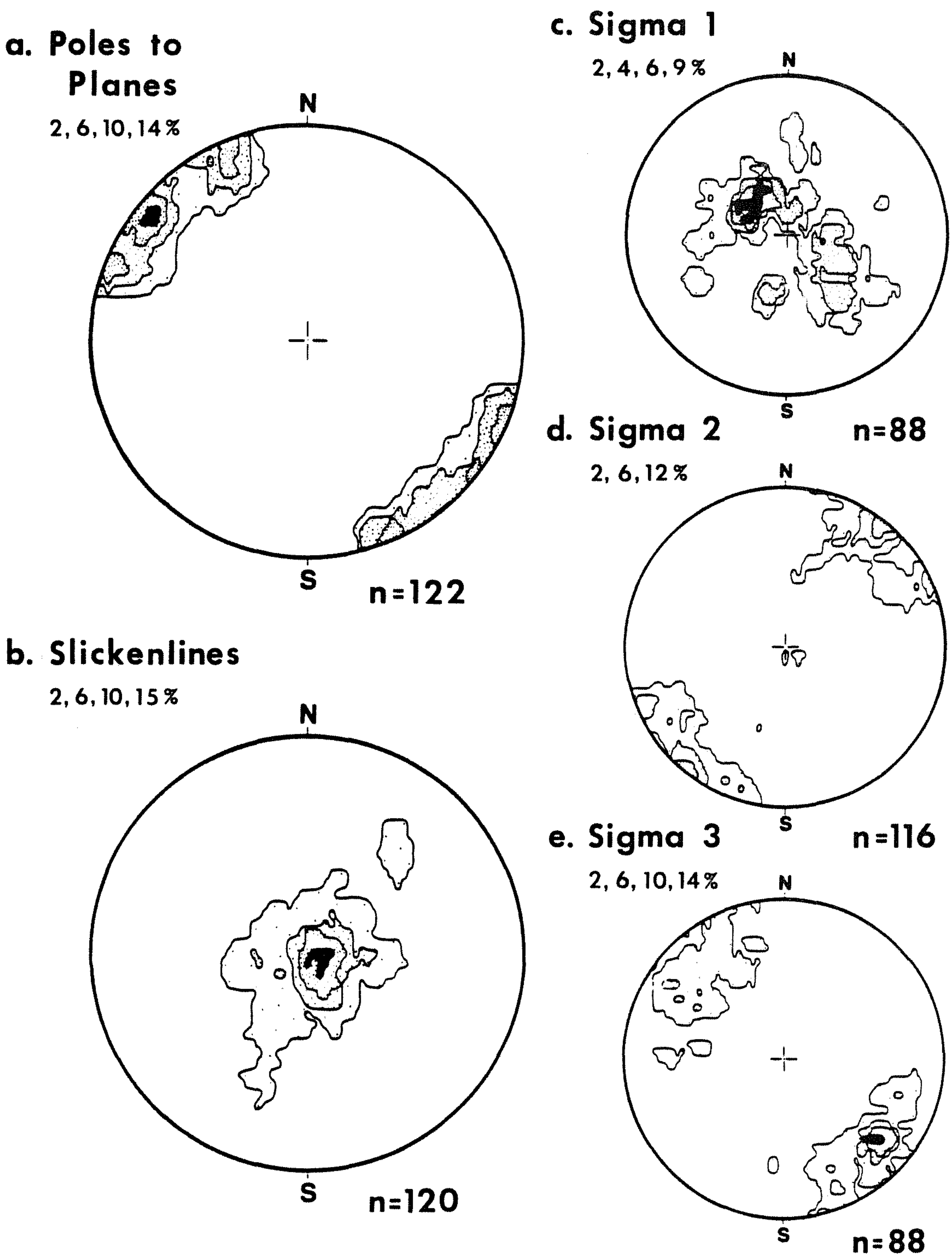

Figure 39. Classification of minor faults by orientation. NE-striking (Merrimack Trend), vertical faults (mostly dip-slip). Contours on equal area nets are in percent per 1% area.

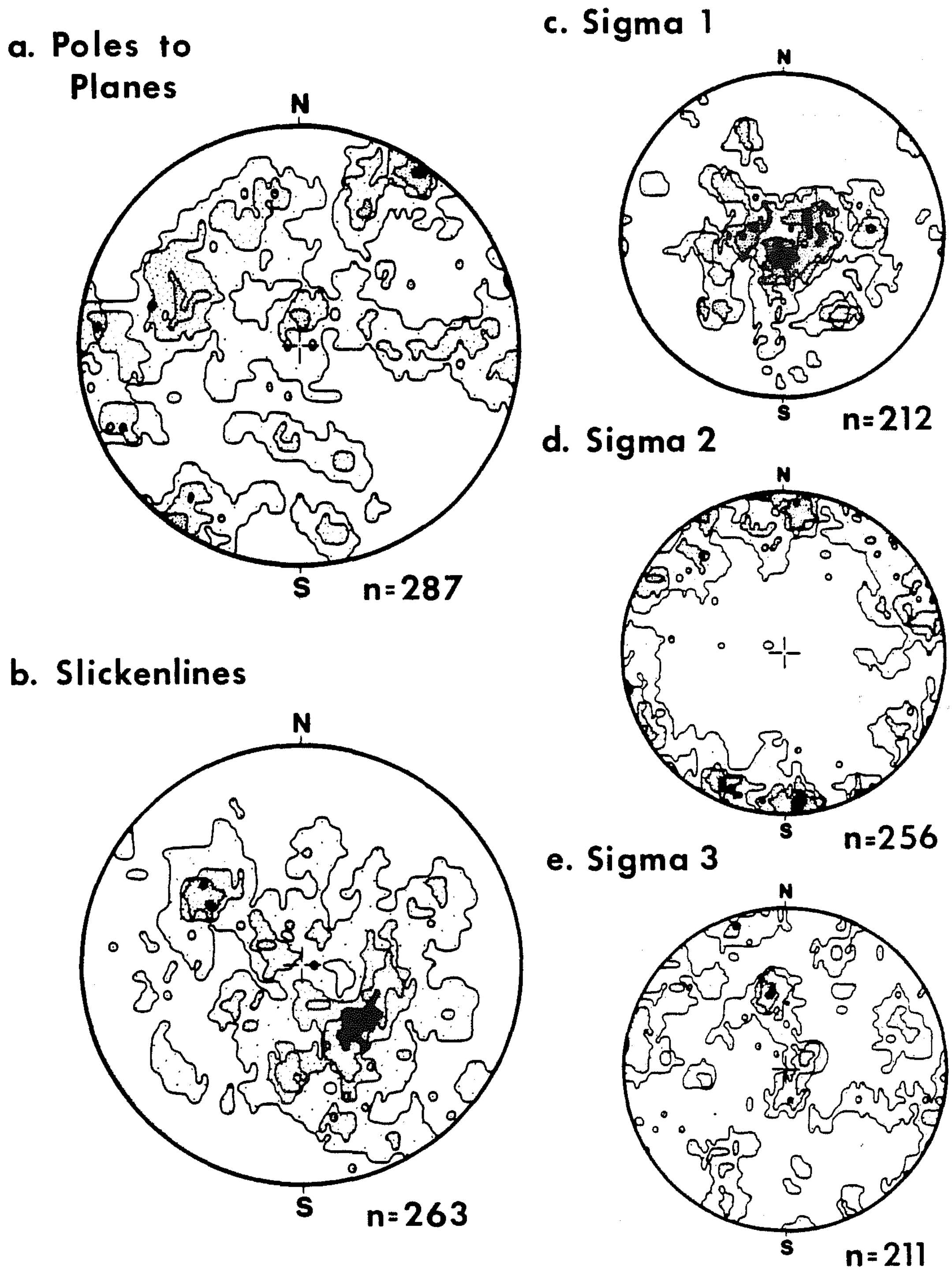

Figure 40. Faults that do not fit an orientational classification scheme. Contours on equal area nets are in percent per 1% area.

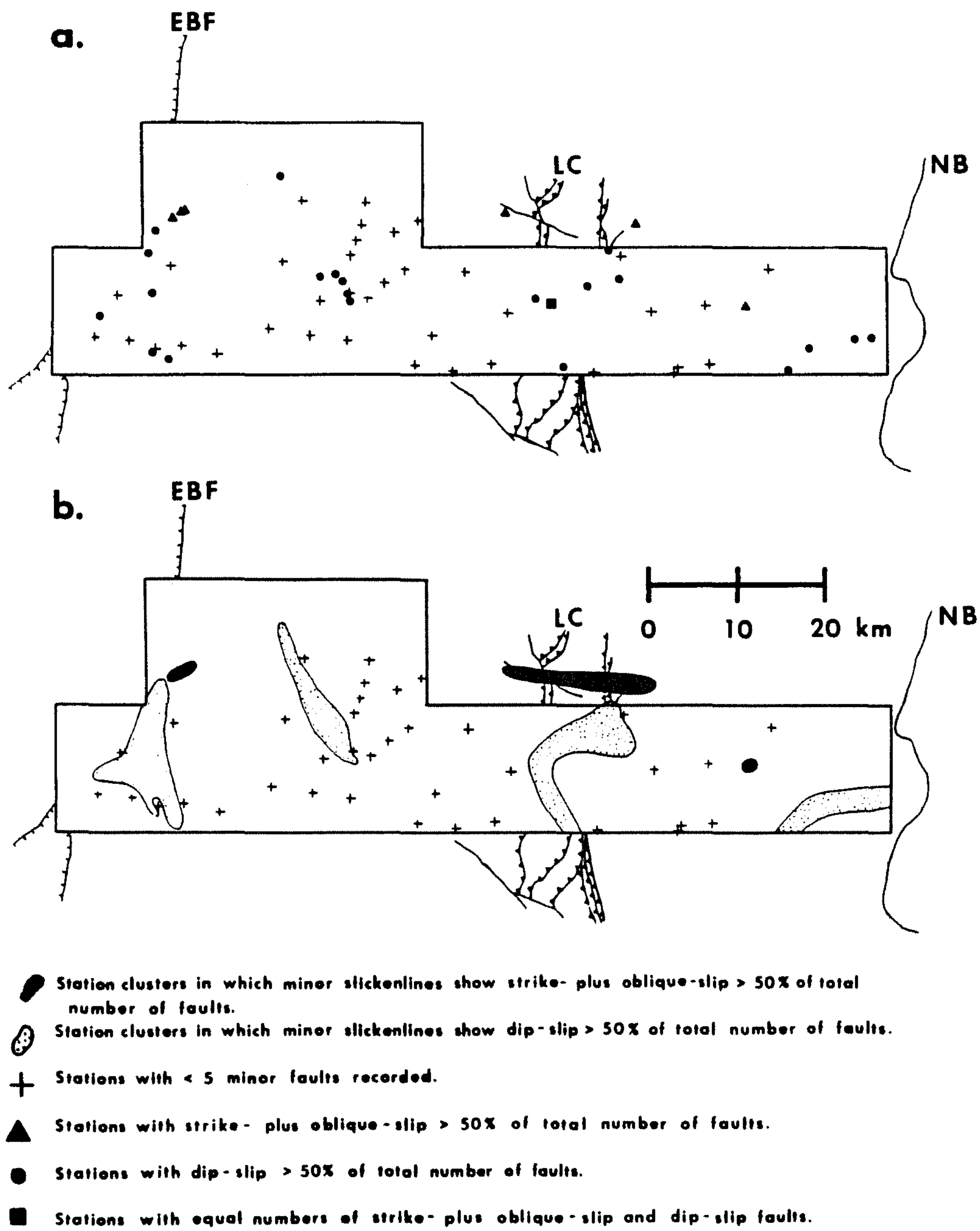

Figure 41. Character of minor faulting motions at fracture stations. The stations shown in a. and b. may represent combinations of two or more individual fracture stations.

APPENDIX III

TREND SURFACE ANALYSIS

The SYMAP package employed in this study has the capability of fitting mathematical surfaces to areally distributed data, a technique known as trend surface analysis (Dougenik and Sheehan, 1979). Trend surface analysis may be the statistical technique most commonly used by geologists to examine areally distributed data (Whitten, 1981). The distribution of NNE-trending quartz veins and minor brittle faults in the area was studied using this technique.

A trend surface is a theoretically noise-free mathematical surface which approximates the distribution of data values. Typically, a trend surface is produced by developing a power series of the form:

$$z=a+by+cx+dy^2+eyx+fx^2+gy^3+hxy^2+iyx^2+jx^3........,$$

where z is a dependent variable and x and y are east-west and north-south coordinates. In this expression, the argument, a, is a noise term corresponding to both error and variation of possible geological significance. The expressions, b, c, d, etc., are linear or nonlinear coefficients derived by the method of least squares to best fit the data (Louden, 1979).

Using trend surface techniques the variability of any areally distributed data may be separated into regional effects or trends and random components or noise terms such as local features of possible geological significance. Trend surfaces, then, may be used as a filtering technique to separate local variation from regional trends (Whitten, 1975). In the case of minor faulting, variation in frequency not explained by the regional surface may be genetically related to a major structural or tectonic feature if it is geographically coincident with or related to the structure.

APPENDIX IV

STATION DESCRIPTIONS

Station numbers refer to the locations shown in Figure 42.

<u>Glastonbury Quadrangle</u>

Station 1: Natural exposure in Glastonbury Gneiss west of Woodland St. 1 km south of intersection with Hopewell St.

Station 2: Ministation. Roadcut in Glastonbury Gneiss on north side of London Turnpike 1.4 km north of intersection with Chestnut Hill Rd.

Station 3: Quarry in Glastonbury Gneiss south of London Turnpike 1 km north of intersection with Chestnut Hill Rd.

Station 4: Natural exposure in Glastonbury Gneiss north of Brook St. 0.4 km west of intersection with Manchester Rd.

Station 5: Ministation. Roadcut in Glastonbury Gneiss north of Hebron Ave. at intersection with Weir St.

Station 6: Ministation. Roadcut in Glastonbury Gneiss on north side of Hebron Ave. 0.2 km east of intersection with Weir St.

Station 7: Ministation. Roadcut in Glastonbury Gneiss on north side of Wassuc Rd. 0.3 km west of intersection with Thompson St.

Station 8: Ministation. Manmade exposure in Glastonbury Gneiss in real estate development north of Wassuc Rd. 0.3 km east of Thompson St.

Station 9: Ministation. Small exposure in Glastonbury Gneiss on east side of Thompson Rd. 0.5 km north of intersection with Wassuc Rd.

Station 10: Roadcut in Bolton Schist on Route 2 0.8 km east of Wassuc Rd. entrance ramp.

Marlborough Quadrangle

Station 11: Roadcut in Monson Gneiss on Route 2 at West Rd. ramp.

Station 12: Manmade exposure in Monson Gneiss in real estate development west of West Rd. 0.4 km north of intersection with Route 2.

Station 13: Roadcut in Brimfield Schist and Hebron Formation on Route 2 west of intersection with Route 66.

Station 14: Manmade exposure in Glastonbury Gneiss south of Route 94 0.4 km east of intersection with Coups Sawmill Rd.

Station 15: Ministation. Roadcut in Glastonbury Gneiss on Route 94 0.2 km west of intersection with Rockwell St.

Station 16: Ministation. Roadcut in Glastonbury Gneiss on north side of Route 94 0.3 km east of intersection with Rockwell St.

Station 17: Natural exposure in Littleton Formation west of Birch Mountain Rd. 2 km north of intersection with Route 94.

Station 18: Natural exposure in Littleton Formation east of Birch Mountain Rd. 4 km north of intersection with Route 94.

Station 19: Natural exposure in Glastonbury Gneiss 0.6 km east of Gardner St. (Glastonbury Quadrangle).

Station 20: Ministation. Natural exposure in septum of Hebron Formation within diabase north of Johnson Rd. 1.3 km south of Route 66.

Station 21: Natural exposure in Hebron Formation and Devonian Pegmatite west of Parker Rd. 1.1 km north of intersection with Route 66.

Station 22: Natural exposure in Hebron Formation and Devonian Pegmatite north of Parker Rd. 1 km west of intersection with West St.

Station 23: Natural exposure in Hebron Formation west of Paper Mill Rd. 2 km south of intersection with Route 66.

Station 24: Natural exposure in Hebron Formation and Devonian Pegmatite south of Route 66 0.2 km east of intersection with Paper Mill Rd.

Station 25: Natural exposure in Hebron Formation and Devonian Pegmatite north and south of Slocum Rd. 0.6 km east of Mack Hill.

Station 26: Natural exposure in Hebron Formation and Devonian Pegmatite north of Route 66 east of intersection with Burrows Hill Rd.

Rockville Quadrangle

Station 27: Roadcut in Glastonbury Gneiss on I-84. First outcrop of crystalline rocks east of redbeds.

Station 28: Roadcut in Bolton Schist on I-84 east of Station 27.

Station 29: Roadcut in Bolton Schist on south side of I-84 west of intersection with Route 44A and U.S. Route 6.

Station 30: Roadcut in Hebron Formation on north side of U.S. Route 6 east of intersection with I-84.

Columbia Quadrangle

Station 31: Ministation. Roadcut in Devonian Pegmatite within Hebron Formation on Route 85 0.3 km west of intersection with Route 207.

Station 32: Ministation. Natural exposure in Hebron Formation and Devonian Pegmatite on the west shore of Amston Lake 0.2 km ENE of end of access road to lake.

Station 33: Ministation. Natural exposure in Hebron Formation and Devonian Pegmatite on the west shore of Amston Lake 0.2 km north of Station 32.

Station 34: Ministation. Natural exposure in Hebron Formation 0.1 km NNW of Station 33 on ridge west of Amston Lake.

Station 35: Quarry and natural exposure in Canterbury Gneiss north and south of Robinson Rd. 0.8 km east of intersection with Route 6A.

Station 36: Ministation. Roadcut in Hebron Formation on Route 6A 0.4 km east of intersection with West St.

Station 37: Ministation. Roadcut in Tatnic Hill Formation on Route 6A 0.3 km west of intersection with Trumbull Highway.

Station 38: Natural exposure in Tatnic Hill Formation and Devonian Pegmatite west of Hop River Rd. 1.9 km north of intersection with Route 6.

Station 39: Ministation. Natural exposure in Tatnic Hill Formation on Hop River Rd. 1.6 km north of intersection with Route 6.

Station 40: Natural exposure in Tatnic Hill and Quinebaug Formations west of defunct Penn Central Railroad tracks 0.2 km south of intersection with Route 87.

Station 41: Ministation. Natural exposure in Quinebaug Formation on east side of Cooks Hill Rd. <0.1 km north of intersection with Route 87.

Station 42: Natural exposure in Tatnic Hill Formation and Devonian Pegmatite along Tenmile River on west side of Cooks Hill Rd.

Station 43: Roadcut in Tatnic Hill Formation on I-84 west of intersection with Route 32.

<u>South Coventry Quadrangle</u>

Station 44: Natural exposure west of Brigham Tavern Rd. 2.9 km north of intersection with Route 44A.

Station 45: Natural exposure north of Route 32 0.2 km east of intersection with Hopkins Rd.

<u>Willimantic Quadrangle</u>

Station 46: Quarry in Lebanon Gabbro on Owunnegunsett Hill east of Village Hill Rd. 0.9 km north of intersection with Chappell Rd.

Station 47: Roadcut in Tatnic Hill Formation on west side of Route 289 (Mountain St.) 1.2 km south of intersection with Pleasant St.

Station 48: Natural exposure in Tatnic Hill Formation at summit of Hosmer Mountain 0.2 km WSW of reservoir.

Station 49: Natural exposure in Tatnic Hill Formation on north flank of Hosmer Mountain south of Johnson St. dead end.

Station 50: Natural exposure in plagioclase gneiss 0.2 km NNE of intersection of Route 32 and U.S. Route 6.

Station 51: Roadcut in plagioclase gneiss on entrance ramp of Route 32 to I-84 East.

Station 52: Natural exposure in Willimantic Gneiss north of Pudding Lane 0.2 km east of intersection with Ash St.

Station 53: Natural exposure in Tatnic Hill Formation south of Route 32 on the grounds of the Immaculata Retreat and on the hill side between the Retreat access road and the Willimantic Camp Ground.

Station 54: Natural exposure in Tatnic Hill Formation west of Tuckie Rd. 1 km north of intersection with Route 14.

Station 55: Natural exposure in Tatnic Hill Formation east of Route 203 2.0 km north of intersection with Route 14.

Station 56: Natural exposure in Canterbury Gneiss on and west of Ballymahack Brook 0.6 km south of Beaver Hill Rd.

Station 57: Natural exposure in Scotland Schist and Hebron Formation on southeastern flanks of Avery Hill and Pleasure Hill west and northwest of Pond Rd. at intersection with Route 207 and eastern flank of Ayers Mountain west of Mountain Rd. at intersection with Route 207.

<u>Spring Hill Quadrangle</u>

Station 58: Natural exposure in Tatnic Hill Formation in and east of Schoolhouse Brook <0.1 km north of Nipmuk Trail Crossing.

Station 59: Natural exposure in Willimantic Gneiss on Nipmuk Trail 0.5 km south of intersection with Crane Hill Rd.

Station 60: Natural exposure in Tatnic Hill Formation east of Route 195 0.7 km north of intersection with Chaffeeville Rd.

Station 61: Natural exposure north of Bradley Rd. 1.5 km east of intersection with Chaffeeville Rd.

Station 62: Natural exposure in Tatnic Hill Formation north of Bassett Bridge Rd. 0.3 km west of intersection with Hall Rd.

Station 63: Natural exposure on Natchaug River east of Route 198 crossing.

Scotland Quadrangle

Station 64: Roadcut and natural exposure in Scotland Schist north of Shetuckett River on north side of Station Rd. 0.4 km west of intersection with Merrick Brook.

Station 65: Natural exposure in Tatnic Hill Formation on east shore of Shetuckett River west of Route 97 1.6 km south of intersection with Salt Rock Rd.

Station 66: Ministation. Roadcut in Tatnic Hill Formation on east side of Route 97 0.9 km south of intersection with Salt Rock Rd.

Station 67: Ministation. Roadcut in Tatnic Hill Formation on Route 97 0.55 km south of intersection with Salt Rock Rd.

Station 68: Ministation. Natural exposure in Scotland Schist east of Route 97 0.7 km south of intersection with Brooklyn Rd.

Station 69: Natural exposure in Scotland Schist and Hebron Formation on east flank of Pudding Hill east of Route 97 0.7 km south of intersection with Brooklyn Rd.

Station 70: Roadcut and natural exposure in Tatnic Hill Formation on west side and west of Water St. 1.2 km north of intersection with Potash Hill Rd.

Station 71: Ministation. Natural exposure in Tatnic Hill Formation on west side of Water St. 1.5 km north of intersection with Potash Hill Rd.

Station 72: Ministation. Roadcut in Tatnic Hill Formation on west side of Lisbon Rd. 1.1 km north of intersection with Bates Pond Rd.

Station 73: Ministation. Natural exposure in Tatnic Hill Formation east of Cory Rd. 0.4 km west of intersection with Lisbon Rd.

Station 74: Natural exposure in Tatnic Hill Formation and Canterbury Gneiss north and south of Kinne Rd. 0.4 km north of intersection with Cory Rd.

Hampton Quadrangle

Station 75: Ministation. Roadcut in Scotland Schist on north side of Route 6 1.4 km west of intersection with Upper Rd.

Station 76: Ministation. Roadcut in Scotland Schist on north side of Route 6 east of intersection with Upper Rd.

Station 77: Roadcut in Canterbury Gneiss on Route 6 on east side of Hampton town line.

Plainfield Quadrangle

Station 78: Ministation. Roadcut in Tatnic Hill Formation on north side of Route 14 1.2 km west of intersection with Mudhole Rd.

Station 79: Roadcut in Tatnic Hill Formation on north side of Route 14 0.3 km west of intersection with Mudhole Rd.

Station 80: Ministation. Natural exposure in Quinebaug Formation west of Depot Rd. 0.3 km south of road between General Putnam Highway and Packer Rd.

Station 81: Ministation. Roadcut in Quinebaug Formation on north side of Route 14A 0.6 km east of intersection with Black Hill Rd.

Station 82: Roadcut in Quinebaug Formation on west side of Route 52 0.4 km south of Rhode Road underpass.

Station 83: Ministation. Roadcut in Quinebaug Formation on east side of Route 52 0.2 km north of Rhode Road underpass.

Station 84: Natural exposure in Quinebaug Formation on east flank of hillside west of Route 12 1 km south of intersection with Route 14.

Station 85: Ministation. Natural exposure in Hope Valley Alaskite Gneiss on north side of Hell Hollow Rd. 0.6 km east of intersection with Sullivan Rd.

Station 86: Natural exposure in Hope Valley Alaskite Gneiss north and south of Hell Hollow Rd. 1.3 km east of intersection with Sullivan Rd.

Station 87: Roadcut in Quinebaug Formation on Route 52 1.4 km north of Moosup Pond Rd. overpass.

Oneco Quadrangle

Station 88: Roadcut in Hope Valley Alaskite Gneiss on Route 14 in Almyville 0.2 km west of Moosup River crossing.

Station 89: Natural exposure in Plainfield Formation on east flank of hillside facing Moosup Pond Rd. west of intersection with Harris Rd.

Station 90: Ministation. Roadcut in Scituate Granite Gneiss on south side of Route 14 1.4 km west of abandoned Sterling Mill.

Station 91: Quarry in Scituate Granite Gneiss west of Pine Hill Rd. Access road at 0.1 km south of Route 95.

Station 92: Natural exposure in Ponaganset Gneiss, Porphyritic Granite Gneiss of Sterling Plutonic Group, and Hope Valley Alaskite Gneiss on south shore of Hazard Pond west of Hazard Rd. 1 km south of intersection with Muddy Brook Rd.

Station 93: Natural exposure in Scituate Granite Gneiss east of Hazard Rd. 0.4 km south of intersection with Muddy Brook Rd.

Station 94: Natural exposure in Plainfield Formation and Ponaganset Gneiss on south flank of Carbuncle Hill south of Route 95 1.6 km west of Fairbanks Corner.

Station 95: Gravel pit in Scituate Granite Gneiss west of Brown Rd. 1 km west of intersection with Plain Rd.

East Killingly Quadrangle

Station 96: Roadcut on Connecticut Turnpike east of Snake Meadow Rd. overpass and 3.2 km east of Route 52 intersection.

Coventry Center Quadrangle

Station 97: Roadcut and natural exposure on west side and west of Route 117 0.1 km south of intersection with Cahoone Rd.

Station 98: Natural exposure in Scituate Granite Gneiss in Wickaboxet State Forest 0.5 km north on park road from intersection with Plain Meeting House Rd.

Station 99: Railroad cut in Scituate Granite Gneiss along old railroad grade east of Route 102.

Station 100: Quarries and natural exposure in Scituate Granite Gneiss south of end of Nipmuk Rd. on south flank of Nipmuk Hill.

Station 101: Roadcut in Hope Valley Alaskite Gneiss on west side of I-95 2.3 km south of intersection with Route 3 (Crompton Quadrangle).

Station 102: Quarry in Ten Rod Gneiss west of Route 3 at end of unimproved road 3.8 km south of I-95 underpass.

Crompton Quadrangle

Station 103: Roadcut in Scituate Granite Gneiss on I-95 at intersection with Route 3.

Station 104: Roadcut in Scituate Granite Gneiss on south side of I-95 at intersection with New London Turnpike.

Station 105: Roadcut in Scituate Granite Gneiss on south side of I-95 2.3 km west of intersection with New London Turnpike.

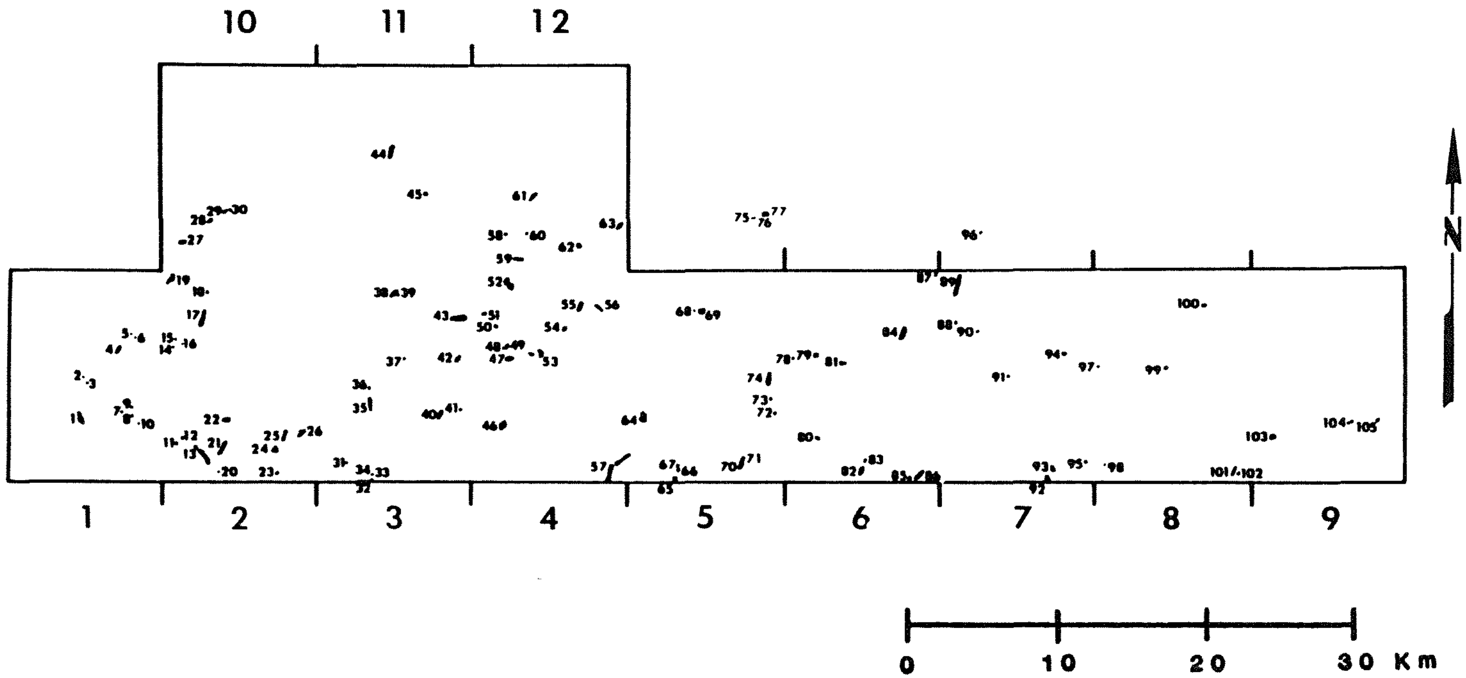

Figure 42. Fracture station locations.